Appendix D Seismic hazard assessment



Efaté Earthquake Engineering Technical Assistance

Port Vila CBD Seismic Hazard Assessment

Prepared for: Egis NZ Limited

Prepared by: Tonkin & Taylor International Ltd

Job Number: 1097984.1000 v02

Date: June 2026

Document control and review

Title: Efaté Earthquake Engineering Technical Assistance					
Date	**Version**	**Description**	**Prepared by**	**Reviewed by**	**Authorised by**
10/06/2026	01	For client review	A Balachandra M Ogden	J Lim	N Hickman
15/06/2026	02	For client review – updated ground zone	A Balachandra M Ogden	J Lim	N Hickman

Table of contents

1 Introduction 1

2 Project location 2

3 Geology and tectonic setting 3

3.1 Published geology 3

3.2 Regional tectonic setting 3

3.3 Historical earthquakes 4

4 Seismic site characterisation 7

4.1 General 7

4.2 Ground conditions 7

4.2.1 General 7

4.2.2 Zone A 9

4.2.3 Zone B 10

4.2.4 Zone C 11

4.2.5 Zone D 13

4.3 Summary 14

5 Seismic source characterisation model 15

5.1 General 15

5.2 Method summary 15

5.3 SSC model logic tree 15

5.4 Ground motion models 16

5.5 Logic tree 17

5.6 Near-fault factors 17

6 Results and discussion 18

6.1 Hazard curves 18

6.2 Uniform hazard spectra 20

6.3 Sensitivity to site V_{s30} value 22

6.4 Comparison with Vanuatu Building Code 24

6.5 Comparison with other studies 26

6.6 Hazard disaggregation 27

7 Recommendations 30

7.1 V_{s30} 30

7.2 Uniform hazard spectra 30

7.3 Ground motion parameters for geotechnical design 30

7.4 Setting within the Vanuatu Building Code framework 31

8 Further study 32

9 References 33

10 Applicability 35

Appendix A Seismic source characterisation methodology

Appendix B Uniform Hazard Spectra

Appendix C Hazard disaggregation

Executive summary

Tonkin & Taylor International Ltd (T+TI) has been engaged by Egis NZ Ltd to provide specialist geotechnical engineering services for the New Zealand Ministry of Foreign Affairs and Trade (MFAT) Efaté Earthquake Engineering Technical Assistance (EEETA) programme.

This report presents the seismic hazard assessment (SHA) undertaken as part of the commission for the Port Vila Central Business District (CBD) in Vanuatu. The assessment characterises the ground shaking expected over the study area for a range of annual probability of exceedance to inform the design of redevelopment works following the 17 December 2024 Port Vila earthquake, which caused significant damage to buildings and infrastructure in Port Vila.

Vanuatu lies on one of the most seismically active plate boundaries in the world, where the Australian plate subducts beneath the Pacific plate. As a result, Port Vila is exposed to large earthquakes from three tectonic settings – shallow crustal events in the overriding plate, large interface earthquakes along the Vanuatu subduction zone, and intermediate-depth events within the subducting slab. All three were considered in this assessment. A seismic source model has been developed based on earthquake catalogue data to end of 2025 for the study area. A detailed discussion of the methodology is provided in **Appendix A**.

The ground shaking hazard at the site is influenced by underlying ground conditions. As such, the study area was divided into four ground zones (A to D) based on the underlying geology and available geotechnical and geophysical data. Time averaged shear wave velocity over the upper 30 m (V_{s30}), used as a proxy to characterise the underlying ground conditions, were developed for each zone from downhole testing and surface-wave (MASW) surveys, and the seismic hazard was computed for the full range of V_{s30} values relevant to the site. The V_{s30} values adopted for the study are discussed further in **Section 4**.

Peak ground acceleration and earthquake magnitude for the purpose of geotechnical design and 5% critically damped acceleration response spectra for the purpose structural design were assessed for all four ground zones for a range of annual probability of exceedance. The recommended design actions are presented in **Section 7**.

Hazard disaggregation, which identifies the earthquake sources that are most likely to result in the assessed design seismic actions, are presented in **Section 6.6**. Based on the hazard disaggregation, interface earthquakes and earthquake in the subducting slab largely dominate the assessed ground shaking hazard.

Finally, the ground shaking hazard derived from this SHA were compared to design actions prescribed in the Vanuatu Building Code Edition 2025 and other recent seismic hazard studies. The seismic actions assessed in this study are generally higher than the equivalent actions in the Vanuatu Building Code 2025 Edition. For building periods less than 0.8 seconds, the 1-in-250 AEP spectrum from this study is approximately equivalent to the 1-in-500 AEP code spectrum, and the 1-in-1000 AEP spectrum is approximately equivalent to the 1-in-2500 AEP code spectrum. The basis for the hazard factor adopted in the Vanuatu Building Code is not known and as such it is not possible to further evaluate potential source of difference.

The results of this SHA are broadly consistent with the ground shaking hazard presented in the Global Earthquake Model (GEM) Seismic Hazard Map. However, there are opportunities for further work and refinement, particularly as more information becomes available for the Vanuatu region and are discussed further in **Section 8**.

Glossary of Terms

Term	Definition
AEP	Annual exceedance probability. Probability that a ground motion intensity measure (IM) will exceed a defined value at a given site within any one-year period.
GMM	Ground Motion Model (also referred to as Ground Motion Prediction Equation or Ground Shaking Intensity Model). Gives the probability that a particular ground motion intensity measure (e.g., peak ground acceleration or spectral acceleration) will exceed a specified value at a given distance from the source, for a given earthquake rupture.
HVSR	Horizontal-to-vertical spectral ratio analysis
IMT	Intensity Measurement Type.
M_w	Moment magnitude. A measure of an earthquakes size or strength as a function of the amount of total energy that is released by the rupture.
MASW	Multi-channel analysis of surface waves to measure shear wave velocity.
PGA	Peak Ground Acceleration (units of g)
PSHA	Probabilistic seismic hazard assessment. A method to calculate the probabilistic earthquake shaking intensity hazard at a site based on a combination of the hazard from many individual earthquake sources.
SA	Spectral acceleration (units of g).
SA (T=x)	Spectral acceleration experienced by a single degree of freedom system with a period of T = x (seconds).
SHA	Seismic hazard assessment. A study to determine earthquake design loadings based on probabilistic and/or deterministic methods.
SSC model	Seismic source characterisation model. Defines the earthquake rupture sources (e.g. location, geometry, faulting type, magnitude) and their probability of occurrence within a given time period.
UHS	Uniform Hazard Spectra. Represents a locus of spectral accelerations at various vibration periods which have the same annual frequency of exceedance (or equivalently, return period).
V_s	Shear wave velocity. A measure of how fast seismic (shear) waves travel through a medium.
V_{s30}	The time-averaged shear wave velocity of the upper 30 m of soil and rock at a site.
$Z_{1.0}$	Depth to a soil or rock shear wave velocity of 1.0 km/s.
$Z_{2.5}$	Depth to a soil or rock shear wave velocity of 2.5 km/s.

1 Introduction

Tonkin & Taylor International Ltd (T+TI) has been engaged by Egis NZ Limited (Egis) to provide specialist geotechnical engineering services for the New Zealand Ministry of Foreign Affairs and Trade (MFAT) Efaté Earthquake Engineering Technical Assistance (EEETA) programme. This programme supports the Government of Vanuatu in its recovery efforts following the 17 December 2024 earthquake, which caused significant damage to buildings and infrastructure in Port Vila.

As part of the specialist geotechnical engineering services, T+TI was engaged to undertake:

- Desktop study and preliminary hazard zoning;
- Detailed geotechnical investigations;
- Seismic (ground shaking) hazard assessment; and
- Assessment of geohazards associated with the anticipated ground conditions. The purpose of this assessment is to support development of geotechnical guidance to aid in the recovery works.

This report presents the seismic hazard assessment (SHA) for the Port Vila Central Business District (CBD). The SHA provides an assessment of shaking hazard for the site and will be used as a basis for earthquake-resistance design as part of the recovery efforts.

The key components of a SHA are:

- The seismic source characterisation (SSC) model. These models define the earthquake rupture sources and rate of seismic activity.
- Ground motion models (GMM). These models are predictive relationships that estimate the ground motion intensity at a site due to any potential rupture.
- Ground characterisation, which is considered by the GMMs to assess the impact of underlying ground conditions on the ground shaking hazard at the ground surface.

This report presents the methodology, results and recommendations from the SHA for the Port Vila CBD.

2 Project location

The SHA has been completed for the detailed and broader study area as shown in Figure 2.1 below. The area within the red outline encompasses the Port Vila CBD. It is likely that the majority of the significant structures will be within this area. The blue extent denotes the full extent of the study area, with lower density of structures typically comprising short and/or lightweight structures.

The probabilistic calculations for the SHA have been undertaken for a single central coordinate location at longitude 168.317°, latitude -17.744°. Sensitivity analyses showed that the results of this SHA are reasonably insensitive to variation in location over the study area (i.e. the shaking hazard is independent of location across the study area but is dependent on-site specific ground conditions). As such, the SHA has considered one coordinate location and several possible ground conditions over the study area based on geotechnical and geophysical testing completed to date.

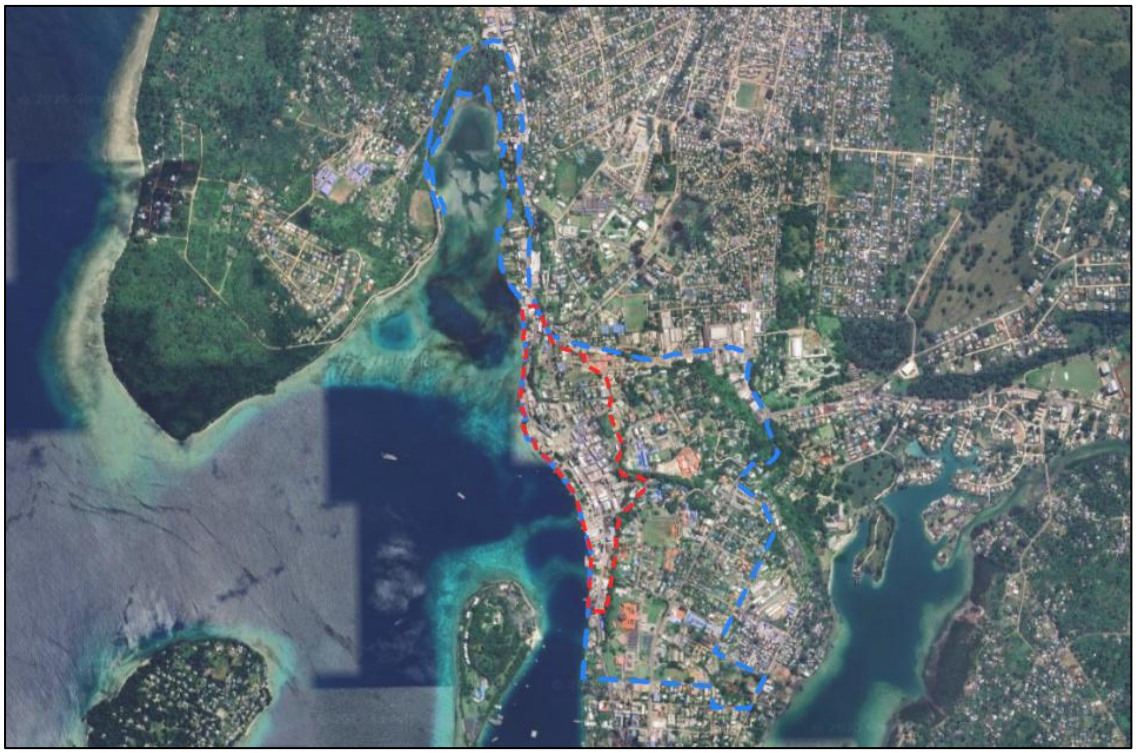

Figure 2.1: Detailed study area (outlined red) and broader study area (outlined blue).

3 Geology and tectonic setting

3.1 Published geology

The island of Efaté is predominantly volcanic in origin and lies within the Tertiary to Recent volcanic island arc system that forms Vanuatu. The volcanic sequence is dominated by the Efaté Pumice Formation, which consists of a succession of non-welded pumice breccia and beds of sand and silt deposited during a major eruptive event approximately 1 Ma (million years ago).

The upper section of the Efaté Pumice Formation consists of the Rentabau Tuffs, a sequence of well-sorted sand to silt beds. These beds were deposited within a submarine environment, likely via density currents. These materials are extremely weak to very weak in strength.

Upon the cessation of volcanic activity in the Pleistocene, abundant fringing coral reef growth occurred around Efaté, unconformably overlying the older volcanic deposits. These reef deposits form the Reef Limestone Formation. Periods of uplift and fluctuating sea levels during glacial and interglacial periods of the Quaternary have resulted in the formation of several coral reef terraces up to 400 m above sea level in Efaté. Large areas of Efaté Island's coastal edge have a capping of coral reefs.

The published geological map presented in Figure 3.1 indicates that Port Vila is underlain by recent raised reef, older raised reef and Efaté Pumice Formation.

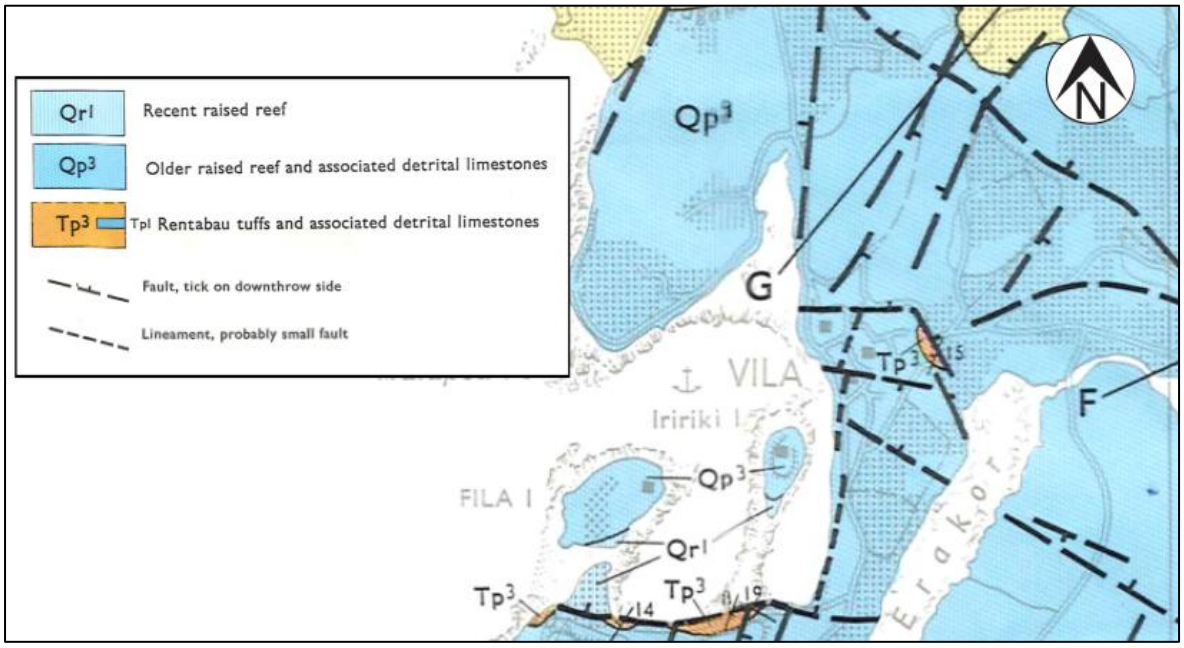

Figure 3.1: Geological setting of Port Vila (Geology of Efaté 1:100,000 New Hebrides Geological Survey Sheet 9).

3.2 Regional tectonic setting

Vanuatu is located in a highly complex and tectonically active region of the South Pacific. The Vanuatu islands extend approximately 1200 km along a north-northwest to south-southeast trend between latitudes 10° and 22° S from the Solomon arc in the north to the Matthew–Hunter Ridge in the south. The tectonic setting for the islands is predominantly governed by the eastward subduction of the Australian Plate beneath the Pacific Plate along the New Hebrides trench (or the Vanuatu subduction zone).

The subduction zone is considered to be strongly segmented, with an estimated convergence rate of ~120 mm/yr towards northern end, 90 to 120 mm/yr along the Efaté islands and towards the

southern end, and significantly lower convergence rate of ~28 to 35 mm/yr in the central portion where the overriding plate collides with the D'Entrecasteaux Ridge (Johnson et al, 2021; Suckale and Grünthal, 2009). These features are illustrated in Figure 3.2 below.

The geometry and kinematics of the subduction system are further complicated by the active back-arc spreading within the North Fiji Basin and the interaction among the several microplates. This complex tectonic setting gives rise to a combination of thrust, strike-slip and extensional faulting regimes across the region.

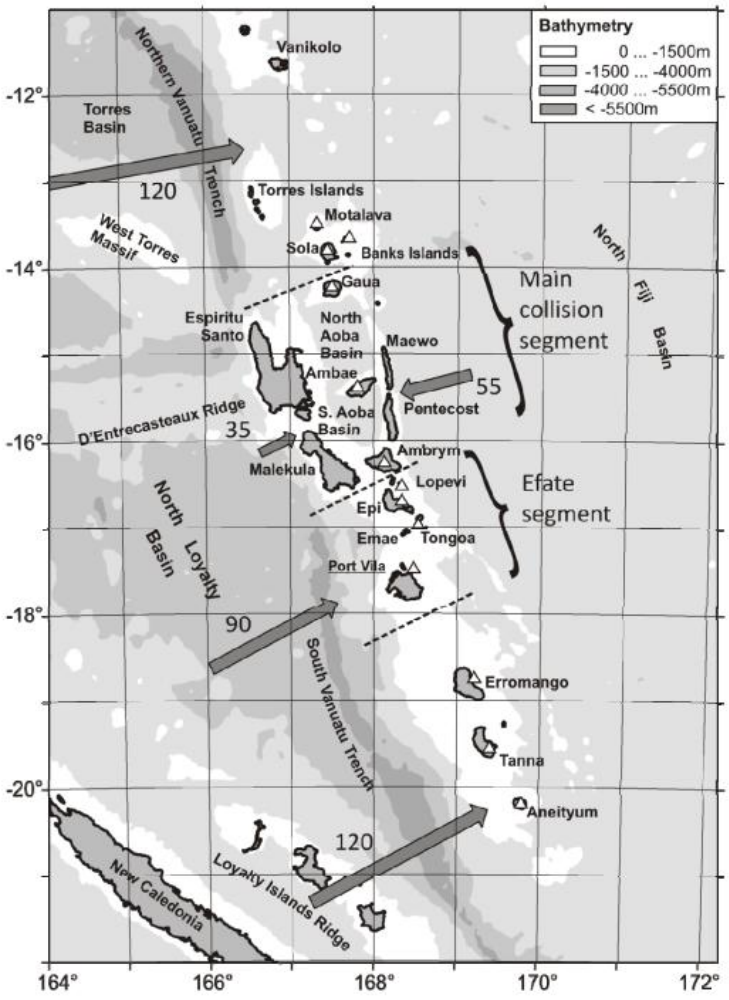

Figure 3.2: Bathymetric map of Vanuatu arc with major islands and important geological features. Figure obtained from Suckale and Grünthal (2009).

3.3 Historical earthquakes

Given the tectonic setting for Vanuatu, large magnitude earthquakes frequently occur in the region, typically along the New Hebrides trench. The recent magnitude 7.3 2024 Port Vila earthquake caused loss of life and extensive damage to land, buildings and infrastructure. The peak ground acceleration in the Port Vila CBD from the event is estimated to be greater than 0.5 g based on reporting of felt intensity.

Between 1907 and 2025, 51 magnitude 7 or higher earthquakes were recorded within the region of interest for this study (typically within 500 km of Port Vila). These events were recorded at a depth of 10 km to 180 km. Figure 3.3 presents the location of these earthquakes relative to Port Vila.

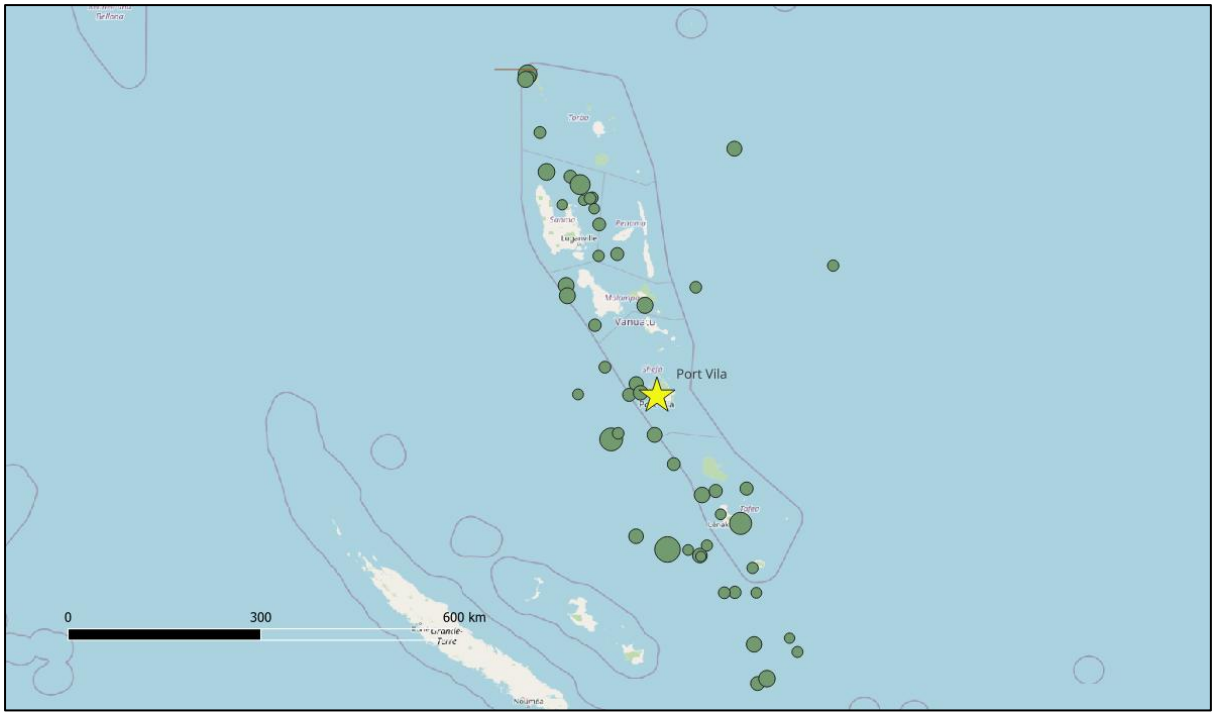

Figure 3.3: Recorded earthquake larger than magnitude 7 within the study region for Port Vila based on earthquake catalogue data compiled. Refer to Section A2 for catalogues considered.

28 of the recorded earthquakes have occurred within 300 km of Port Vila and are summarised in Table 3.1.

Table 3.1: Magnitude 7+ earthquakes within 300 km of Port Vila

Date	Magnitude1	Distance2
1907-10-11	7.1	187
1910-11-9	7.41	214
1910-6-16	7.84	243
1920-9-20	8.09	248
1925-3-22	7.18	113
1927-1-24	7.09	84
1938-5-30	7.03	253
1939-4-5	7.06	253
1944-11-24	7.2	178
1946-1-5	7.07	245
1950-12-2	7.9	99
1953-7-2	7.2	204
1961-7-23	7.33	62
1965-8-13	7.4	228

Date	Magnitude1	Distance2
1972-11-2	7	268
1981-7-15	7.11	93
1990-7-27	7.18	292
1990-8-12	7.03	215
1992-10-11	7.38	174
1994-7-13	7.15	150
1999-11-26	7.42	148
2002-1-2	7.2	43
2007-8-1	7.19	238
2008-4-9	7.31	266
2010-12-25	7.31	229
2010-8-10	7.28	38
2012-2-2	7.04	122
2024-12-17	7.3	25

Note:

1) All earthquake magnitudes are provided in terms of moment magnitude. 2) The distance is measured from Port Vila to the epicentre of the recorded earthquakes. In some cases, the closest distance from Port Vila to the earthquake rupture may be significantly less than the epicentre distance.

4 Seismic site characterisation

4.1 General

Characterising shear wave velocity of the soil and rock underlying a site is an integral component of an SHA. The ground motion models (GMMs) used in this study use V_{s30}, which is the time-averaged shear wave velocity in the upper 30 m of soil and rock at the site, as a proxy for considering the effect of local site conditions on seismic actions.

T+TI engaged Resource Development Consultants Limited (RDCL) to undertake geophysical testing across the study area between 10 February and 6 March 2026 to inform the V_{s30} for this study.

The geophysical testing completed to date comprised:

- Downhole shear wave velocity testing at 6 no. borehole locations;
- Multi-channel analysis of surface waves (MASW) across 5.5 km in length across the study area;
- Seismic refraction tomography across 1 km in length; and
- Horizontal-to-vertical spectral ratio analysis (HVSR) at 12 no. locations.

A site plan showing the location of the above tests and the results are provided in the T+TI (May 2026) Geotechnical Factual Report[1]. A summary of ground conditions across the study area and the V_{s30} values adopted for the study are presented in the sections below.

4.2 Ground conditions

4.2.1 General

The ground conditions across the study area are characterised by four distinct reef terraces. These terrace features are gently tilted towards the south and are located at elevations of approximately -1 to 5 m, 15 to 30 m, 40 to 70 m and 80 to 90 m RL. The terraces are bounded by steep to subvertical north to south trending sea cliffs that are approximately 15 to 20 m high.

The Port Vila CBD area is primarily located on the western fringe of Port Vila on the lowermost terrace bordering the harbour. This area is underlain by predominantly loose to medium dense reclamation fill and intra-reef deposits, comprising coral sands, gravels and cobbles, over reef limestone. The higher terraces are generally underlain by a thin mantle of volcanic ash, residual soils and/ or localised filling overlying very weak to weak reef limestone and extremely weak to very weak siltstone and sandstone (Efaté Pumice Formation).

A schematic geology cross section for the CBD downtown area is shown in Figure 4.1 below. A detailed assessment of ground conditions is provided in the T+TI (June 2026) Geotechnical Assessment Report[2].

[1] T+TI (May 2026). 20260507_EEETA_Port Vila CBD_Geotechnical Factual Report_V01
[2] T+TI (June 2026). EEETA_Port Vila CBD_Geotechnical Assessment Report.

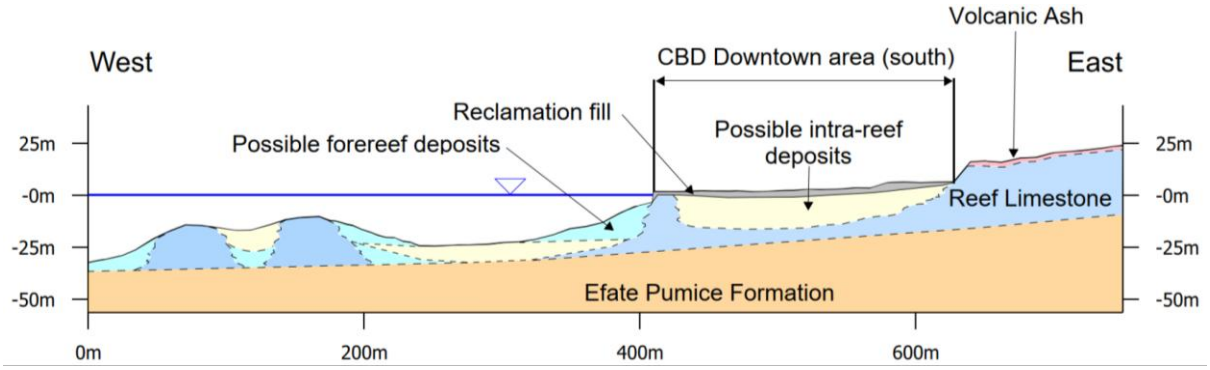

Figure 4.1: Schematic geological cross-section through the CBD Downtown area.

Based on the interpreted geomorphology and ground conditions across the study area, the four assessed ground zones are shown in Figure 4.2. The complete hazard zone maps are provided in Appendix A of the T+TI (June 2026) Geotechnical Assessment Report.

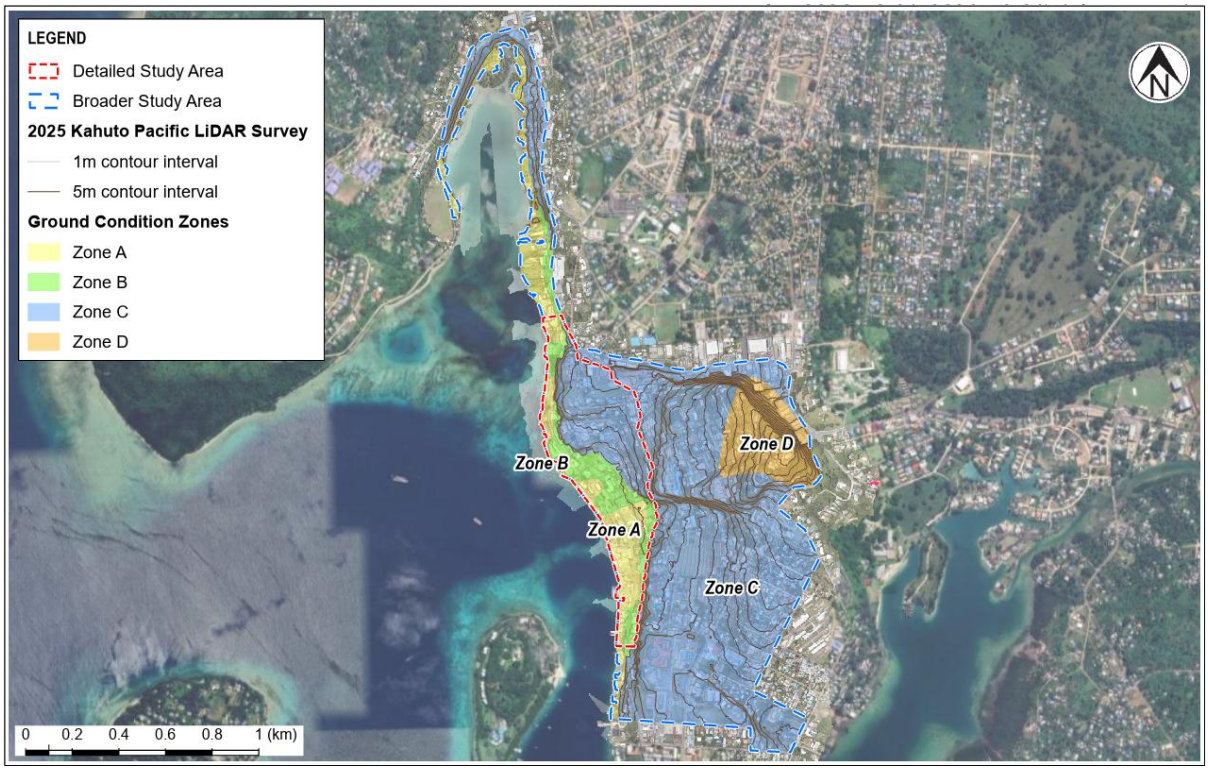

Figure 4.2: Ground zoning for the study area.

For this study, a representative V_{s30} value has been adopted for each zone based on downhole shear wave velocity measurements and MASW testing undertaken within that zone. The ground conditions observed within each zone are discussed further below.

It is important to note that ground zones were defined based on high level ground conditions that are expected within each zone. Ground conditions, and the resulting V_{s30}, are expected to locally vary, and it is important that the V_{s30} at specific sites are confirmed through further testing, particularly for high importance structures that may be sensitive to the adopted V_{s30} value.

The seismic hazard for the adopted V_{s30} values is provided in Section 6 of this report. A discussion of sensitivity to the V_{s30} value at the site is provided in Section 6.3, with recommendations for selecting V_{s30} for specific sites and structures provided in Section 7.1.

4.2.2 Zone A

Zone A is typically underlain by:

- Loose to medium dense sandy gravel (Reclamation Fill), typically to a depth of 2 m to 4 m below ground level, overlying
- Loose to medium dense gravelly sand with some silt (Intra-reef deposits), typically to a depth of 4 m to 15 m below ground level, overlying
- Extremely weak to weak, reef limestone at least to a depth of 30 m.

The geophysical testing in Zone A comprised:

- Three downhole shear wave velocity measurements within BH02, BH03 and BH09 to a depth of 29 m below ground level. Based on measured shear wave arrival times, the assessed V_{s30} ranges from 310 m/s to 430 m/s, with a mean value of 365 m/s.
- MASW lines over a combined length of approximately 1.8 km to generate quasi-2D shear wave velocity profiles. Based on sampling of these profiles, the assessed V_{s30} ranges from 350 m/s to 550 m/s with lower shear wave velocities measured in areas close to the harbour.
- Seven MASW soundings to generate 1D shear wave velocity profile. The assessed V_{s30} ranges from 330 m/s to 420 m/s with a mean value of 374 m/s.

Based on the geophysical testing, a representative V_{s30} of 375 m/s has been adopted for Zone A.

The shear wave velocity profile inferred from downhole testing in Zone A is shown in Figure 4.3. The quasi-2D MASW profile along the waterfront (Line 01), which typically measured the lowest shear wave velocities within the zone, is provided in Figure 4.4.

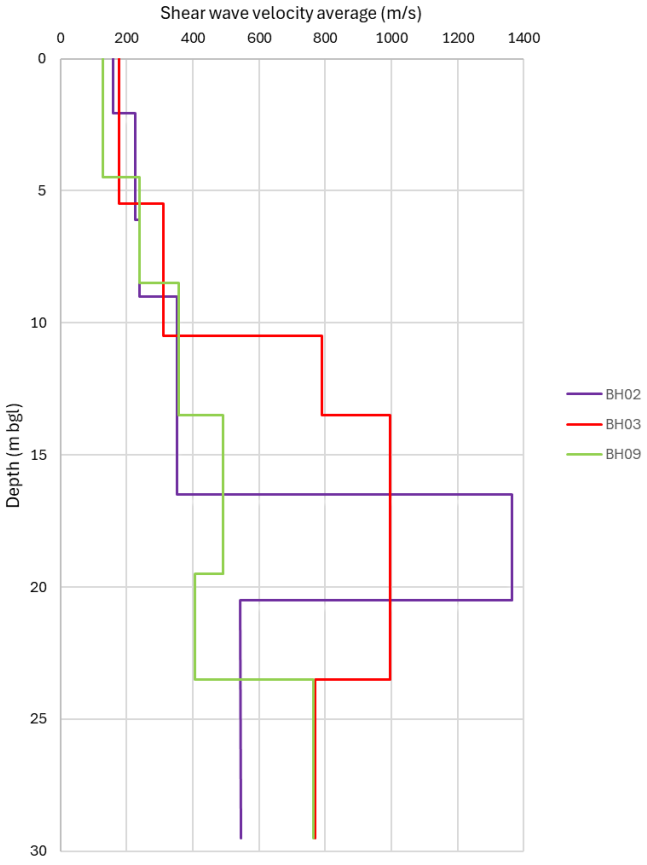

Figure 4.3: Zone A – inferred shear wave velocity profile from downhole testing.

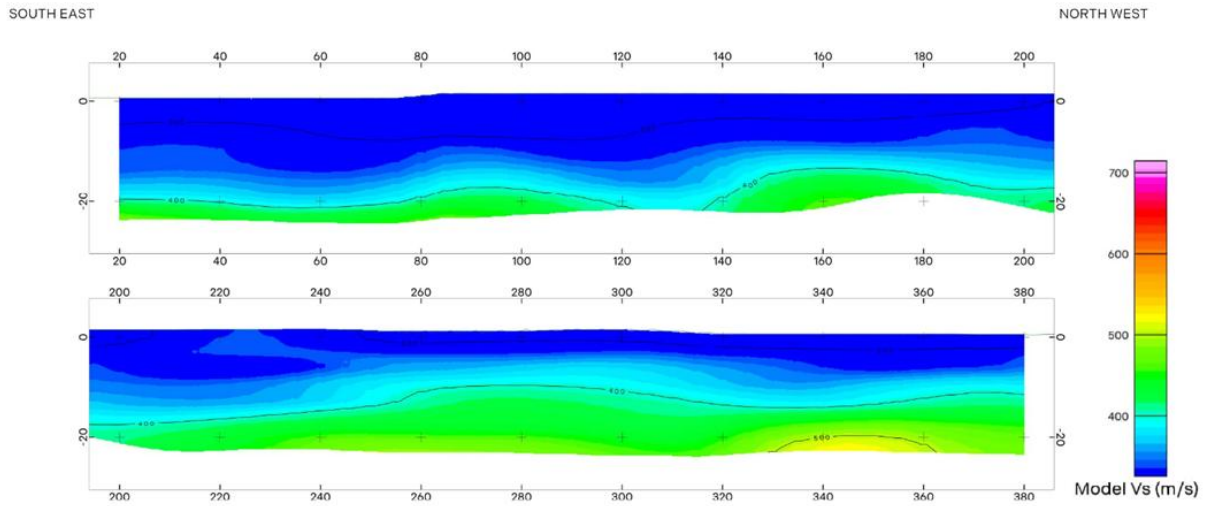

Figure 4.4: Quasi-2D shear wave velocity profile from MASW Line 01 near Zone A waterfront.

4.2.3 Zone B

Zone B is generally at a higher elevation relative to Zone A with reef limestone inferred to be present at shallower depth. The zone is underlain by:

- Loose to dense sandy gravel (Reclamation Fill), typically to a depth of 1 m to 2 m below ground level; overlying
- Loose to medium dense gravelly sand with some silt (Intra-reef deposits), typically to a depth of 2 m to 8 m below ground level; overlying
- Extremely weak to weak, reef limestone at least to a depth of 30 m.

The geophysical testing in Zone B comprised:

- One downhole shear wave velocity measurement within BH07 to a depth of 14.5 m below ground level. Based on measured shear wave arrival times, the V_{s30} is assessed to be 405 m/s.
- MASW lines over a combined length of approximately 700 m to generate quasi-2D shear wave velocity profiles. Based on sampling of these profiles, the assessed V_{s30} ranges from 400 m/s to 600 m/s with a median value of approximately 473 m/s. V_{s30} typically increases with elevation due to the reef limestone unit being encountered at a shallower depth.
- Five MASW soundings to generate 1D shear wave velocity profile. The assessed V_{s30} ranges from 350 m/s to 410 m/s with a mean value of 391 m/s.

Based on the geophysical testing, a V_{s30} of 450 m/s has been adopted for Zone B.

The shear wave velocity profile inferred from downhole testing in Zone B is shown in Figure 4.5. The quasi-2D shear wave velocity profile from MASW Line 03 between chainage 0 and 360 m, which is predominantly within Zone B, is shown in Figure 4.6.

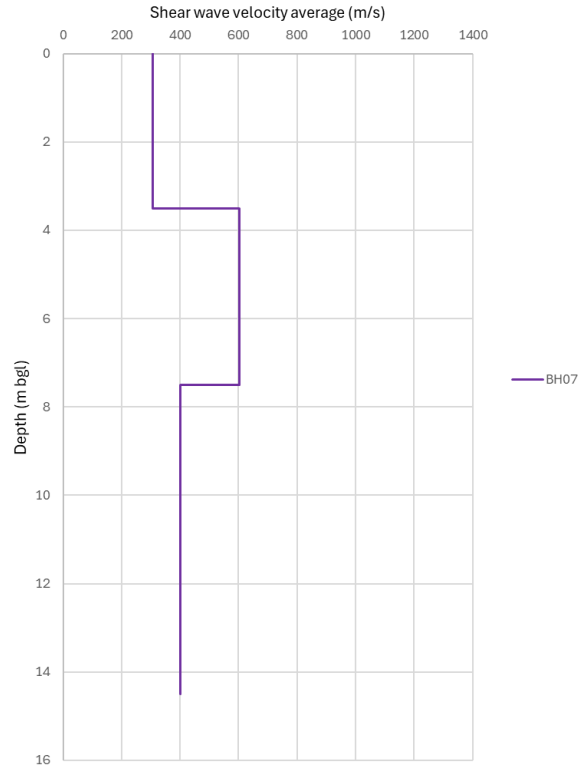

Figure 4.5: Zone B – inferred shear wave velocity profile from downhole testing.

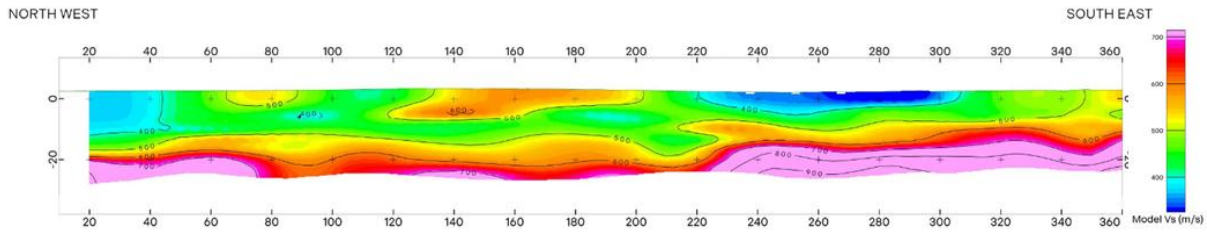

Figure 4.6: Quasi-2D shear wave velocity profile from MASW Line 03.

4.2.4 Zone C

Zone C covers a central raised area across the study area, with a relatively thin mantle of soil. The zone is typically underlain by:

- Localised fill comprising sandy gravel, typically loosely packed, and volcanic ash comprising stiff silt with some clay; overlying
- Extremely weak to weak, reef limestone typically at depths less than 3 m below ground level and extending at least to a depth of 30 m.

The geophysical testing in Zone C comprised:

- One downhole shear wave velocity measurement within BH06 to a depth of 28.5 m below ground level. Based on measured shear wave arrival times, the V_{s30} is assessed to be 785 m/s.
- MASW lines over a combined length of approximately 1.0 km to generate quasi-2D shear wave velocity profiles. The available MASW testing is predominantly along Line 15 towards the

northwestern extent of the study area. Based on sampling of these profiles, the assessed V_{s30} ranges from 450 m/s to 875 m/s, with a median value of approximately 570 m/s.

Based on the geophysical testing, a V_{s30} of 600 m/s has been adopted for Zone C.

The quasi-2D shear wave velocity profile from Line 15 is shown in Figure 4.7, with the measurements between Ch. 160 m and 820 m generally representative of Zone C. The shear wave velocity profile inferred from downhole testing in Zone C is shown in Figure 4.8.

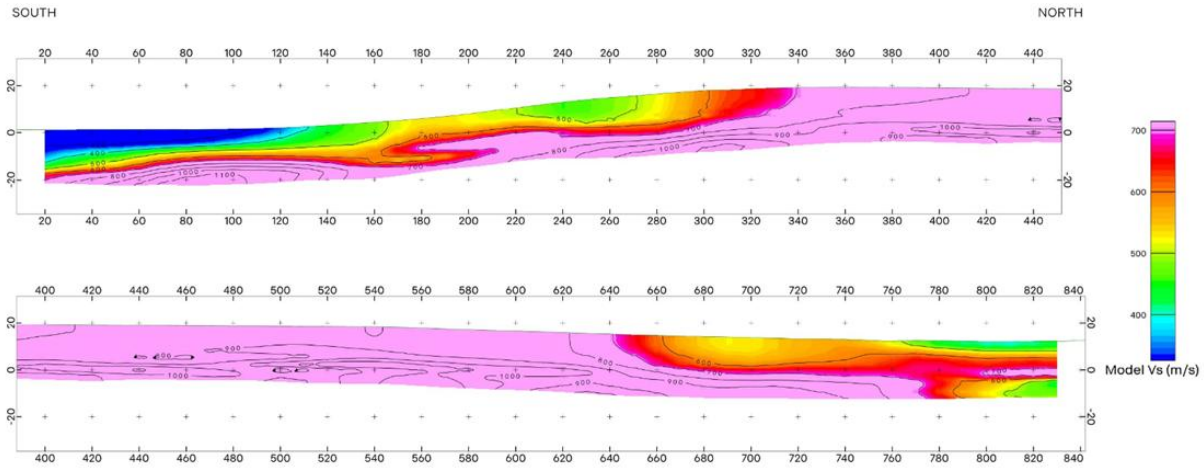

Figure 4.7: Quasi-2D shear wave velocity profile from MASW Line 15.

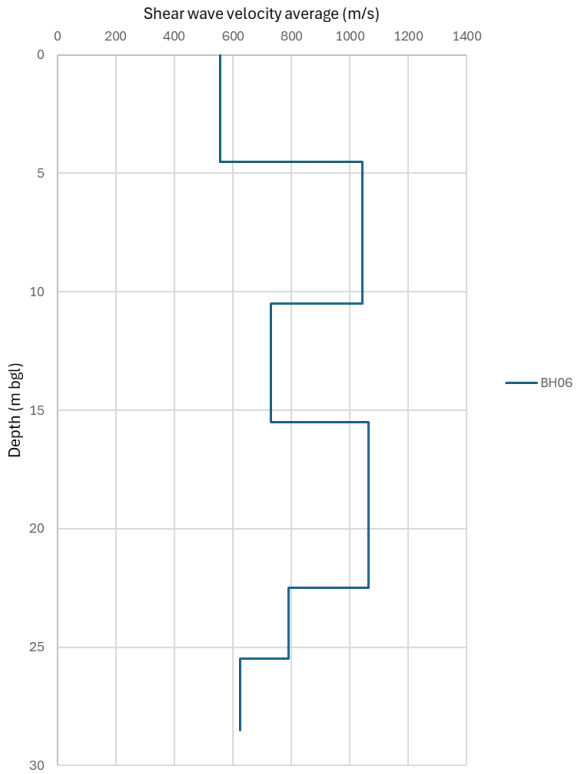

Figure 4.8: Zone C – inferred shear wave velocity profile from downhole testing.

4.2.5 Zone D

Zone D covers an elevated section across the study area, where the Efaté Pumice Formation was typically encountered in the upper 30 m. Investigations undertaken with Zone D indicate a thicker unit of soil (typically comprising more broken coral reef deposit and residual to weathered Efaté Pumice Formation soil), particularly at the boundary between the reef limestone and Efaté Pumice Formation. Hence, the shear wave velocity of the underlying material is expected to be lower than the neighbouring Zone C.

Zone D is typically underlain by:

- Localised fill comprising sandy gravel, typically loosely packed and volcanic ash, comprising stiff silt with some clay; overlying
- Coral gravels, loosely packed, and extremely weak to weak, reef limestone typically at depths less than 3 m below ground level extending to a depth of 5 m to 20 m below ground level; overlying
- Efaté Pumice Formation comprising, residual and completely weathered soils that are typically stiff to very stiff overlying extremely weak to weak pumiceous siltstone and sandstone.

The geophysical testing in Zone D comprised:

- One downhole shear wave velocity measurement within BH12 to a depth of 29.5 m below ground level. Based on measured shear wave arrival times, the V_{s30} is assessed to be 318 m/s.
- MASW lines over a combined length of approximately 270 m to generate quasi-2D shear wave velocity profiles. Based on sampling of these profiles, the assessed V_{s30} ranges from 350 m/s to 600 m/s with a mean value of 440 m/s.

Based on the geophysical testing, a V_{s30} of 450 m/s has been adopted for Zone D.

The quasi-2D shear wave velocity profile from Line 11 is shown in Figure 4.9. The shear wave velocity profile inferred from downhole testing in Zone D is shown in Figure 4.10.

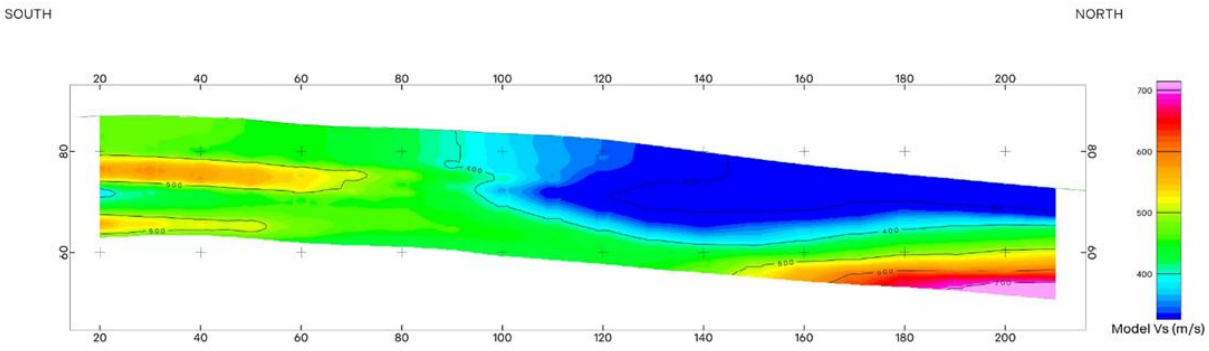

Figure 4.9: Quasi-2D shear wave velocity profile from MASW Line 11.

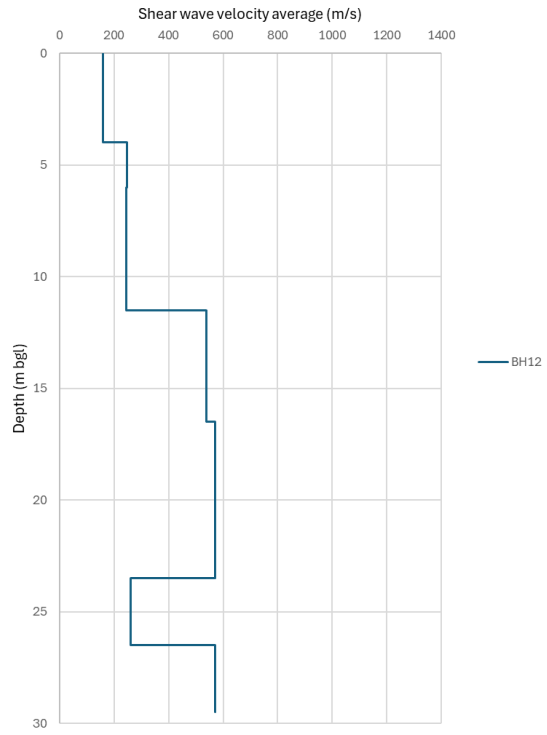

Figure 4.10: Zone D – inferred shear wave velocity profile from downhole testing.

4.3 Summary

The V_{s30} values adopted for this SHA are summarised in Table 4.1. In addition to the representative V_{s30} value for each zone, additional V_{s30} values have been considered to assess sensitivity to small variation in V_{s30} and to provide seismic actions should further investigations be undertaken to refine V_{s30} values at specific locations.

It is important that the results presented in this study are reviewed for any V_{s30} value outside the range presented below.

Table 4.1: Shear wave velocity parameters adopted for this SHA.

Study area/ geological condition	V_{s30} (m/s)
Zone A	375
Zone B	450
Zone C	600
Zone D	450
Typical 'rock' site	760
Additional V_{s30} values to cover typical V_{s30} range within each zone	300 and 500

Although the near surface ground stiffness (e.g. V_{s30}) is generally the most important factor when estimating the local site effects on ground shaking, the ground conditions at depth can also be important, particularly for long period motions. This study uses $Z_{1.0}$ (depth to a V_s of 1000 m/s) and $Z_{2.5}$ (depth to a V_s of 2500 m/s) to characterise the deep ground stiffness at the site. $Z_{1.0}$ and $Z_{2.5}$ values for this study are estimated using correlations with V_{s30} (Boore et al. 2014, Campbell and Bozorgnia 2014).

5 Seismic source characterisation model

5.1 General

The SSC model for the Port Vila CBD SHA has been developed based on historical seismicity using the approach described in Baker et al. (2021) and generally following a similar methodology to that used by Johnson et al (2021) to develop a high-level PSHA for South Pacific Islands. The following scope of work has been undertaken to date in developing the SSC model.

- Developed an earthquake catalogue with homogenised earthquake magnitudes
- Classified the earthquakes based on location of hypocentre to distinguish between subduction interface, subduction slab and crustal earthquakes
- Defined segmentation for the subduction interface and subduction slab sources
- Declustered the catalogue to remove pre- and aftershocks
- Assessed the magnitude completeness for the declustered catalogue
- Assessed fault mechanism and earthquake recurrence parameters
- Prepared SSC model (i.e. fault geometry and mechanism, recurrence rates, relative weighting etc) for input into probabilistic calculations

5.2 Method summary

The detailed methodology used to develop the SSC model is presented in Appendix A and is summarised here at a level appropriate for the main report.

The earthquake catalogue was compiled from three sources: the ISC-GEM Global Instrumental Earthquake Catalogue (1904 to 2021), the ISC Reviewed Bulletin (1900 to 2023), and the ANSS Comprehensive Earthquake Catalog (2023 to 2025). Following catalogue merging and removal of duplicate events, the combined catalogue was clipped to a study region around Port Vila and all magnitudes were homogenised to moment magnitude (M_w). The final declustered catalogue, with completeness constraints applied for recurrence analysis comprises 10,439 events.

Catalogue events were classified into three tectonic regimes – subduction interface, subduction slab, and shallow crustal – using the SLAB2.0 subduction geometry of Hayes et al. (2018) and the CRUST1.0 Moho model (Laske et al., 2013). The subduction interface was modelled as either a single unsegmented source or as three segments (Northern, Central, Southern). The subduction slab was modelled with the same segmentation. Shallow crustal seismicity was assigned to four crustal source zones based on areas of internally similar tectonics and seismicity rates.

Recurrence parameters (Gutenberg-Richter a- and b-values, and maximum magnitudes) were derived for each source using the Weichert (1980) maximum-likelihood method, which accounts for the time-varying completeness thresholds in the catalogue. Adopted parameters for every source and segment are tabulated in Appendix A6.

5.3 SSC model logic tree

The alternative SSC model parameters for segmented vs non-segmented for earthquakes along the subduction zone (i.e. interface and slab earthquakes), distributed vs uniform rate model for crustal earthquake and maximum magnitudes that are 0.3 to 0.5 higher than maximum observed have been considered with a logic tree. The weighting adopted for each alternative model is shown in Figure 5.1.

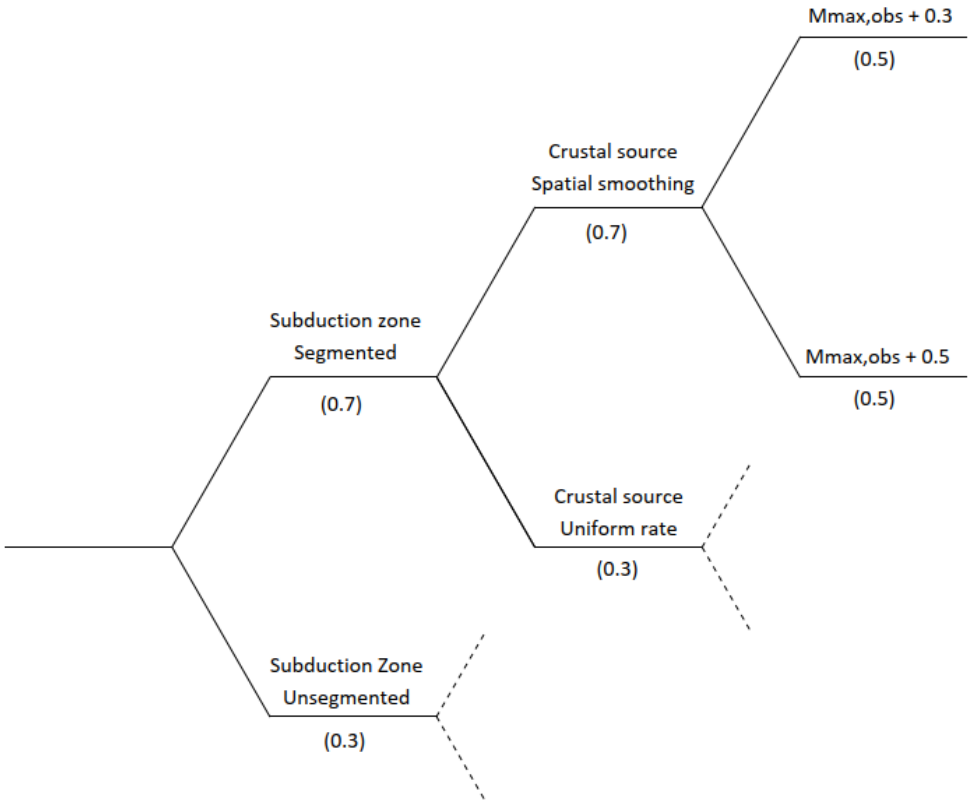

Figure 5.1: Logic tree for the SSC model.

5.4 Ground motion models

Ground motion models (GMMs) used in the SHA are drawn from the NGA-West2 project (Bozorgnia et al., 2014) for shallow crustal seismicity and from the NGA-Sub project (Bozorgnia et al., 2021) for subduction interface and subduction slab seismicity. The adopted GMMs and their weights are listed in Table 5.1.

Aleatory variability in each GMM was truncated at three standard deviations away from the median prediction, consistent with common practise.

The NGA-West2 and NGA-Sub models are currently used to develop the U.S. National Seismic Hazard Maps for the western United States and have a strong precedent of use in international seismic hazard studies for locations that do not have any robust region-specific models. The availability of strong ground motion station data in the study region is limited and would not be enough to provide meaningful statistical analysis of model residuals. Therefore, no further validation of the adopted models is undertaken at this time, and equal weightings have been used for each GMM within each tectonic regime branch, (i.e. 0.25 weighting for each of four GMMs for shallow crustal events, and 0.33 weighting for each of three GMMs for subduction events).

Within-model epistemic uncertainty was represented by three branches per GMM (10th, 50th and 90th percentile of the model's predicted distribution) with weights of 0.30, 0.40 and 0.30 respectively. For the subduction interface and slab GMMs, the distribution is provided directly by the model authors. The uncertainty distribution for the crustal GMMs were taken from Rezaeian et al. (2014).

Table 5.1: Ground motion models and weightings used for this study. Lower, central and upper values correspond to the 10th, 50th and 90th percentile predictions of the mean based on the 'within-model epistemic uncertainty' distributions

ID	GMM	Shallow crustal			Subduction Interface			Subduction intraslab		
		lower	central	upper	lower	central	upper	lower	central	upper
ASK14	Abrahamson et al. (2014)	0.075	0.10	0.075	-	-	-	-	-	-
BSSA14	Boore et al. (2014)	0.075	0.10	0.075	-	-	-	-	-	-
CB14	Campbell and Bozorgnia (2014)	0.075	0.10	0.075	-	-	-	-	-	-
CY14	Chiou and Youngs (2014)	0.075	0.10	0.075	-	-	-	-	-	-
AG20	Abrahamson and Gülerce (2020)	-	-	-	0.10	0.133	0.10	0.10	0.133	0.10
PSBAH20	Parker et al. (2020)	-	-	-	0.10	0.133	0.10	0.10	0.133	0.10
KBCG20	Kuehn et al. (2020)	-	-	-	0.10	0.134	0.10	0.10	0.134	0.10
SUM		**1.0**			**1.0**			**1.0**		

5.5 Logic tree

The full SSC logic tree comprises 8 SSC model branches and 972 GMM logic tree branches, giving a total of 7,776 logic tree combinations. The SSC logic tree structure itself is illustrated in Figure 5.1.

5.6 Near-fault factors

For sites located near a fault directivity effects produce larger long-period ground motions when rupture occurs towards the site of interest and smaller motions when rupture propagates away from the site. Near-fault factors are a tool that can be used to allow for these rupture directivity effects to be considered.

For the study area, the seismic hazard is largely dominated by subduction interface and intraslab earthquakes generally located at a distance of 40 km or more (refer to hazard disaggregation outputs in Appendix C). The contribution from nearby shallow crustal earthquakes is relatively small. Hence, near fault directivity effects are considered to be negligible for the study area and have not been applied to the design actions recommended in this study.

6 Results and discussion

6.1 Hazard curves

A hazard curve presents the probability that a specific ground motion intensity measure will be exceeded in a given time frame. Figure 6.1, Figure 6.2, and Figure 6.3 present hazard curves for PGA, SA(0.5s) and SA(2s) for the representative V_{s30} values adopted for each ground zone.

The figures include 10th and 90th percentile hazard curves, which offer insight into the degree of epistemic uncertainty based on the logic tree discussed in Section 5.5. For instance, 90% of all weighted model combinations predict a hazard curve at or below the 90th percentile value. A narrow range between the 10th and 90th percentile values suggest good agreement among alternative models, while a larger range indicates a correspondingly larger range in predicted values depending on the models used. The weighted mean value represents the best-estimate hazard value.

Site-specific acceleration values presented herein correspond to the 'RotD50' average ground motion orientation definition, which is the 50th percentile (i.e. median) of the SA value obtained by rotating the horizontal ground motion components through all angles.

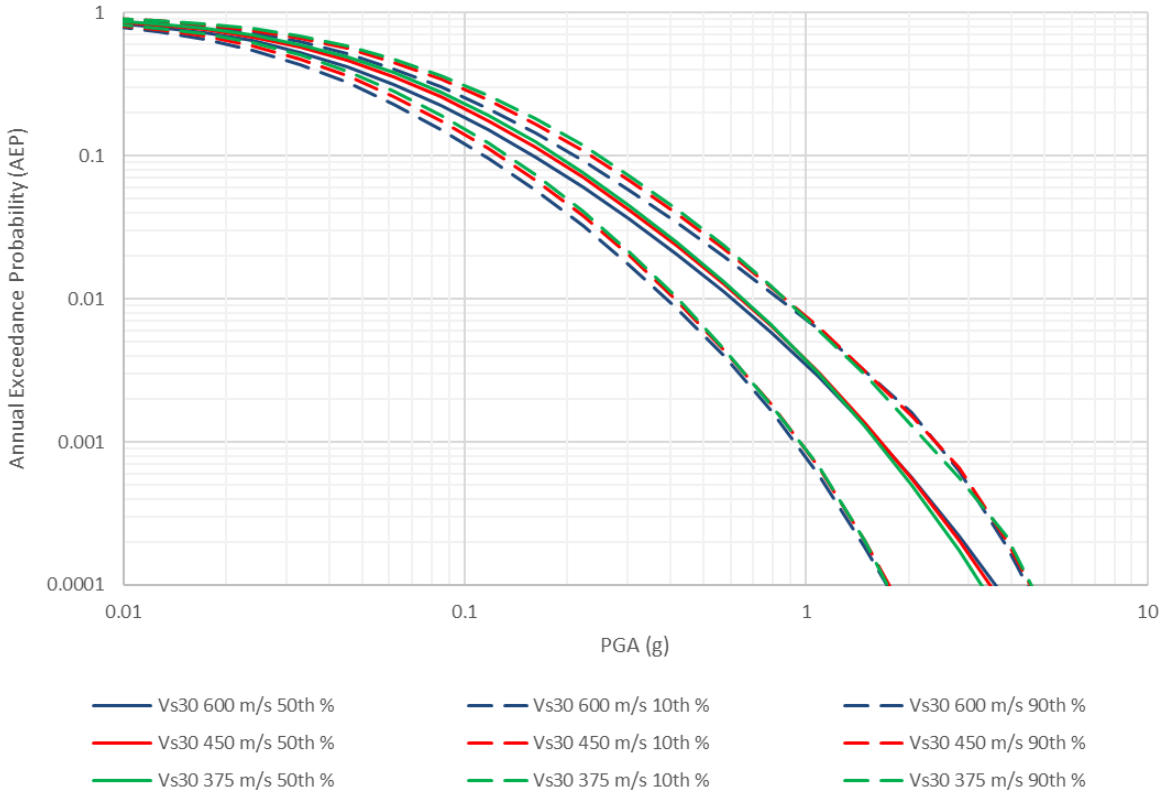

Figure 6.1: Hazard curve for PGA.

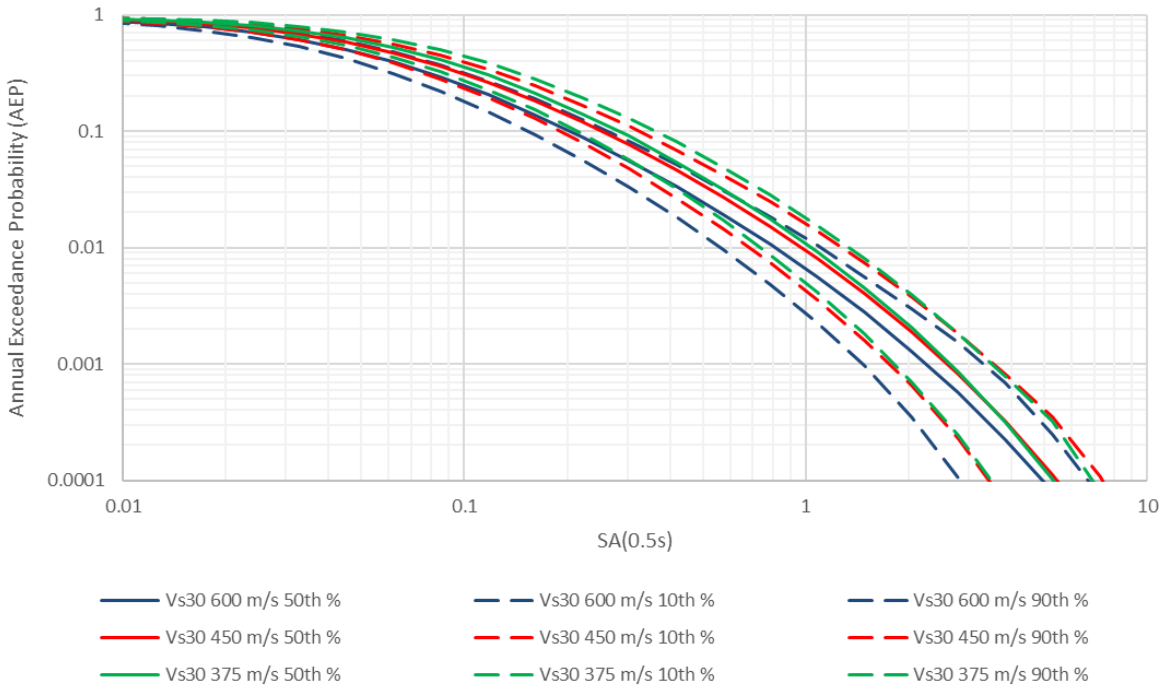

Figure 6.2: Hazard curve for SA(0.5s).

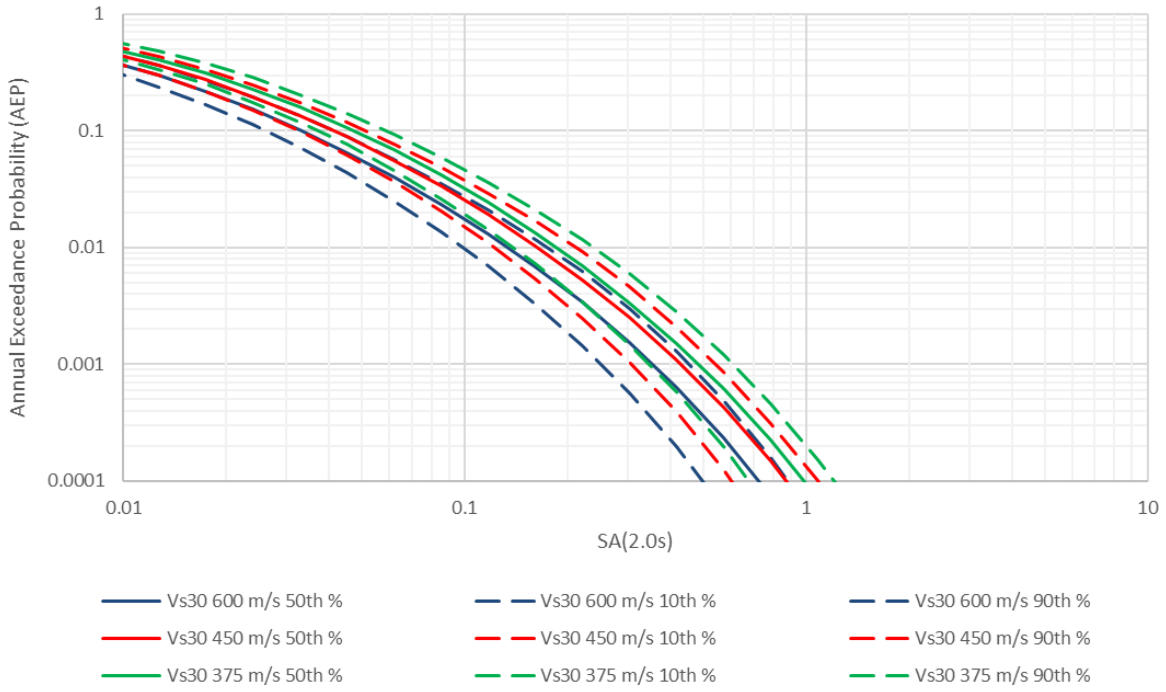

Figure 6.3: Hazard curve for SA(2.0s).

6.2 Uniform hazard spectra

A Uniform Hazard Spectrum (UHS) represents a collection of spectral accelerations at various vibration periods that share the same annual probability of exceedance (or return period).

It is important to note that dominant earthquake sources for a specific spectral period may differ from those at other spectral periods. Therefore, no single earthquake rupture should be expected to produce a ground motion like the UHS over a wide range of vibration periods.

Figure 6.4, Figure 6.5, and Figure 6.6 present 5% damped UHS for 1 in 25, 1 in 100, 1 in 250, 1 in 500, 1 in 1000 and 1 in 2500 AEPs, and for V_{s30} values of 375 m/s, 450 m/s and 600 m/s. Tabulated spectral acceleration values for all of the above AEPs and V_{s30} values of 300 m/s, 375 m/s, 450 m/s, 500 m/s, 600 m/s and 760 m/s are provided in Appendix B. Select 5% damped UHS with 10th and 90th percentile spectra are also provided in Appendix B to show the assessed epistemic uncertainty.

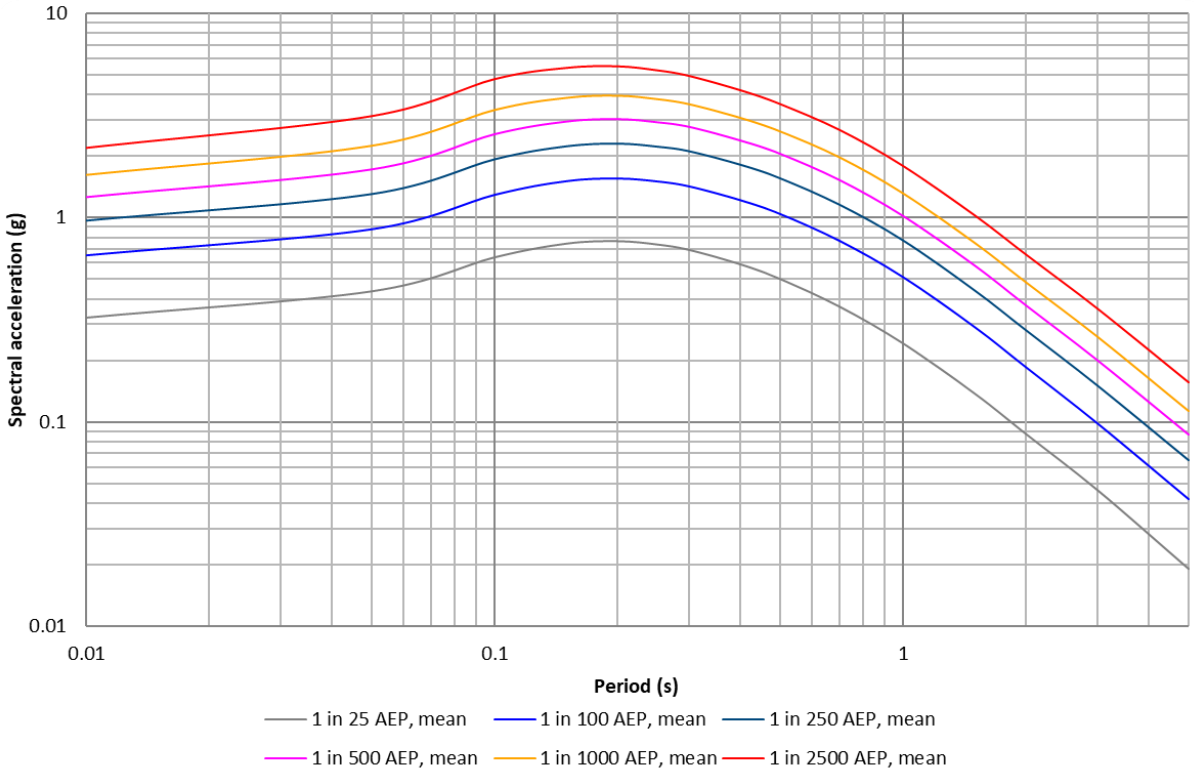

Figure 6.4: 5% damped uniform hazard spectra for V_{s30} of 375 m/s.

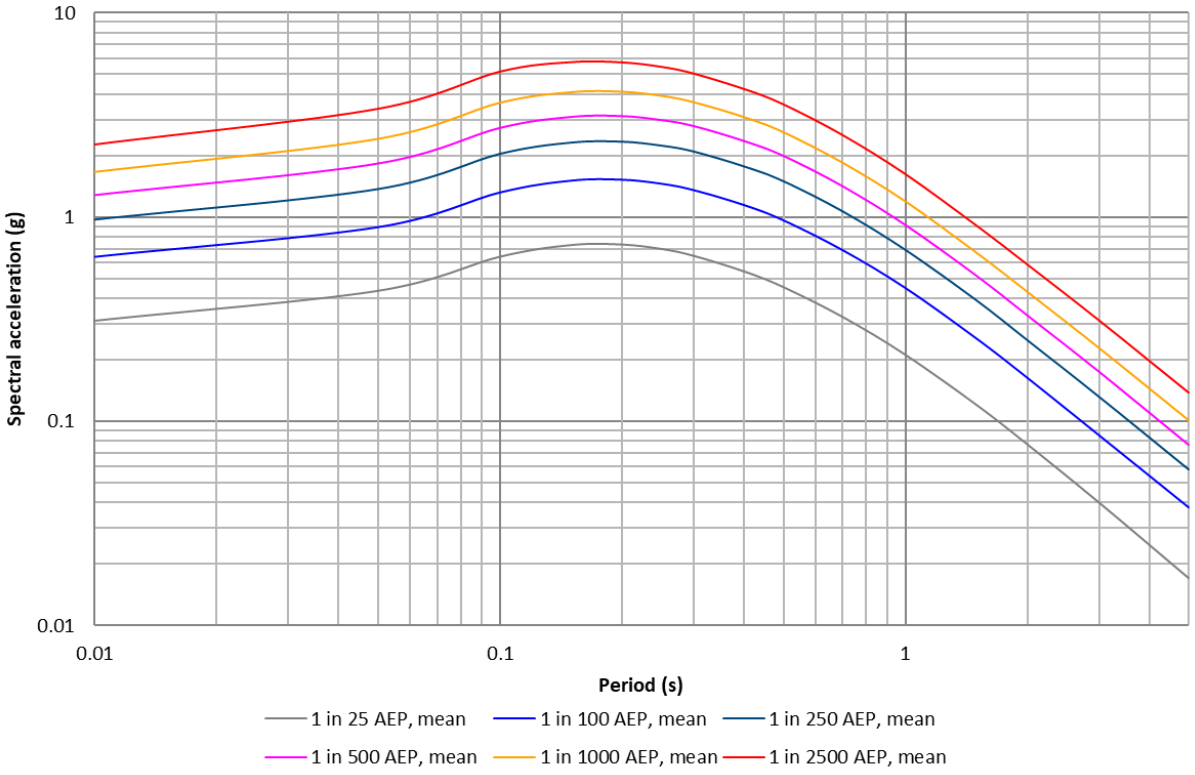

Figure 6.5: 5% damped uniform hazard spectra for V_{s30} of 450 m/s.

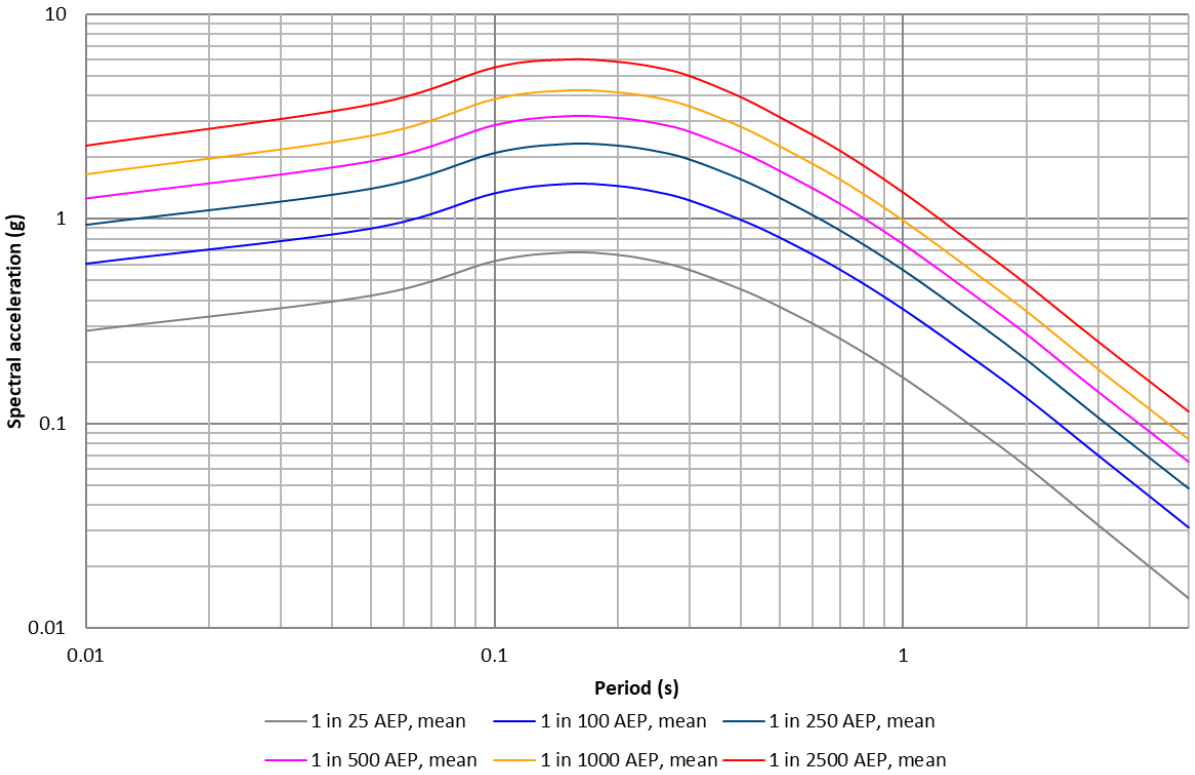

Figure 6.6: 5% damped uniform hazard spectra for V_{s30} of 600 m/s.

6.3 Sensitivity to site V_{s30} value

Figure 6.7, Figure 6.8, and Figure 6.9 present spectral acceleration ratio for 1 in 25, 1 in 500 and 1 in 2500 AEP. The figures show the ratio of spectral accelerations for V_{s30} values of 300 m/s, 400 m/s, 500 m/s and 600 m/s over the spectral acceleration for V_{s30} of 760 m/s.

The intensity of earthquake shaking and the spectral period of interest both have an influence on the degree to which underlying ground conditions influence the seismic actions at ground surface. A discussion of sensitivity to varying the V_{s30} from 300 m/s to 760 m/s is provided in Table 6.1.

Table 6.1: Sensitivity to V_{s30} value

Intensity measure	Sensitivity to site Vs30 value
PGA	• For lower intensity shaking (such as 1 in 25 AEP), PGA over the study area generally increases with decreasing V_{s30} value. • For lower intensity shaking, PGA over the study area for a V_{s30} of 300 m/s is approximately 30% higher than the PGA for a V_{s30} of 760 m/s. • At higher levels of shaking (such as due to a 1 in 500 or 1 in 2500 AEP event), PGA over the study area is relatively insensitive to the V_{s30}. PGA typically varies by ±7% over a V_{s30} range of 300 m/s to 760 m/s.
0.05 s ≤ T < 0.3 s (typical period of interest for short/ stiff structures)	• At low intensity shaking, spectral accelerations at short spectral periods of interest follow a similar trend to PGA as described above. • At higher levels of shaking: – Spectral accelerations at short periods of interest are relatively insensitive over a V_{s30} range of 760 m/s to 400 m/s – Spectral accelerations decrease by up to 25% for a V_{s30} value of 300 m/s relative to a bedrock site. This is likely to be a result of more significant non-linear behaviour induced in the softer soil at high levels of shaking, resulting in more strain within soil and hence more significant damping of high frequency ground motion.
T ≥ 0.3 s (typical periods for medium to tall structures/ flexible structures)	• The spectral accelerations typically increase with decreasing V_{s30} at all levels of shaking. • The seismic hazard at long spectral periods is sensitive to the adopted V_{s30} value. Long spectral periods are likely to be of interest for tall, base-isolated and/or highly flexible structures. • As such, it is generally more important to confirm V_{s30} through additional site-specific testing for structures with a longer period of interest (in particular periods greater than 0.5 seconds).

In practice, spatially averaged ground conditions across the site are expected to influence ground surface motions more strongly than point-specific V_{s30} variations. As such, any further investigations at site-specific locations should consider these values along with broader area-wide data to verify and select an appropriate V_{s30} value for the structure.

For sensitive structures, the variability in the spectral accelerations identified below may be used in structural sensitivity analyses. If such analyses indicate significant differences in performance – particularly for long-period structures on softer ground—additional site-specific geophysical testing may be beneficial to confirm or refine the V_{s30}.

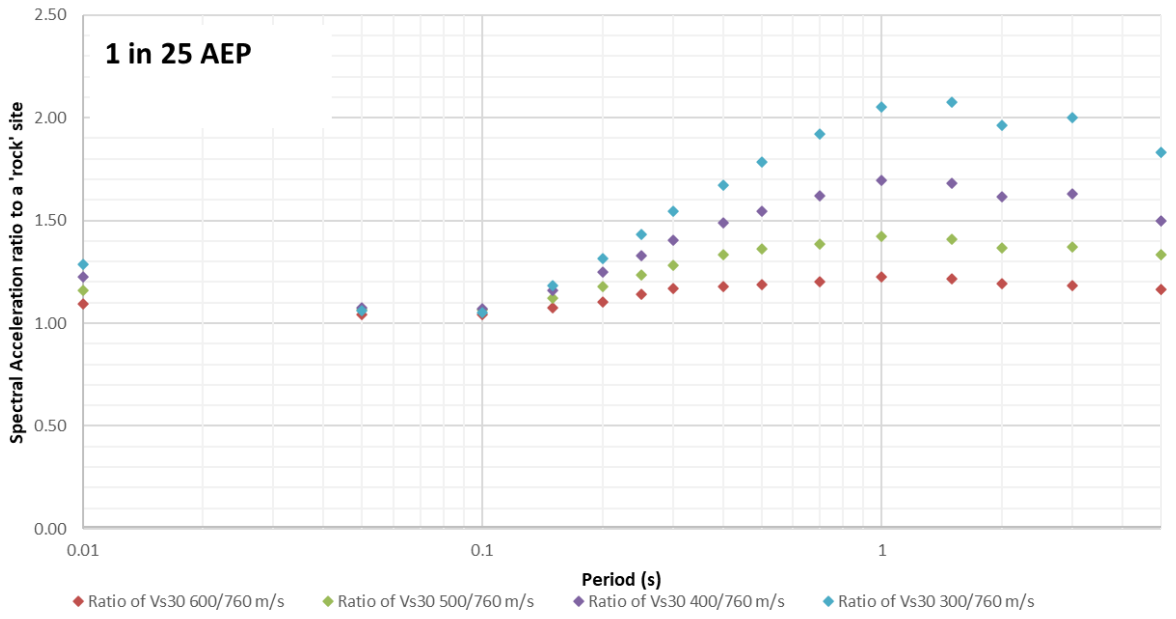

Figure 6.7: Spectral acceleration ratio for 1 in 25 AEP.

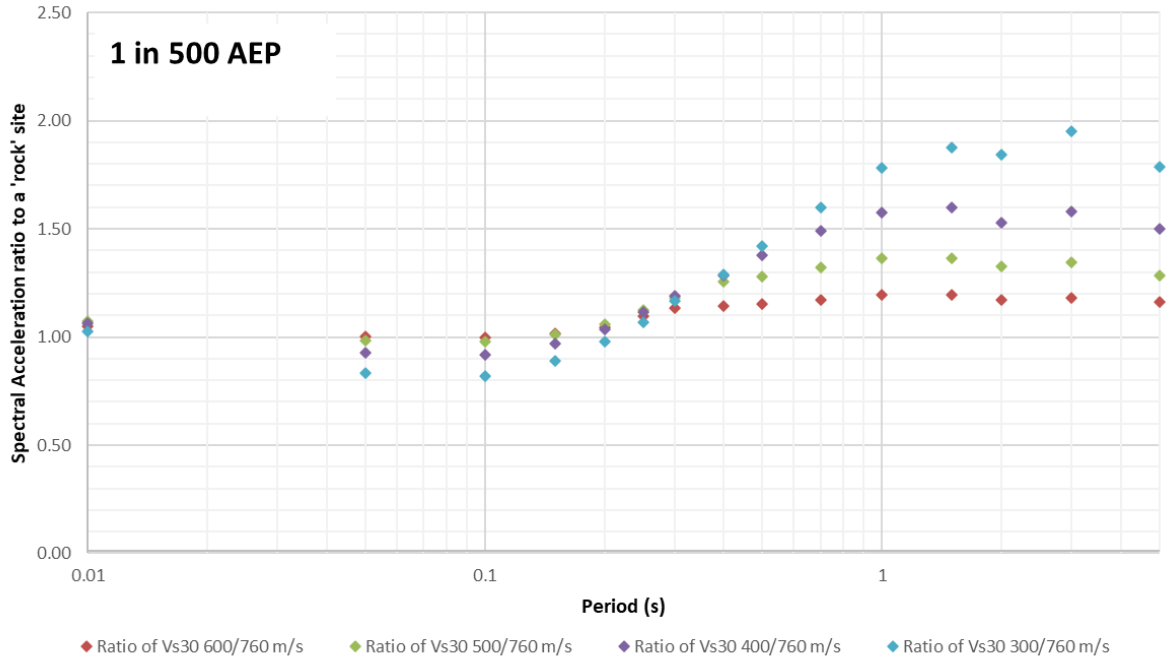

Figure 6.8: Spectral acceleration ratio for 1 in 500 AEP.

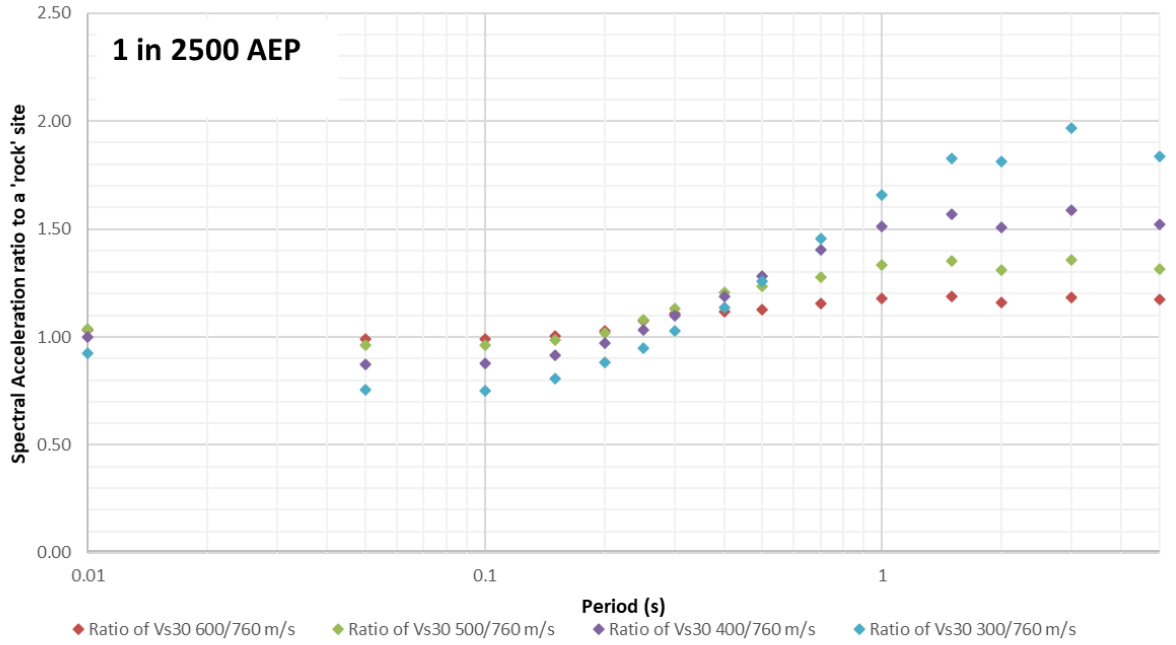

Figure 6.9: Spectral acceleration ratio for 1 in 2500 AEP.

6.4 Comparison with Vanuatu Building Code

The Vanuatu Building Code 2025 Edition was released in December 2025. The codified acceleration response spectra are based on the provisions in NZS1170.5:2004 – New Zealand Standard for Earthquake Actions and hazard factors specific to Vanuatu.

In particular, the Vanuatu Building Code requires:

- A hazard factor of 0.7 to be used with NZS1170.5:2004 for Port Vila,
- Design actions based on a site-specific hazard analysis to be no less than accelerations based on a minimum hazard factor of 0.7;
- For AEPs less than 1 in 250, the near fault factors to be equal to the Nmax(T) as determined from NZS1170.5:2004. Note that near-fault directivity is considered to be negligible for the study area as the hazard is largely dominated by subduction interface and intraslab earthquakes. Further discussion is provided in Section 5.6;
- The maximum hazard is not required to exceed a ZRu value of 1.44, where Z is the hazard factor and Ru is the return period factor. The code also states that a site-specific hazard study may be submitted to seek approval for a lower ZRu value; and
- The code does not appear to cap seismic hazard from seismic hazard assessments to the acceleration response spectra evaluated using the maximum ZRu value.

Figure 6.10 and Figure 6.11 present UHS from this study compared against the acceleration response spectra from the Vanuatu Building Code for 1 in 500, 1 in 2500 AEP, and the maximum hazard acceleration response spectra for V_{s30} values of 760 m/s and 450 m/s respectively.

There is no direct correlation between V_{s30} and the site class system used in NZS1170.5 (and hence adopted by the Vanuatu Building Code). However, Class B is considered to be approximately equivalent to V_{s30} of 760 m/s and Class C is considered to be approximately equivalent to V_{s30} of 450 m/s.

The comparison shows that the seismic actions assessed in this study are generally higher than equivalent seismic actions from the Vanuatu Building Code Edition 2025. The comparison shows:

- The UHS from this study for a 1 in 250 AEP is approximately equivalent to a 1 in 500 AEP code acceleration response spectra for periods less than 0.8 seconds;
- A UHS for a 1 in 1000 AEP from this study is approximately equivalent to a 1 in 2500 AEP code acceleration response spectra for periods less than 0.8 seconds;
- At periods greater than 0.8 seconds the code spectrum is typically greater than the results from this study; and
- The code maximum spectrum typically falls between the UHS spectra for 1 in 1000 and 1 in 2500 AEP from this study.

The seismic hazard assessment used to develop the Vanuatu Building Code 2025 Edition is not publicly available, so the reasons for any differences cannot be further evaluated. An earlier draft of the Vanuatu Building Code, released for public consultation in April 2025, proposed a hazard factor of 1.3 for Port Vila. Although the basis for this value is also unknown, it is generally consistent with the findings of this study.

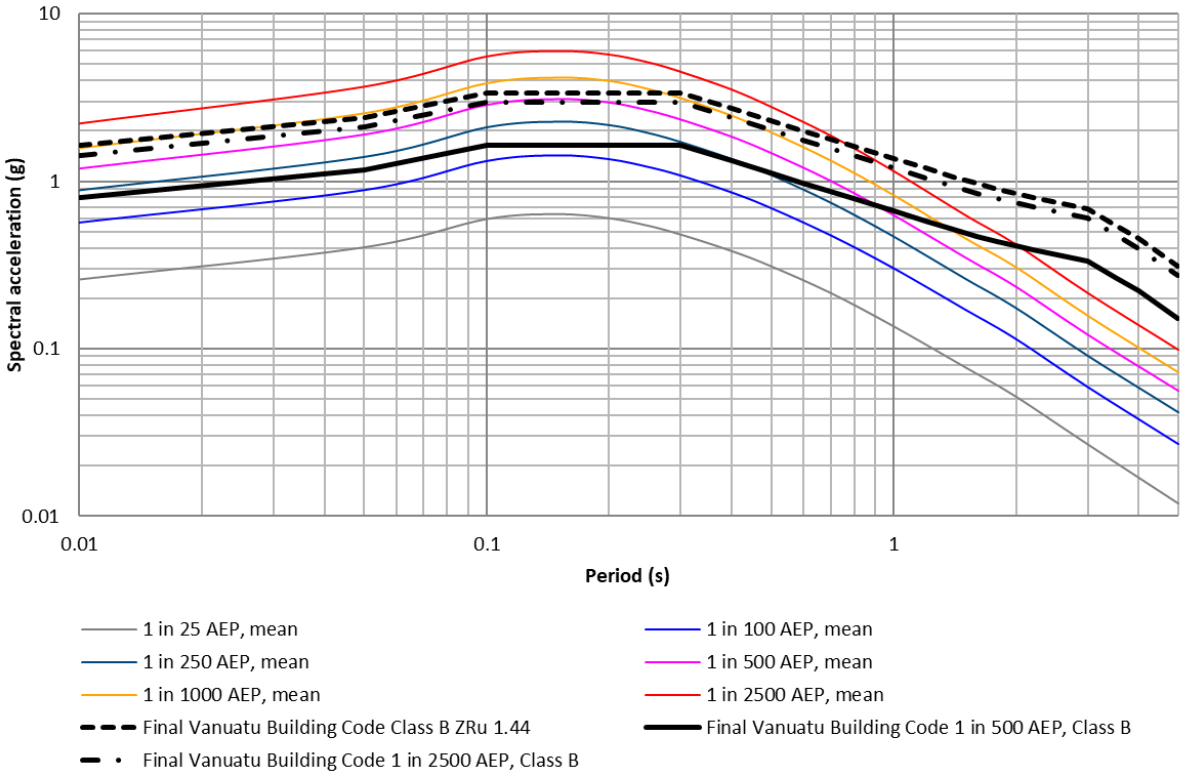

Figure 6.10: UHS from this study for a V_{s30} of 760 m/s compared against the acceleration response spectra from the Vanuatu Building Code 2025 Edition for Class B site.

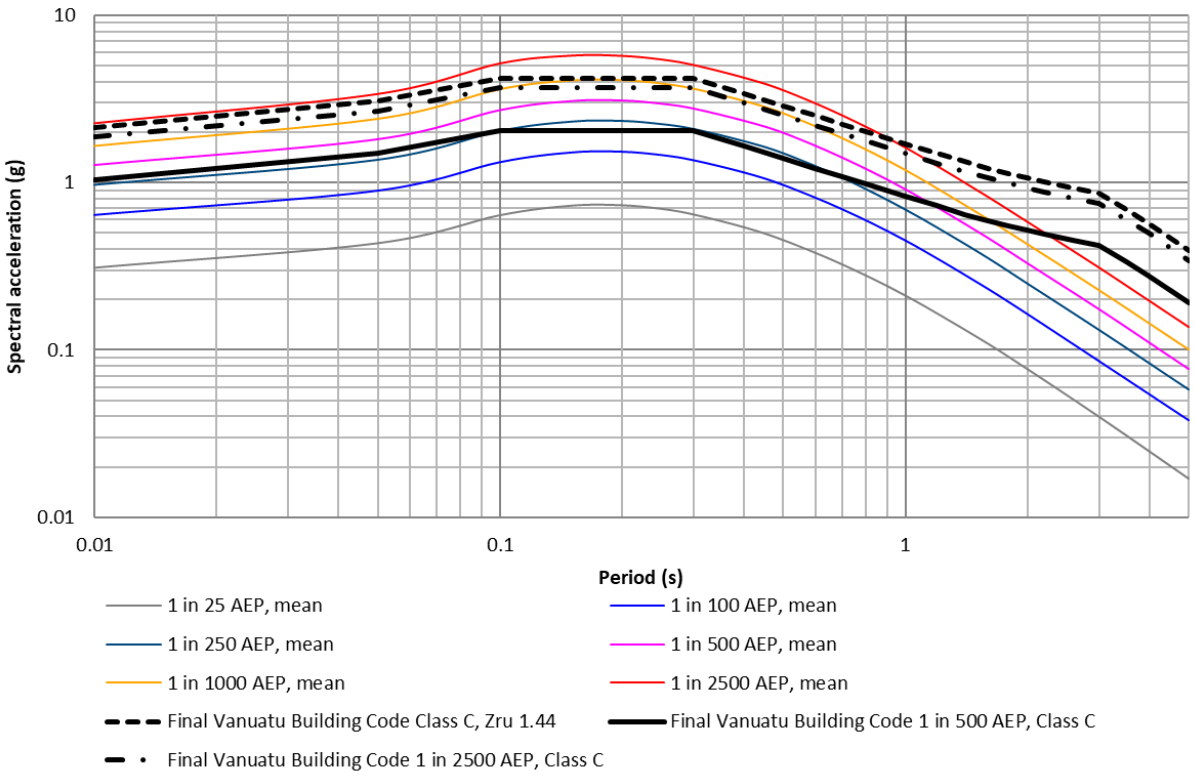

Figure 6.11: UHS from this study for a V_{s30} of 450 m/s compared against the acceleration response spectra from the Vanuatu Building Code 2025 Edition for Class C site.

6.5 Comparison with other studies

There is limited publicly available seismic hazard information for Vanuatu. Table 6.2 compares PGA assessed from this study against publicly available information and other recent seismic hazard information that is known to us.

The comparison shows:

- The assessed seismic hazard from this study is broadly consistent with the PGA reported in the GEM 2023.1 version of the Seismic Hazard Map;
- The seismic hazard from this study is generally higher than slightly older seismic hazard studies;
- As discussed above, the seismic hazard from this study is greater than the seismic actions recommended in the Vanuatu Building Code Edition 2025. However, it is broadly consistent with the earlier hazard included in the draft document for public consultation.

Vanuatu is located in a highly complex and highly seismic region of the South Pacific. There has been limited region-specific research, with seismic hazard assessment generally relying on global models.

There appears to be a trend of increasing assessed seismic hazard in Vanuatu with time. This may be due to:

- Increased quantity of data and in particular number of high-magnitude earthquake events; and
- Release of new state-of-the-art ground motion models such as the NGA Subduction models released in 2021.

Table 6.2: Comparison of the assessed seismic hazard from this study against other published studies

Study	$PGA_{vs30=400}$ (1 in 500 AEP)	$PGA_{vs30=760}$ (1 in 500 AEP)	$PGA_{vs30=760}$ (1 in 2500 AEP)
This study	**1.27 g**	**1.20 g**	**2.22 g**
Global Earthquake Model (GEM) Seismic Hazard Map (version 2023.1 - June 2023) – Johnson et al. (2023)	-	1.20 g	-
Johnson et al. (2021) – Informed the GEM Seismic Hazard Map – 2019.1[1]	-	0.83 g	1.37 g
Beca study for South Paray Wharf (2020)[2]	1.03 g	-	-
Vanuatu Building Code Edition 2025[3] (Hazard Factor 0.7 for Port Vila)	0.93 g	0.7 g	1.26 g
Draft Vanuatu Building Code for consultation (April 2025)[3] (Hazard Factor 1.3 for Port Vila)	1.73 g	1.3 g	2.34 g

Note 1: Considers earthquake catalogue data to 2015.

Note 2: Based on seismic source model developed by GNS Science. Full report not available to review the source model and GMMs adopted.

Note 3: Class C is considered approximately equivalent to V_{s30} 400 m/s and Class B is considered approximately equivalent to V_{s30} 760 m/s for this comparison.

6.6 Hazard disaggregation

The hazard curves and uniform hazard spectra discussed above represent the aggregate seismic hazard from all modelled earthquake sources. However, it is useful to understand the relative contribution from each of the sources. This information can be used for determining appropriate scenario earthquakes for analysis, determining appropriate earthquake magnitudes for geotechnical design and for selecting appropriate earthquake records for time history modelling.

Disaggregation by tectonic region is provided in Appendix C. These disaggregation figures provide:

- The contribution to the seismic hazard for the respective AEP, V_{s30} value and vibration period from each tectonic regime;
- The relative contribution from various magnitude-distance scenarios;
- The mean causal magnitude and distance; and
- The mean epsilon (ε).

The mean causal magnitude and distance for various AEP and V_{s30} values is summarised in Table 6.3 to Table 6.6. The relative contribution from each tectonic regions is summarised in Table 6.7 and Table 6.8.

The hazard disaggregation shows that:

- The mean causal magnitude and distance, and relative contribution from each tectonic region are generally insensitive to V_{s30};
- Interface and intraslab seismic sources along the Vanuatu subduction zone generally control the assessed seismic hazard across the study area. In particular, earthquakes in the subducting

slab that extends beneath Port Vila are the most important sources driving the seismic hazard for the study area; and

- The contribution from subduction sources increases with decreasing AEP. At low AEPs, the relative contribution from active shallow crustal sources is relatively negligible.

Table 6.3: Mean causal magnitude and distance for V_{s30} 375 m/s

AEP	PGA		SA(0.5s)		SA(2s)	
	Magnitude	Distance (km)	Magnitude	Distance (km)	Magnitude	Distance (km)
1 in 25	7.0	74	7.2	80	7.4	87
1 in 100	7.3	66	7.4	69	7.6	68
1 in 250	7.4	62	7.5	63	7.7	58
1 in 500	7.5	60	7.6	60	7.7	53
1 in 1000	7.5	58	7.6	57	7.7	49
1 in 2500	7.6	57	7.7	55	7.8	45

Table 6.4: Mean causal magnitude and distance for V_{s30} 450 m/s

AEP	PGA		SA(0.5s)		SA(2s)	
	Magnitude	Distance (km)	Magnitude	Distance (km)	Magnitude	Distance (km)
1 in 25	7.1	73	7.2	80	7.4	88
1 in 100	7.3	65	7.4	68	7.6	68
1 in 250	7.4	61	7.5	63	7.7	59
1 in 500	7.5	60	7.6	60	7.7	54
1 in 1000	7.6	58	7.6	57	7.8	50
1 in 2500	7.6	57	7.7	55	7.8	46

Table 6.5: Mean causal magnitude and distance for V_{s30} 600 m/s

AEP	PGA		SA(0.5s)		SA(2s)	
	Magnitude	Distance (km)	Magnitude	Distance (km)	Magnitude	Distance (km)
1 in 25	7.1	73	7.2	81	7.4	89
1 in 100	7.3	64	7.4	69	7.6	70
1 in 250	7.5	61	7.5	63	7.7	61
1 in 500	7.5	59	7.6	60	7.8	56
1 in 1000	7.6	58	7.6	58	7.8	52
1 in 2500	7.6	56	7.7	56	7.8	49

Table 6.6: Mean causal magnitude and distance for V_{s30} 760 m/s

AEP	PGA		SA(0.5s)		SA(2s)	
	Magnitude	Distance (km)	Magnitude	Distance (km)	Magnitude	Distance (km)
1 in 25	7.1	72	7.2	81	7.5	90
1 in 100	7.3	64	7.5	69	7.7	71
1 in 250	7.5	61	7.5	63	7.7	62
1 in 500	7.5	59	7.6	60	7.8	57
1 in 1000	7.6	57	7.6	59	7.8	53
1 in 2500	7.6	56	7.7	57	7.9	50

Table 6.7: Relative contribution from each tectonic region for V_{s30} of 375 m/s

AEP	PGA			SA(0.5s)			SA(2s)		
	Crustal	Interface	Intraslab	Crustal	Interface	Intraslab	Crustal	Interface	Intraslab
1 in 25	12%	27%	61%	15%	29%	57%	23%	37%	40%
1 in 100	7%	26%	67%	11%	26%	63%	20%	38%	42%
1 in 250	5%	23%	71%	10%	24%	67%	20%	37%	43%
1 in 500	4%	21%	75%	9%	21%	70%	21%	35%	43%
1 in 1000	3%	18%	78%	8%	19%	73%	23%	33%	44%
1 in 2500	2%	14%	83%	8%	15%	77%	26%	30%	44%

Table 6.8: Relative contribution from each tectonic region for V_{s30} of 760 m/s

AEP	PGA			SA(0.5s)			SA(2s)		
	Crustal	Interface	Intraslab	Crustal	Interface	Intraslab	Crustal	Interface	Intraslab
1 in 25	12%	27%	61%	11%	30%	60%	15%	40%	45%
1 in 100	7%	24%	69%	7%	26%	67%	12%	41%	47%
1 in 250	5%	21%	74%	6%	22%	72%	12%	40%	49%
1 in 500	4%	18%	78%	5%	18%	77%	12%	38%	50%
1 in 1000	3%	15%	82%	4%	15%	81%	12%	36%	52%
1 in 2500	2%	11%	88%	3%	10%	87%	13%	33%	54%

7 Recommendations

7.1 V_{s30}

Representative V_{s30} values were assessed for each of the ground zones as discussed in Section 4. PGA and earthquake magnitude (M_w), and 5% damped uniform hazard spectra are provided for these V_{s30} values and three additional values. Sensitivity to the site V_{s30} was discussed in Section 6.3.

It is important to note that while a representative mean V_{s30} value has been assessed for each ground zone, it is expected that V_{s30} will vary within each zone. As such it is recommended that:

- For high importance structures or structures that are likely to be sensitive to the adopted V_{s30} value (such as tall or flexible structures), site-specific investigations are undertaken to confirm the V_{s30} value at the specific location. These site-specific investigations should be considered along with area wide investigations to select an appropriate V_{s30} value for the structure.
- For lower importance structures or lightweight or short, stiff structures, design actions based on the representative V_{s30} value for each ground zone may be adopted. For PGA and spectral accelerations at periods less than 0.3 seconds, the design actions are expected to vary by up to 10% based on the site V_{s30} value.
- If the V_{s30} value at a site is assessed to be greater than 760 m/s, it is recommended that the design actions for a V_{s30} value of 760 m/s is adopted.
- If the V_{s30} value at a site is assessed to be less than 300 m/s, this is outside the V_{s30} range considered in this study based on measurements completed to date. T+TI should be informed to verify the applicability of this study.

7.2 Uniform hazard spectra

Tabulated spectral accelerations for 5% critical damping are provided in Appendix B. The values provided are for the 'RotD50' average ground motion orientation definition. Near-fault directivity effects are considered to be negligible for the study area and have not been applied to the recommended design actions.

7.3 Ground motion parameters for geotechnical design

Table 7.1 presents ground motion parameters for geotechnical design such as geotechnical stability analyses, liquefaction assessment, retention design etc.

Table 7.1: Ground motion parameters for geotechnical design.

Return period	PGA (g)						Earthquake magnitude
	V_{s30} 300 m/s	V_{s30} 375 m/s	V_{s30} 450 m/s	V_{s30} 500 m/s	V_{s30} 600 m/s	V_{s30} 760 m/s	
1 in 25 AEP	0.34	0.32	0.31	0.3	0.28	0.26	7.1
1 in 100 AEP	0.65	0.65	0.64	0.63	0.61	0.57	7.3
1 in 250 AEP	0.95	0.97	0.97	0.96	0.93	0.88	7.5
1 in 500 AEP	1.23	1.26	1.28	1.28	1.26	1.2	7.5
1 in 1000 AEP	1.55	1.62	1.66	1.67	1.65	1.58	7.6
1 in 2500 AEP	2.06	2.18	2.27	2.31	2.3	2.22	7.6

7.4 Setting within the Vanuatu Building Code framework

The Vanuatu Building Code 2025 Edition sets the minimum requirements for construction and design to protect public safety, health and welfare. A comparison of outcomes from this SHA has been compared to the seismic hazard set out in the Code and is provided in Section 6.4.

Generally, the seismic hazard from this study is greater than minimum provisions in the Code up to a building period of 0.8 second. At building periods greater than 0.8 seconds, the assessed seismic hazard from this study is typically less than the minimum Code provisions.

The results from this study may be used to justify a departure from the Vanuatu Building Code, as long as the minimum provisions in the Code are adhered to, namely:

- The earthquake actions used from this SHA are not less than the hazard developed using a minimum Hazard Factor (Z_{min}) of 0.7.
- The SHA may be used to seek approval to reduce the limiting ZR_u to less than 1.44 where appropriate.

The seismic hazard that is used for design should be confirmed on a project-by-project basis based on the nature of the project and performance expectations.

This SHA presents the assessed seismic hazard based on currently available information for the region. This report does not provide performance level requirements for structures (i.e. what annual exceedance probability structures are designed for) or guidance for designing to the assessed seismic actions.

The design should use appropriate local and international standards and guidelines (such as the proposed geotechnical guidance for Port Vila prepared by T+TI) to select suitable design methodologies to accommodate the assessed seismic hazard.

8 Further study

This assessment is based on:

- Site specific ground conditions;
- Earthquake catalogue that is specific to the region of interest (i.e. approximately 500 km radius of Port Vila);
- A 3D subduction geometry model for Vanuatu but developed as part of a global study; and
- Global ground motion models and magnitude scaling relationships.

Developing models that are tailored to the South Pacific is a significant undertaking that is outside the scope of this study. However, there may be benefit in exploring the areas below to further refine the seismic hazard for Port Vila and Vanuatu.

- Ground motion stations or strong-motion network in Port Vila to collect region specific information. This can be used to provide greater weighting to ground motion models that fit ground motion data in Vanuatu and/ or tailor ground motions models for use in the South Pacific.
- Technical advisory group or expert peer review for independent review and expert elicitation.
- Refinement of the 3D subduction model for Vanuatu (such as slab thickness and variability in the inclination of the subducting slab) as more seismicity information becomes available for the region. More robust consideration of uncertainties in the geometry of the subduction zone. This is likely to require a larger and higher quality database of seismicity.
- Periodic review on release of revised ground motion models or earthquake catalogues. The hazard estimates presented in this report reflect the NGA-West2 and NGA-Subduction ground motion models and the seismicity catalogue available as at the date of issue. Periodic review (recommended at intervals of no greater than five years, or sooner following a significant local earthquake) is recommended to capture the impact of revised models, expanded catalogues, or improved tectonic understanding on the recommended seismic hazard values.

9 References

Abrahamson, N. A. et al. (2013). Update of the AS08 Ground-Motion Prediction Equations Based on the NGA-West2 Data Set. PEER Report 2013/04. Pacific Earthquake Engineering Research Center Headquarters, University of California, Berkeley.

Abrahamson and Gülerce (2020). Regionalized ground-motion models for subduction earthquakes based on the NGA-SUB database. PEER Report 2020/25. Berkeley, CA: Pacific Earthquake Engineering Research Center, University of California, Berkeley.

Boore, D. M. et al. (2013). NGA-West2 Equations for Prediction Response Spectral Accelerations for Shallow Crustal Earthquakes. PEER Report 2013/05. Pacific Earthquake Engineering Research Center Headquarters, University of California, Berkeley.

Bozorgnia et al. (2014). NGA-West2 Research Project. Earthquake Spectra. 30(3): 973-987.

Bozorgnia et al. (2021). NGA-Subduction research program. Earthquake Spectra, 38(2).

Baker, J., Bradley, B., & Stafford, P. (2021). Seismic hazard and risk analysis. Cambridge University Press.

Campbell, K. W. & Bozorgnia, Y. (2013). NGA-West2 Campbell-Bozorgnia Ground motion model for the horizontal components of PGA, PGV and 5% damped elastic Pseudo-Acceleration Response Spectra for Periods Ranging from 0.01 to 10s. PEER Report 2013/06. Pacific Earthquake Engineering Research Center Headquarters, University of California, Berkeley.

Chiou, B. S. J. & Youngs, R. R. (2013). Update of the Chiou and Youngs NGA Ground Motion Model for Average Horizontal Component of Peak Ground Motion and Response Spectra. PEER Report 2013/07. Pacific Earthquake Engineering Research Center Headquarters, University of California, Berkeley.

Christophersen, A., Litchfield, N., Berryman, K., Thomas, R., Basili, R., Wallace, L., ... & Yeats, R. (2015). Development of the Global Earthquake Model's neotectonic fault database. Natural Hazards, 79(1), 111-135.

Di Giacomo et al. (2015). ISC-GEM: Global Instrumental Earthquake Catalogue (1900–2009), III. Re computed MS and mb, proxy MW, final magnitude composition and completeness assessment Phys. Earth planet. Inter. 239 33 47

Gardner & Knopoff (1974). Is the sequence of earthquakes in Southern California, with aftershocks removed, Poissonian? Bulletin of the Seismological Society of America, 64(5).

Hayes et al. (2018). Slab2, a comprehensive subduction zone geometry model. Science, 362(6410).

International Seismological Centre (2025a). ISC-GEM Earthquake Catalogue, https://doi.org/10.31905/d808b825

International Seismological Centre (2025b). On-line Bulletin, https://doi.org/10.31905/D808B830

J. Lecolle & M. Bernat (1985), "Late Quaternary surrection history of Efaté Island, New Hebrides Island arc (Vanuatu)

Johnson, K. L., Pagani, M., & Styron, R. H. (2021). PSHA of the southern Pacific Islands. Geophysical Journal International, 224(3), 2149-2172.

Johnson et al. (2023). Global Earthquake Model (GEM) Seismic Hazard Map (version 2023.1 - June 2023), DOI: https://doi.org/10.5281/zenodo.8409647

Kuehn et al. (2020). Partially non-ergodic ground-motion model for subduction regions using NGA-Subduction database. PEER Report 2020/04. Berkeley, CA: Pacific Earthquake Engineering Research Center, University of California, Berkeley.

Laske et al. (2013). Update on CRUST1.0 - A 1-degree Global Model of Earth's Crust, Geophys. Res. Abstracts, 15, Abstract EGU2013-2658, 2013.

Pagani et al. (2014). OpenQuake Engine: An Open Hazard (and Risk) Software for the Global Earthquake Model. Seismological Research Letters, 85(3): 692-702.

Pagani et al. (2018). Global Earthquake Model (GEM) Seismic Hazard Map (version 2018.1 – December 2018), DOI: 10.13117/GEM-GLOBAL-SEISMIC-HAZARD-MAP-2018.1

Pagani et al. (2020). Modelling subduction sources for probabilistic seismic hazard analysis, Geol. Soc. Lond. Spec.Publ., 501, doi:10.1144/SP501-2019-120.

Parker et al. (2020). NGA-Subduction global ground-motion models with regional adjustment factors. PEER Report 2020/03. Berkeley, CA: Pacific Earthquake Engineering Research Center, University of California, Berkeley.

Rezaeian et al. (2014). Implementation of NGA-West2 ground motion models in the 2014 U.S. National Seismic Hazard Maps. Earthquake Spectra 30: 1319–1333.

Roas, A. M., & McPhie, J. (2003). The submarine record of a large-scale explosive eruption in the Vanuatu Arc: ~ 1 Ma Efaté Pumice Formation. Explosive Subaqueous Volcanism, Geophysical Monograph 140, 273-283. American Geophysical Union.

Stiphout et al. (2012). Seismicity declustering, Community Online Resource for Statistical Seismicity Analysis, doi:10.5078/corssa-52382934.

Suckale, J., & Grünthal, G. (2009). Probabilistic seismic hazard model for Vanuatu. Bulletin of the Seismological Society of America, 99(4), 2108-2126.

Thingbaijam et al. (2017). New Empirical Earthquake Source-scaling Laws. Bulletin of the Seismological Society of America, 107(5).

U.S. Geological Survey, Earthquakes Hazard Program (2017). Advanced National Seismic System (ANSS) Comprehensive Catalog of Earthquake Events and Products: Various, https://doi.org/10.5066/F7MS3QZH.

Uhrhammer (1986). Characteristics of northern and southern California seismicity. Earthquake Notes 57, p. 21

Weatherill et al. (2016). Exploring earthquake databases for the creation of magnitude-homogeneous catalogues: tools for application on a regional and global scale. Geophysical Journal International, 206.

Weichert (1980). Estimation of the earthquake recurrence parameters for unequal observation periods for different magnitude. Bulletin of the Seismological Society of America, 70(4).

Wells, D. L., & Coppersmith, K. J. (1994). New empirical relationships among magnitude, rupture length, rupture width, rupture area, and surface displacement. Bulletin of the seismological Society of America, 84(4), 974-1002.

10 Applicability

This report has been prepared for the exclusive use of our client Egis NZ Limited, with respect to the particular brief given to us and it may not be relied upon in other contexts or for any other purpose, or by any person other than our client, without our prior written agreement.

Earthquake hazard science is a constantly evolving field. Accordingly, it is possible that the results of future research may indicate a seismic hazard that is lower or higher than the hazard estimated by this SHA.

The ground motion parameters provided here are for free-field ground conditions and do not consider possible topographic amplification effects. The possibility and applicability of additional amplification factors should be considered on a case-by-case basis depending on the failure mechanism and analysis method being considered.

Tonkin & Taylor International Ltd
Environmental and Engineering Consultants

Report prepared by:



Ananth Balachandra
Principal Geotechnical Engineer

Report prepared by:

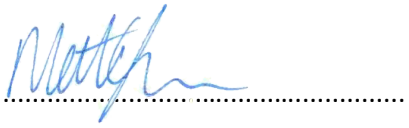

Matt Ogden
Senior Data Scientist

Report reviewed by:

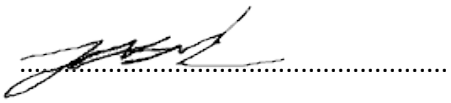

Jason Lim
Principal Geotechnical Engineer

Authorised for Tonkin & Taylor International Ltd by:

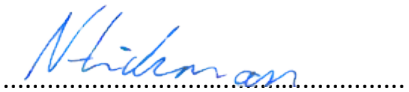

Nathan Hickman
Project Director

\\ttgroup.local\corporate\christchurch\tt projects\1097984\1097984.1000\issueddocuments\20260615_eeeta_port vila cbd_seismic hazard assessment_v02.docx

Appendix A Seismic source characterisation methodology

A1 General

This appendix presents the detailed methodology for the seismic source characterisation (SSC) model summarised in Section 5 of the main report. It covers the earthquake catalogue, classification of events by tectonic regime, declustering, magnitude completeness analysis, earthquake recurrence parameters and seismic source logic tree implemented for probabilistic calculations.

A2 Earthquake catalogue

The earthquake catalogue used to inform the SSC model was compiled from the following sources:

1 ISC-GEM Global Instrumental Earthquake Catalogue (version 12), covering 1904 to 31 December 2021.

2 ISC Reviewed Bulletin, covering 1 January 1900 to 1 November 2023.

3 ANSS Comprehensive Earthquake Catalog (ComCat), covering 1 November 2023 to 26 November 2025.

The ISC-GEM catalogue is a refined version of the ISC bulletin, with all event magnitudes homogenised to the Mw scale. It presents an improvement on the accuracy of the location and magnitude for events with Mw > 5.5 occurring between 1900 and 2021. This catalogue is prioritised over the other global bulletins because it has data quality specifically improved for the requirements of modelling seismic hazard and risk. The ISC Reviewed Bulletin and ANSS ComCat catalogues were used to supplement the ISC-GEM catalogue with smaller and more recent events relevant to the study area.

The combined catalogue was clipped to a study region bounded by latitudes -13° to -22° and longitudes 162° to 173°, which encompasses the Vanuatu subduction zone and the immediately adjacent crustal source regions.

Magnitude values were homogenised to moment magnitude (M_w) using the following hierarchy, based on our experience of global conversion models evaluated against catalogue data in the region, where $(Mw)^{GCMT}$ denotes the Global Centroid Moment Tensor solution and other terms are defined in the source references:

1 $M_w = {M_w}^{GCMT}$

2 $M_w = 1.021{M_w}^{NEIC} - 0.091$ *(Weatherill et al. 2016)*

3 $M_w = e^{-0.222+0.233m_s} + 2.863$ *(Di Giacomo et al. 2015)*

4 $M_w = 1.38m_b - 1.79$ *(Di Giacomo et al. 2015)*

Events for which no body-wave magnitude (mb), surface-wave magnitude (ms) or Mw could be assigned were removed from the catalogue. This was generally limited to only earthquakes with very low magnitude. The final homogenised catalogue contains 19,354 events.

A3 Classification of events

Catalogue events were classified into three tectonic regimes (subduction interface, subduction slab and shallow crustal) following a procedure similar to that described by Pagani et al. (2020).

The subduction interface was defined using the SLAB2.0 model of Hayes et al. (2018), with a vertical buffer of 20 km above and below the interface surface and a maximum depth cut-off (transition between interface and intraslab) of 40 km based on the work of Christophersen et al. (2015). Events with hypocentres within this buffer and shallower than the interface/intraslab cut-off were classified as interface events.

The subduction slab was defined using the SLAB2.0 model with a 60 km buffer above and 60 km below the slab surface. Events deeper than the maximum interface/intraslab depth cut-off and within the slab buffer were classified as slab events. The modelled reference slab surface generally approximated the upper surface of the subducting slab with very few recorded events located in the buffer region above the surface. 2D cross sections of the recorded events relative to the modelled reference surfaces were used to check for any events being misclassified as a slab event.

Shallow crustal events were defined as those above the CRUST1.0 Moho (Laske et al. 2013) with an additional 25 km buffer to capture events in the catalogue with a default assigned depth below the Moho. Events were further delineated into the four crustal source zones based on areas on internally similar tectonics and seismicity rates.

Where an event satisfied the geometric criteria for more than one regime, the priority order interface > slab > crustal was applied. All events with Mw > 7.5 were reviewed manually against published focal mechanisms and aftershock distributions; two events (IDs 896121 and 13908747) were reclassified as a result of this review.

The subduction interface and subduction slab were further considered as either a single unsegmented source or as three segments along-strike (Northern, Central and Southern) based on historical seismicity patterns and a review of other studies (e.g. Johnson et al. 2021). The classification results are illustrated in the figures below.

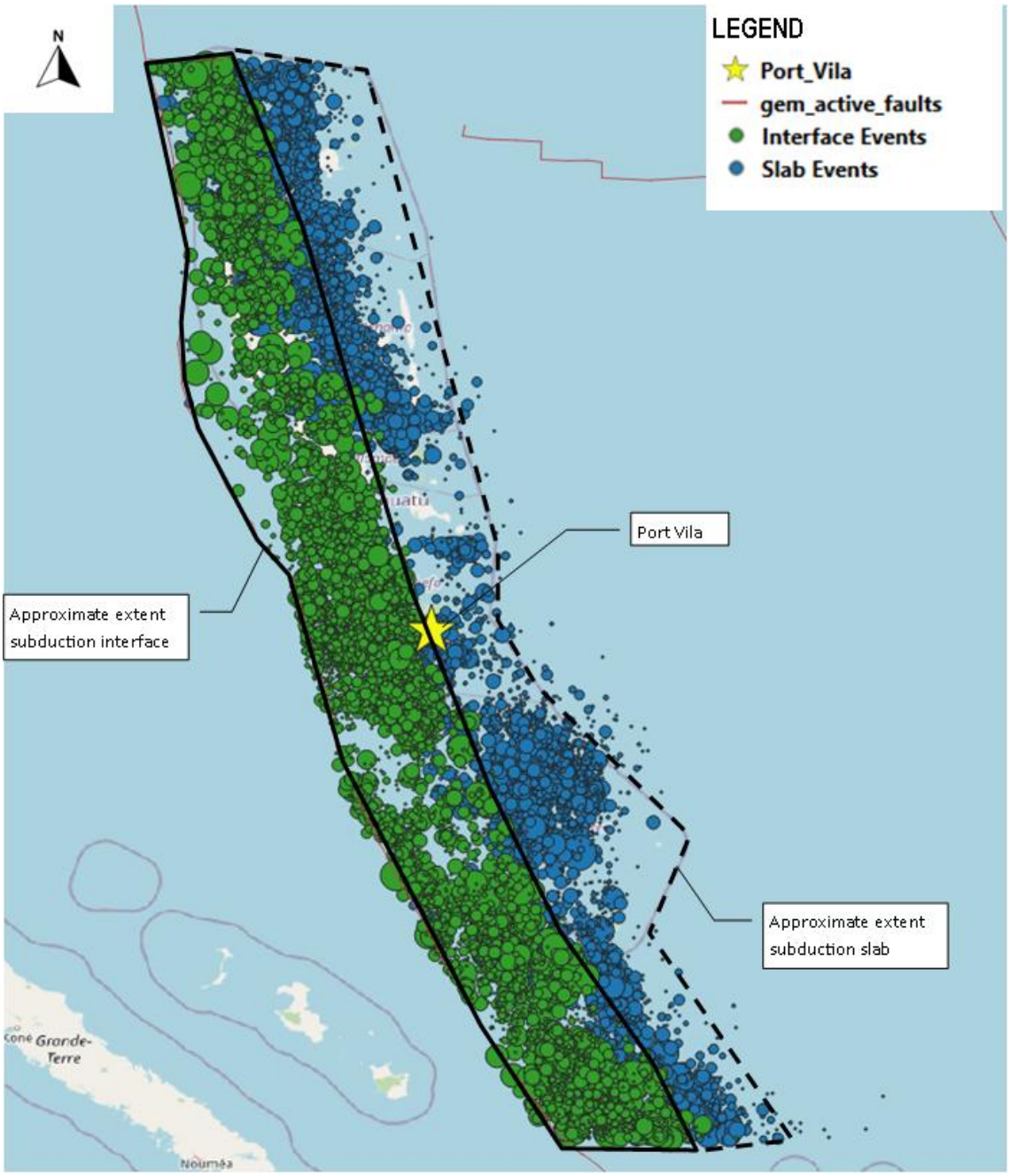

Figure Appendix A.1: Epicentre of catalogue events classified as subduction interface or subduction slab. Interface and slab zones are approximate surface projection of the reference surface used to classify provided to illustrate the classification process.

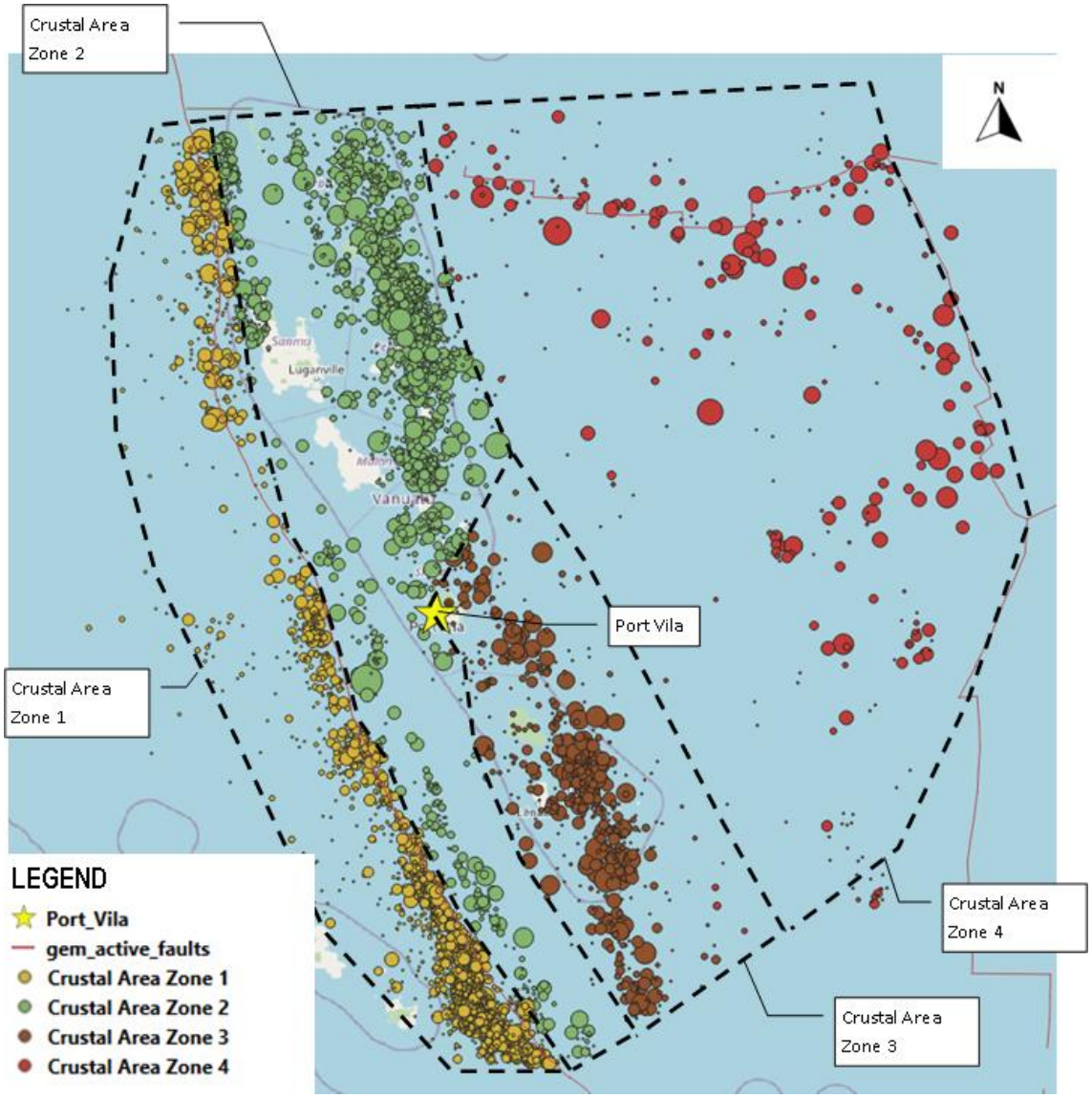

Figure Appendix A.2: Epicentre of catalogue events classified as crustal.

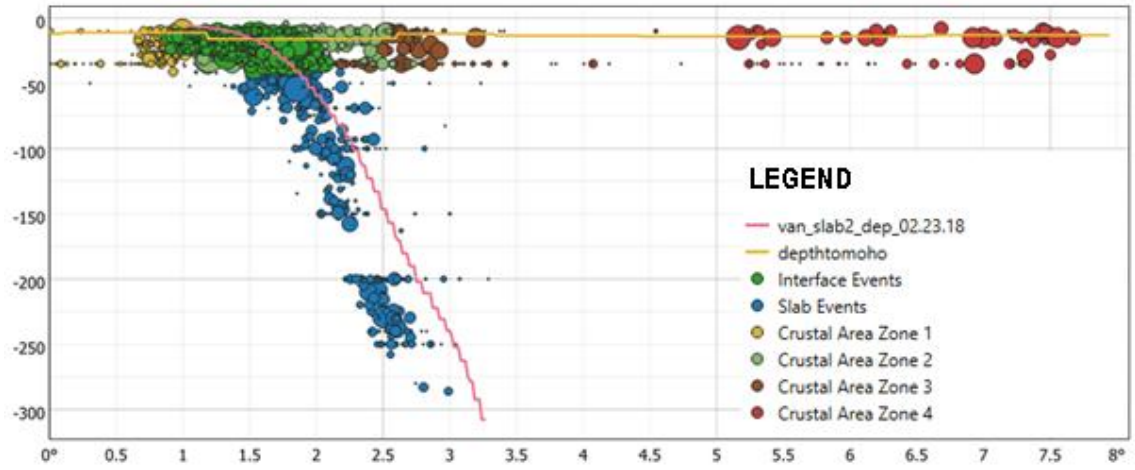

Figure Appendix A.3: Cross-section perpendicular to the strike of the subduction interface and approximately through the Port Vila CBD.

A4 Declustering

Classical probabilistic seismic hazard analysis commonly assumes that earthquake occurrence follows a Poisson process. To comply with this assumption, it is important to consider independent random earthquake events in time and space. Catalogues contain clusters of earthquakes in time and space (i.e. pre-shocks and aftershocks). As such, the combined catalogue was declustered to remove foreshock and aftershock events.

Declustering was done using the method of Gardner & Knopoff (1974), with the alternative time-space-magnitude windows proposed by Grüenthal (van Stiphout et al. 2012) and Uhrhammer (1986) also compared. All three are window-based methods that identify dependent events using space-time windows scaled by mainshock magnitude.

The shallow crustal and subduction interface sub-catalogues were declustered together based on the general expectation that both regimes can trigger aftershock sequences across regime boundaries. The subduction slab sub-catalogue was declustered separately. This also avoided issues with deep intraslab events occupying the triggering window of shallow crustal events, as the method relies on epicentre rather than hypocentre location.

For each set of declustering parameters, the resulting temporal distribution, magnitude-frequency distribution and temporal-spatial distribution of events was evaluated. The final declustering algorithm parameters adopted were those recommended by Uhrhammer (1986), as we found this resulted in a catalogue that was adequately Poissonian (based on a visual inspection of outputs) and contained the largest number of events in the declustered catalogue for statistical analysis of earthquake rates. The original and declustered catalogue using the algorithm recommended by Uhrhammer (1986) is provided in Figure Appendix A.4.

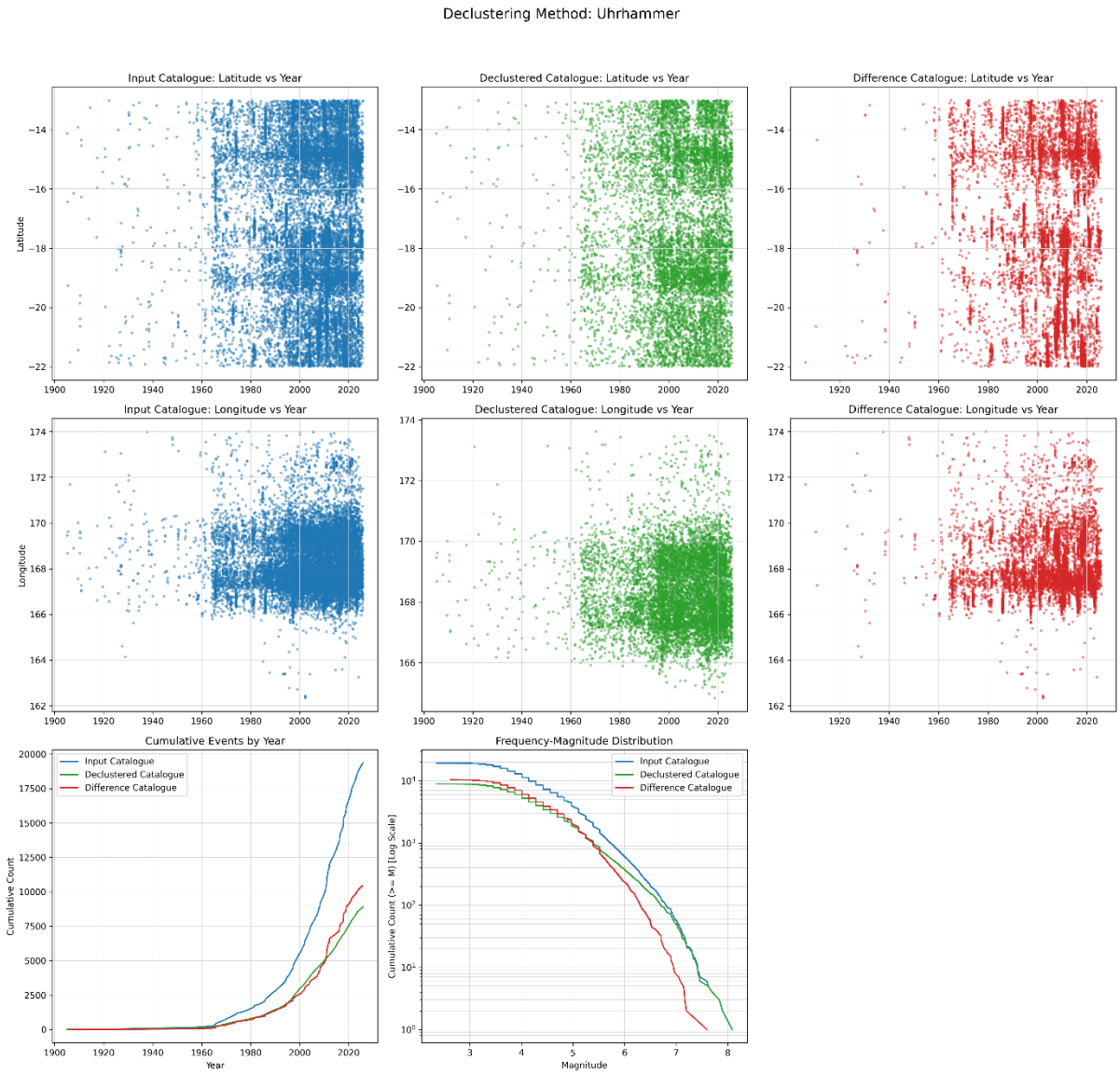

Figure Appendix A.4: Declustered results using the window parameters provided by Uhrhammer (1986).

A5 Magnitude completeness

The magnitude completeness, Mc, is the lowest magnitude above which all events in the catalogue are reliably detected and recorded. Events below Mc are under-represented in the catalogue and were excluded from the derivation of earthquake recurrence parameters.

Mc thresholds for each sub-catalogue time period were derived by inspection of the magnitude-time-density distribution of the declustered catalogue and by stable b-value analysis. The adopted completeness thresholds are listed in Table Appendix A.1 and illustrated in the figure below.

Table Appendix A.1: Magnitude completeness thresholds used for each sub-catalogue time period

Year	1900 to 1921	1922 to 1963	1964 to 2025
Magnitude threshold	7.0	6.0	5.0

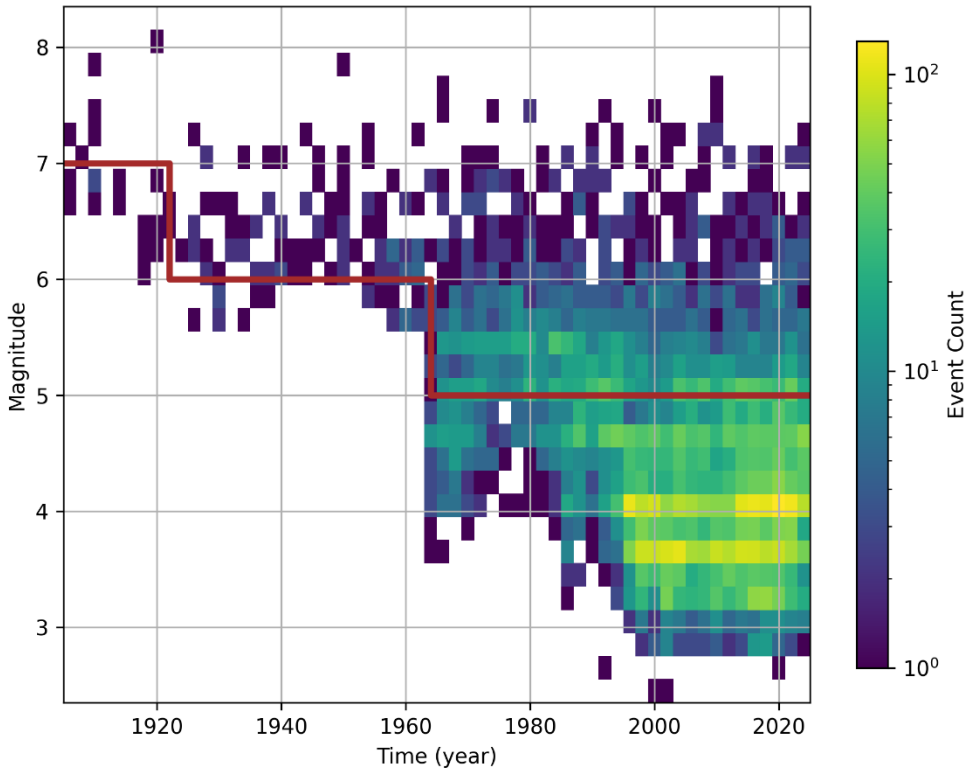

Figure Appendix A.5: Magnitude-time-density plot of the declustered catalogue. The interpreted magnitude completeness is provided as a red line.

A6 Earthquake recurrence parameters

Earthquake recurrence parameters were derived separately for each tectonic regime using the Weichert (1980) maximum-likelihood method, which accommodates the time-varying completeness thresholds in Table Appendix A.1. These have been used to define double-truncated Gutenberg-Richter magnitude-frequency distributions with a minimum magnitude cut-off, M_{min} = 5 and a maximum magnitude cut-off, M_{max} = $M_{max,obs}$ + 0.3 to 0.5 (for shallow crustal and subduction slab sources), where $M_{max,obs}$ is the observed historical maximum within each respective area source zone.

A6.1 Shallow crustal seismicity

Published geological maps for Efate Island identify several possible fault traces in the Port Vila region and Efate Island. However, there is insufficient detailed information of individually mapped faults to accurately model the crustal seismicity using fault planes. Therefore, the crustal seismicity model consists only of area and distributed seismicity sources.

Recurrence parameters for shallow crustal seismicity were derived using the Weichert (1980) maximum-likelihood method. The 2024 Vanuatu earthquake was reviewed but had no material effect on the adopted parameters.

Hypocentral depths and nodal-plane orientations for each crustal source zone were derived from the focal-mechanism recorded in the ISC-GEM database weighted by the relative observed frequency of each style of faulting. The assessed hypocentre depths and fault orientations were sense checked

against other available studies for the region (such as Johnson et al. (2021). The Wells & Coppersmith (1994) magnitude-area scaling factors are used within the hazard calculations to determine rupture dimensions.

Two spatial representations of crustal seismicity were considered:

1 A uniform seismicity source within each crustal area zone, in which seismicity is treated as uniformly distributed.

2 A spatially distributed (smoothed seismicity) model in which observed event locations are smoothed onto a 0.1° × 0.1° grid using a Gaussian kernel, under the assumption that historical spatial distribution of seismicity is representative of the likely distribution of future seismicity.

A6.2 Subduction interface seismicity

Subduction interface seismicity was modelled as a 3D fault source using the SLAB2.0 interface geometry, allowing for 'floating' ruptures on the fault surface (i.e. lower magnitude events that rupture along only a portion of the surface). Maximum magnitude (Mmax) for the double truncated GR magnitude-frequency distribution was derived from the fault rupture area of each segment (and the alternative non-segmented model) using the magnitude-area scaling relation of Thingbaijam et al. (2017) for interface earthquakes. The Thingbaijam et al. (2017) magnitude-area scaling relationship was also used for scaling of floating rupture geometry within the hazard calculations.

A6.3 Subduction slab seismicity

Subduction slab seismicity was modelled using the Weichert (1980) maximum-likelihood method with a double-truncated GR magnitude-frequency distribution. Seismicity was distributed using a 3D Gaussian smoothing algorithm to spatially smooth the total rates across seven representative hypocentre depth bins covering the depth range of slab events in the catalogue.

A6.4 Adopted recurrence parameters

The adopted recurrence parameters for each source zone and segment are listed in Table Appendix A.2. Gutenberg-Richter (GR) plots showing the fit of the adopted parameters to the declustered catalogue, and the smoothed seismicity grids, are presented separately.

Table Appendix A.2: Adopted earthquake recurrence parameters.

Earthquake Source	Description	Mechanism(3) type/strike (weight)	Hypocentre depth, km (weight)	N(Note 2)	GR a-value(Note 1)	GR b-value	Mmax
Zone 1	New Hebrides outer rise seismicity (Australian Plate)	N/ 150 (0.65) SS/ 190 (0.35)	15 (0.4) 25 (0.4) 35 (0.2)	86	6.11	1.2	7.54
Zone 2	Fore/ backarc of New Hebrides (Pacific Plate)	R/ 130 (0.75) SS/ 100 (0.25)	15 (0.5) 25 (0.4) 35 (0.1)	163	4.50	0.82	7.92
Zone 3	North Fiji Basin spreading ridges and transform faults	N/ 120 (0.4) SS/ 180 (0.6)	15 (0.7) 25 (0.15) 35 (0.15)	84	3.49	0.68	7.48
Zone 4	North Fiji Basin spreading ridges and transform faults	N/ 100 (0.55) SS/ 100 (0.45)	15 (0.6) 25 (0.15) 35 (0.25)	74	4.28	0.85	7.83
Subduction interface (unsegmented) – Maximum magnitude based on a total unsegmented length of approximately 1900 km				552	4.67	0.76	8.73
Northern segment	Northern segment approximately 500 km in length. Extending from the northern tip of the New Hebrides trench to a deflection in the trench strike at the d'Entrecasteaux ridge.			78	2.80	0.56	8.09
Central segment	Central segment approximately 300 km in length. Reduced convergence rate where overriding plate collides with the D'Entrecasteaux Ridge			114	3.94	0.74	8.05
Southern segment	Southern segment approximately 670 km in length. Increased convergence rate parallel to Efaté. The trench bends eastwards at the southern end.			360	4.65	0.79	8.23
Subduction intraslab (unsegmented)				871	5.48	0.87	8.34
Northern segment	Approximately coinciding with the northern interface segment			365	4.93	0.84	8.2
Central segment	Approximately coinciding with the central interface segment with reduced activity			116	4.49	0.85	7.8
Southern segment	Approximately coinciding with the southern interface segment, subducting beneath Port Vila			380	5.27	0.9	8.34

Note (1): GR a-values are total rate values for each source. For the subduction intraslab seismicity and distributed crustal seismicity models, rates have been spatially smoothed onto a 0.1° x 0.1° grid based on epicentre location of past events. **(2):** N is the number of events within each sub catalogue, after filtering for region of interest, declustering and magnitude completeness. **(3):** N = normal, R = reverse, SS = strike-slip. Numbers after the style code (e.g. /150) denote nodal-plane strike in degrees.

Appendix B Uniform Hazard Spectra

Table Appendix B.1: Mean 5% critically damped spectral acceleration values for V_{s30} 300 m/s

Period (s)	Mean Spectral Accelerations (g)					
	1 in 25 AEP	1 in 100 AEP	1 in 250 AEP	1 in 500 AEP	1 in 1000 AEP	1 in 2500 AEP
0.01	0.34	0.65	0.95	1.23	1.55	2.06
0.05	0.43	0.83	1.22	1.59	2.05	2.79
0.1	0.63	1.22	1.79	2.35	3.05	4.20
0.15	0.76	1.46	2.12	2.77	3.56	4.86
0.2	0.80	1.54	2.24	2.91	3.74	5.08
0.25	0.78	1.51	2.19	2.85	3.62	4.89
0.3	0.75	1.45	2.11	2.74	3.47	4.66
0.4	0.64	1.27	1.85	2.39	3.03	4.02
0.5	0.56	1.11	1.62	2.10	2.66	3.52
0.7	0.42	0.84	1.24	1.61	2.06	2.73
1	0.28	0.58	0.86	1.12	1.43	1.91
1.5	0.16	0.34	0.50	0.66	0.85	1.14
2	0.10	0.22	0.32	0.43	0.56	0.76
3	0.05	0.12	0.18	0.24	0.31	0.42
5	0.02	0.05	0.08	0.10	0.13	0.18

Table Appendix B.2: Mean 5% critically damped spectral acceleration values for V_{s30} 375 m/s

Period (s)	Mean Spectral Accelerations (g)					
	1 in 25 AEP	1 in 100 AEP	1 in 250 AEP	1 in 500 AEP	1 in 1000 AEP	1 in 2500 AEP
0.01	0.32	0.65	0.97	1.26	1.62	2.18
0.05	0.44	0.87	1.31	1.73	2.25	3.13
0.1	0.64	1.29	1.93	2.57	3.37	4.74
0.15	0.75	1.50	2.24	2.96	3.87	5.38
0.2	0.77	1.55	2.30	3.05	3.96	5.47
0.25	0.74	1.50	2.23	2.94	3.81	5.23
0.3	0.69	1.41	2.11	2.79	3.59	4.91
0.4	0.59	1.21	1.82	2.39	3.08	4.18
0.5	0.50	1.04	1.56	2.06	2.65	3.58
0.7	0.37	0.77	1.16	1.53	1.97	2.67
1	0.24	0.51	0.77	1.02	1.32	1.78
1.5	0.14	0.29	0.44	0.58	0.75	1.02
2	0.09	0.19	0.28	0.37	0.48	0.66
3	0.05	0.10	0.15	0.20	0.26	0.36
5	0.02	0.04	0.06	0.09	0.11	0.16

Table Appendix B.3: Mean 5% critically damped spectral acceleration values for V_{s30} 450 m/s

Period (s)	Mean Spectral Accelerations (g)					
	1 in 25 AEP	1 in 100 AEP	1 in 250 AEP	1 in 500 AEP	1 in 1000 AEP	1 in 2500 AEP
0.01	0.31	0.64	0.97	1.28	1.66	2.27
0.05	0.44	0.90	1.37	1.83	2.41	3.40
0.1	0.64	1.33	2.03	2.73	3.62	5.17
0.15	0.73	1.52	2.31	3.09	4.08	5.75
0.2	0.74	1.53	2.33	3.12	4.10	5.74
0.25	0.70	1.47	2.23	2.98	3.92	5.46
0.3	0.65	1.36	2.09	2.79	3.65	5.06
0.4	0.54	1.15	1.76	2.36	3.08	4.25
0.5	0.46	0.97	1.49	2.00	2.60	3.58
0.7	0.32	0.69	1.06	1.42	1.84	2.53
1	0.21	0.45	0.69	0.92	1.19	1.63
1.5	0.12	0.25	0.39	0.52	0.67	0.91
2	0.08	0.16	0.25	0.33	0.43	0.59
3	0.04	0.09	0.13	0.18	0.23	0.31
5	0.02	0.04	0.06	0.08	0.10	0.14

Table Appendix B.4: Mean 5% critically damped spectral acceleration values for V_{s30} 500 m/s

Period (s)	Mean Spectral Accelerations (g)					
	1 in 25 AEP	1 in 100 AEP	1 in 250 AEP	1 in 500 AEP	1 in 1000 AEP	1 in 2500 AEP
0.01	0.30	0.63	0.96	1.28	1.67	2.31
0.05	0.43	0.91	1.39	1.88	2.49	3.54
0.1	0.64	1.34	2.07	2.81	3.75	5.39
0.15	0.72	1.52	2.33	3.15	4.18	5.93
0.2	0.71	1.51	2.33	3.14	4.16	5.86
0.25	0.67	1.44	2.21	2.99	3.95	5.56
0.3	0.62	1.33	2.06	2.77	3.65	5.11
0.4	0.51	1.11	1.72	2.33	3.07	4.27
0.5	0.43	0.91	1.41	1.90	2.49	3.45
0.7	0.30	0.65	1.00	1.33	1.74	2.40
1	0.19	0.42	0.64	0.86	1.12	1.53
1.5	0.11	0.24	0.36	0.48	0.62	0.85
2	0.07	0.15	0.23	0.31	0.40	0.55
3	0.04	0.08	0.12	0.16	0.21	0.29
5	0.02	0.04	0.05	0.07	0.09	0.13

Table Appendix B.5: Mean 5% critically damped spectral acceleration values for V_{s30} 600 m/s

Period (s)	Mean Spectral Accelerations (g)					
	1 in 25 AEP	1 in 100 AEP	1 in 250 AEP	1 in 500 AEP	1 in 1000 AEP	1 in 2500 AEP
0.01	0.28	0.61	0.93	1.26	1.65	2.30
0.05	0.42	0.90	1.40	1.91	2.55	3.65
0.1	0.63	1.34	2.10	2.86	3.84	5.54
0.15	0.69	1.49	2.32	3.16	4.23	6.05
0.2	0.67	1.46	2.28	3.11	4.15	5.89
0.25	0.62	1.36	2.13	2.91	3.89	5.53
0.3	0.56	1.24	1.95	2.66	3.54	5.02
0.4	0.46	1.00	1.56	2.12	2.82	3.97
0.5	0.37	0.81	1.26	1.71	2.25	3.15
0.7	0.26	0.57	0.88	1.18	1.56	2.17
1	0.17	0.36	0.56	0.75	0.98	1.35
1.5	0.09	0.20	0.31	0.42	0.55	0.75
2	0.06	0.13	0.20	0.27	0.35	0.48
3	0.03	0.07	0.11	0.14	0.19	0.25
5	0.01	0.03	0.05	0.06	0.08	0.12

Table Appendix B.6: Mean 5% critically damped spectral acceleration values for V_{s30} 760 m/s

Period (s)	Mean Spectral Accelerations (g)					
	1 in 25 AEP	1 in 100 AEP	1 in 250 AEP	1 in 500 AEP	1 in 1000 AEP	1 in 2500 AEP
0.01	0.26	0.57	0.88	1.20	1.58	2.22
0.05	0.41	0.88	1.39	1.91	2.56	3.68
0.1	0.60	1.32	2.09	2.87	3.87	5.59
0.15	0.64	1.42	2.26	3.11	4.19	6.02
0.2	0.61	1.35	2.15	2.97	4.01	5.74
0.25	0.55	1.21	1.93	2.66	3.58	5.15
0.3	0.48	1.08	1.71	2.35	3.16	4.53
0.4	0.39	0.86	1.35	1.85	2.48	3.54
0.5	0.31	0.69	1.09	1.48	1.97	2.79
0.7	0.22	0.47	0.74	1.01	1.34	1.88
1	0.14	0.30	0.47	0.63	0.83	1.15
1.5	0.08	0.17	0.26	0.35	0.46	0.63
2	0.05	0.11	0.17	0.23	0.31	0.42
3	0.03	0.06	0.09	0.12	0.16	0.21
5	0.01	0.03	0.04	0.06	0.07	0.10

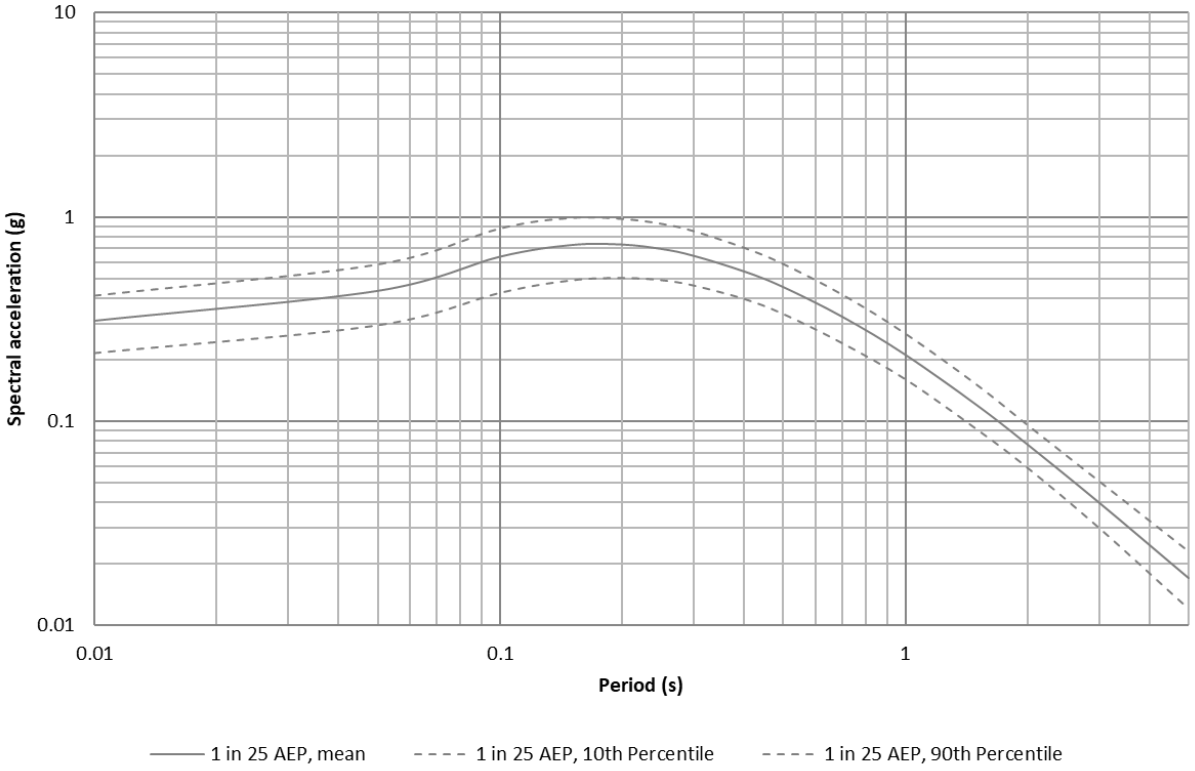

Figure Appendix B.1: 5% critically damped UHS for 1 in 25 AEP and V_{s30} 450 m/s, showing 10th and 90th percentile UHS to demonstrate epistemic uncertainty.

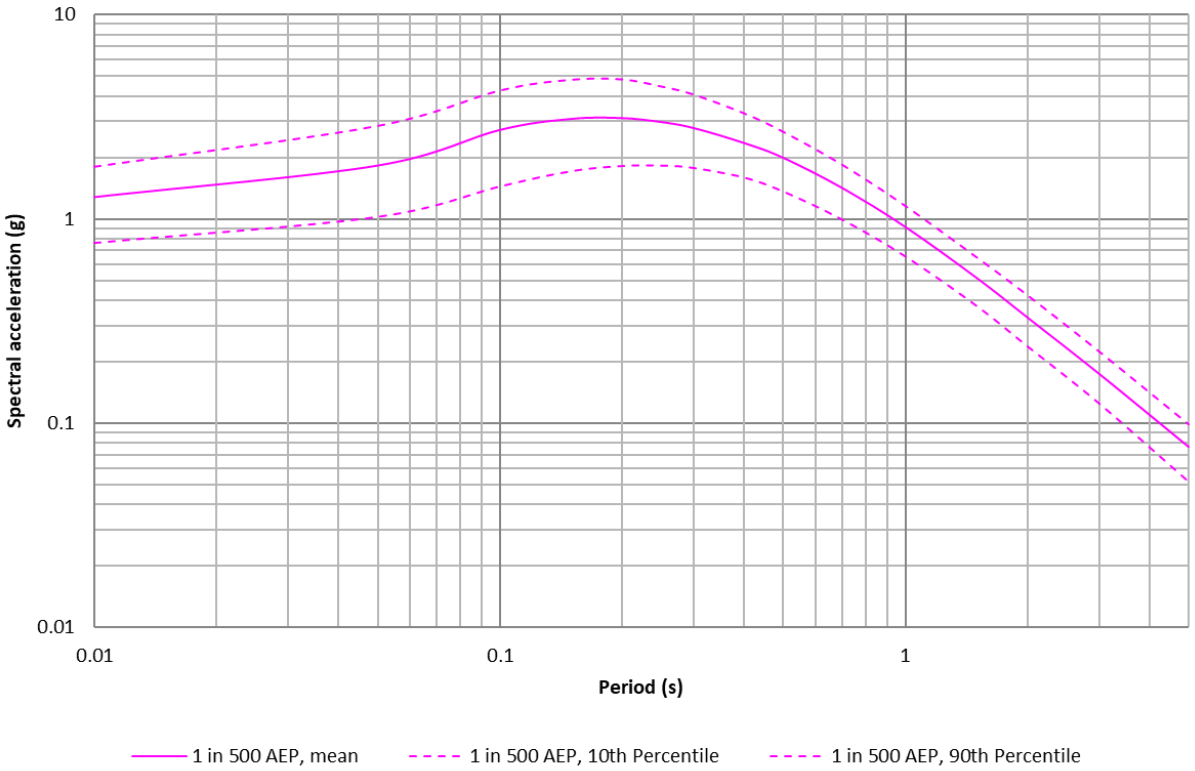

Figure Appendix B.2: 5% critically damped UHS for 1 in 500 AEP and V_{s30} 450 m/s, showing 10th and 90th percentile UHS to demonstrate epistemic uncertainty.

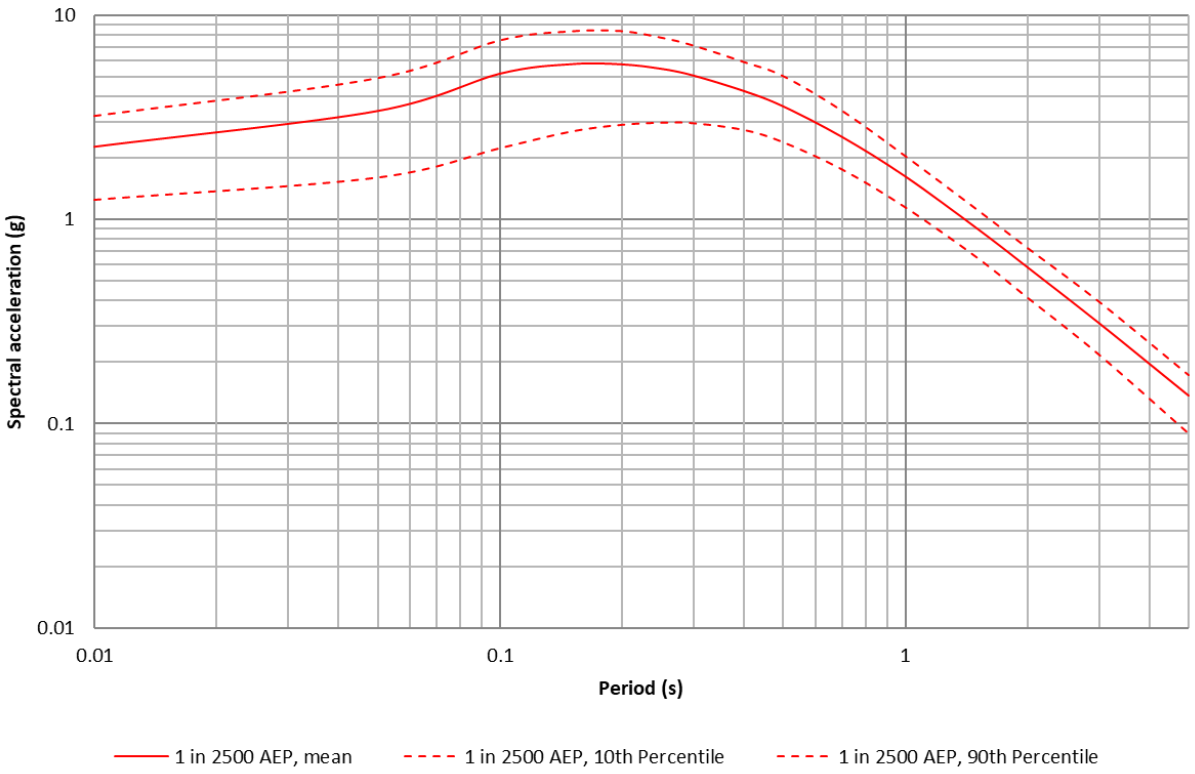

Figure Appendix B.3: 5% critically damped UHS for 1 in 2500 AEP and V_{s30} 450 m/s, showing 10th and 90th percentile UHS to demonstrate epistemic uncertainty.

Appendix C Hazard disaggregation

- **C1 Hazard disaggregation for V_{s30} 375 m/s**
- **C2 Hazard disaggregation for V_{s30} 450 m/s**
- **C3 Hazard disaggregation for V_{s30} 600 m/s**
- **C4 Hazard disaggregation for V_{s30} 760 m/s**

C1 Hazard disaggregation for V_{s30} 375 m/s

C1.1 PGA

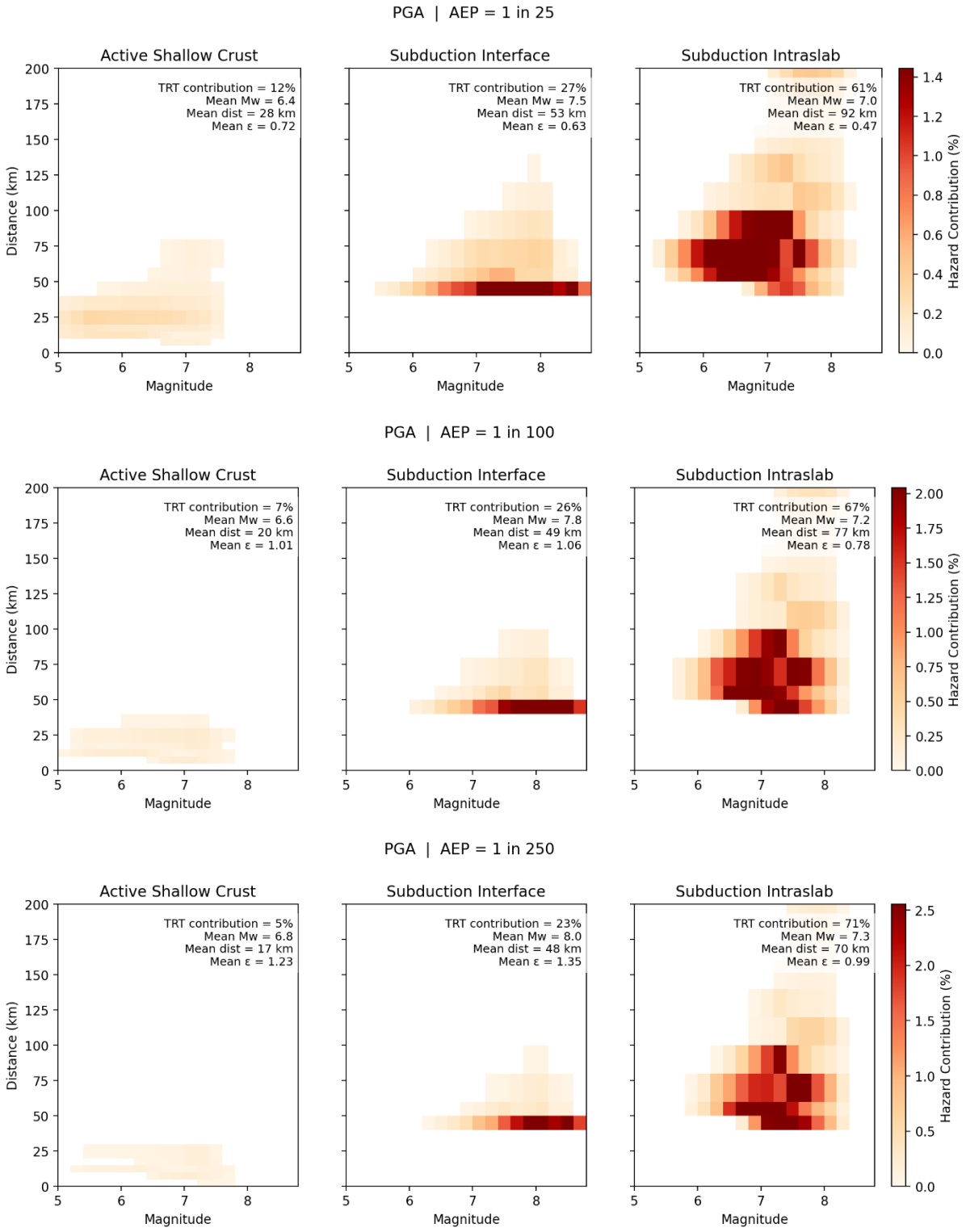

Figure Appendix C.1: PGA hazard disaggregation by magnitude, distance and TRT for 1 in 25, 1 in 100 and 1 in 250 AEP and V_{s30} 375 m/s.

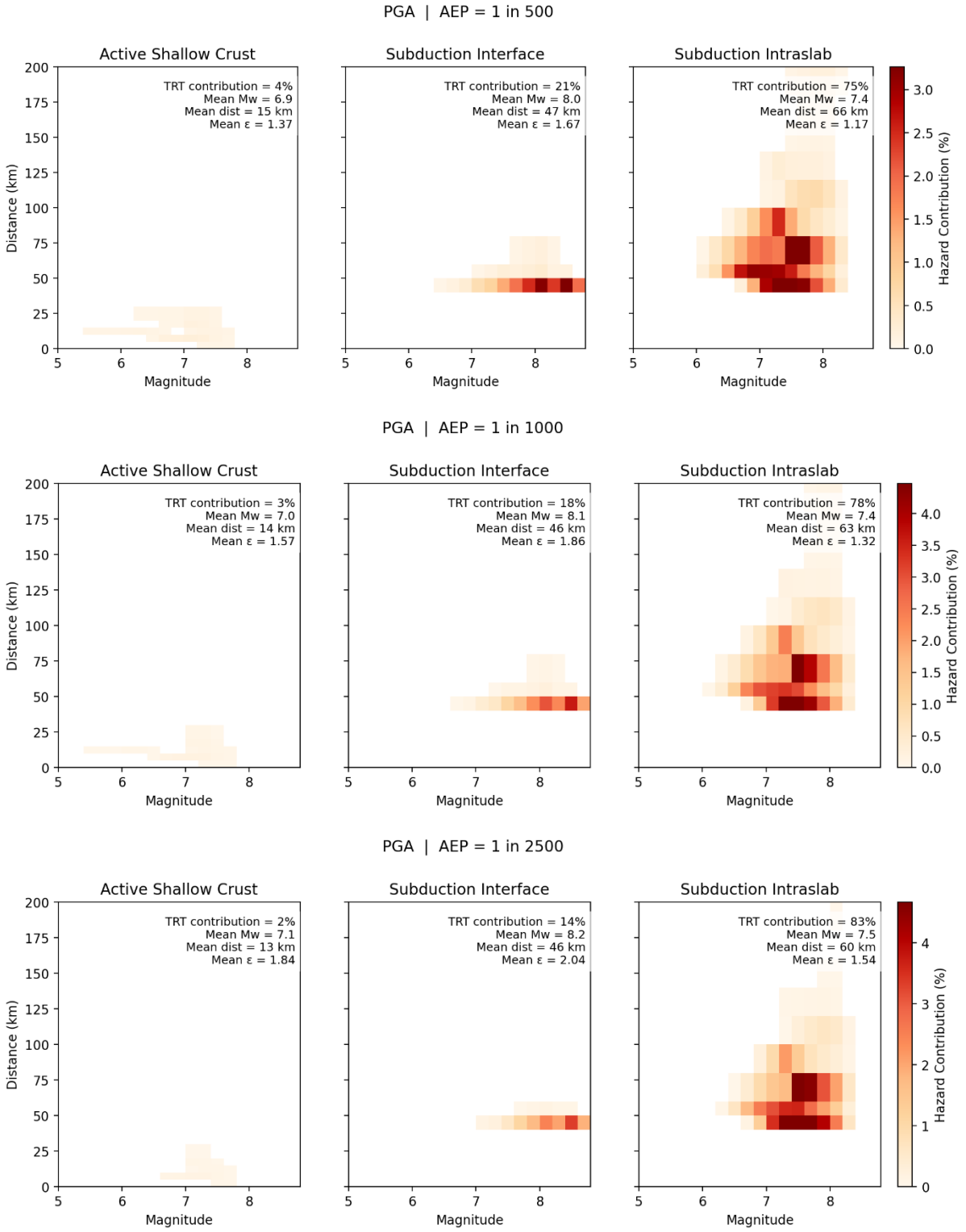

Figure Appendix C.2: PGA hazard disaggregation by magnitude, distance and TRT for 1 in 500, 1 in 1000 and 1 in 2500 AEP and V_{s30} 375 m/s.

C1.2 SA(0.5s)

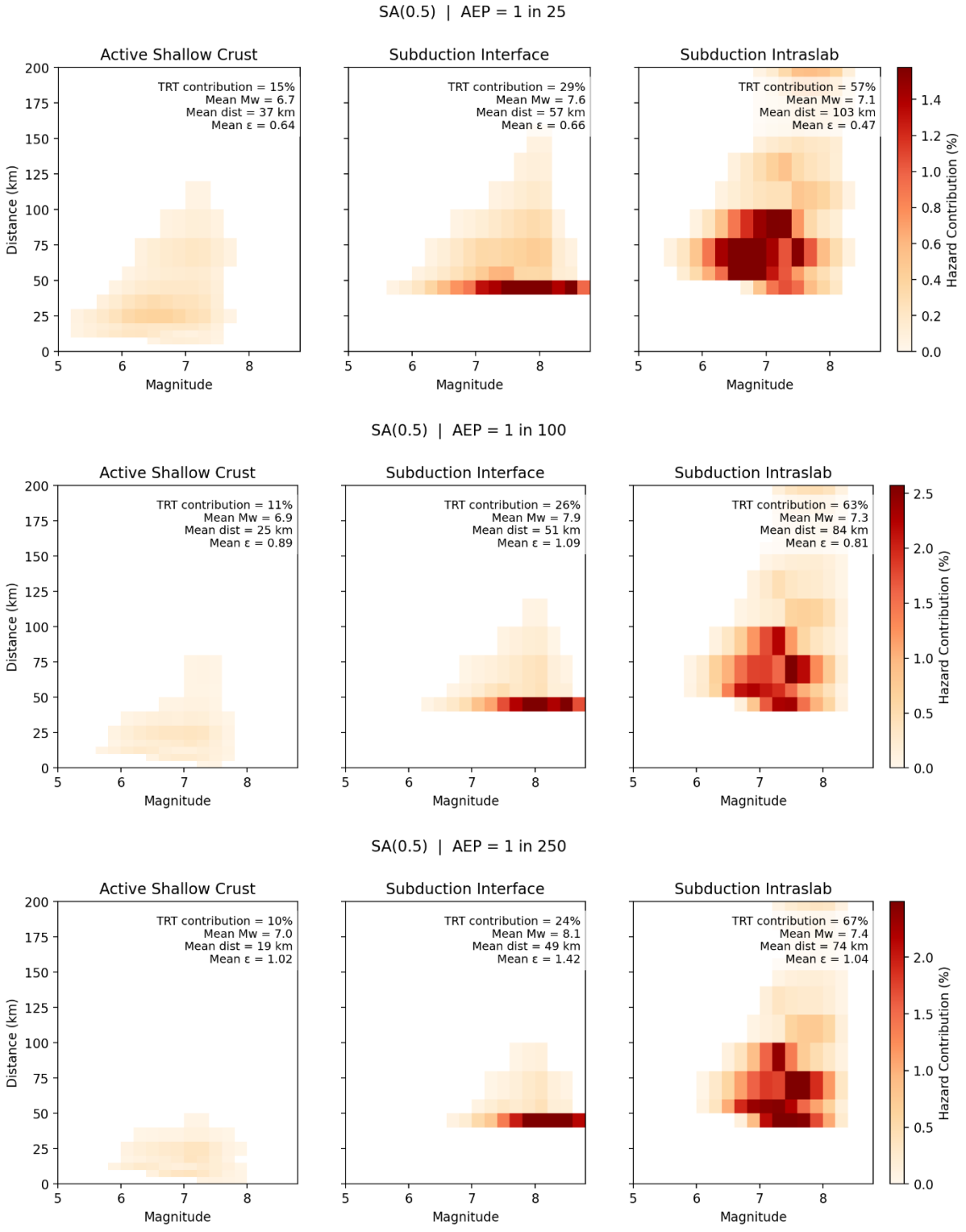

Figure Appendix C.3: SA(0.5s) hazard disaggregation by magnitude, distance and TRT for 1 in 25, 1 in 100 and 1 in 250 AEP and V_{s30} 375 m/s.

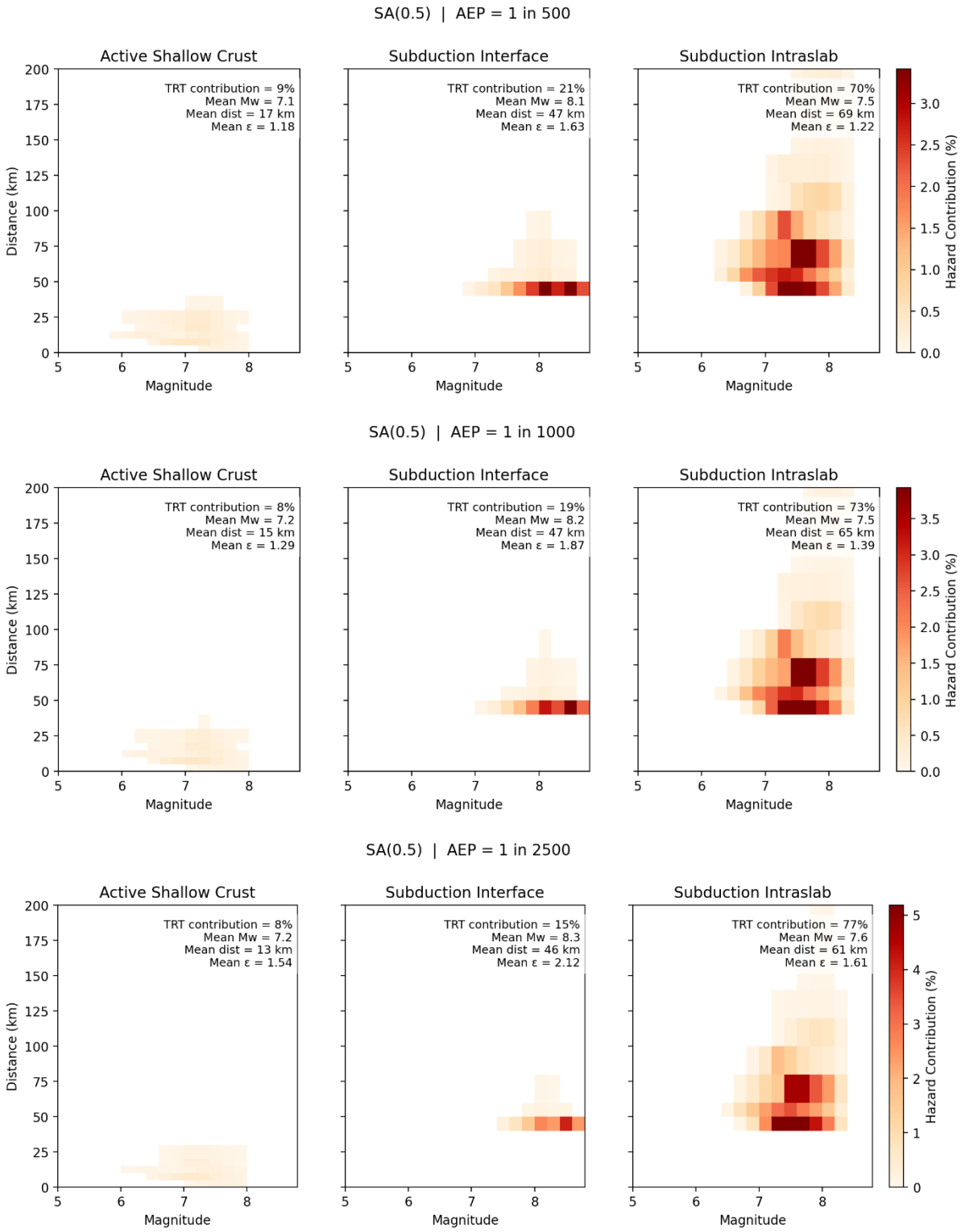

Figure Appendix C.4: SA(0.5s) hazard disaggregation by magnitude, distance and TRT for 1 in 500, 1 in 1000 and 1 in 2500 AEP and V_{s30} 375 m/s.

C1.3 SA(2.0s)

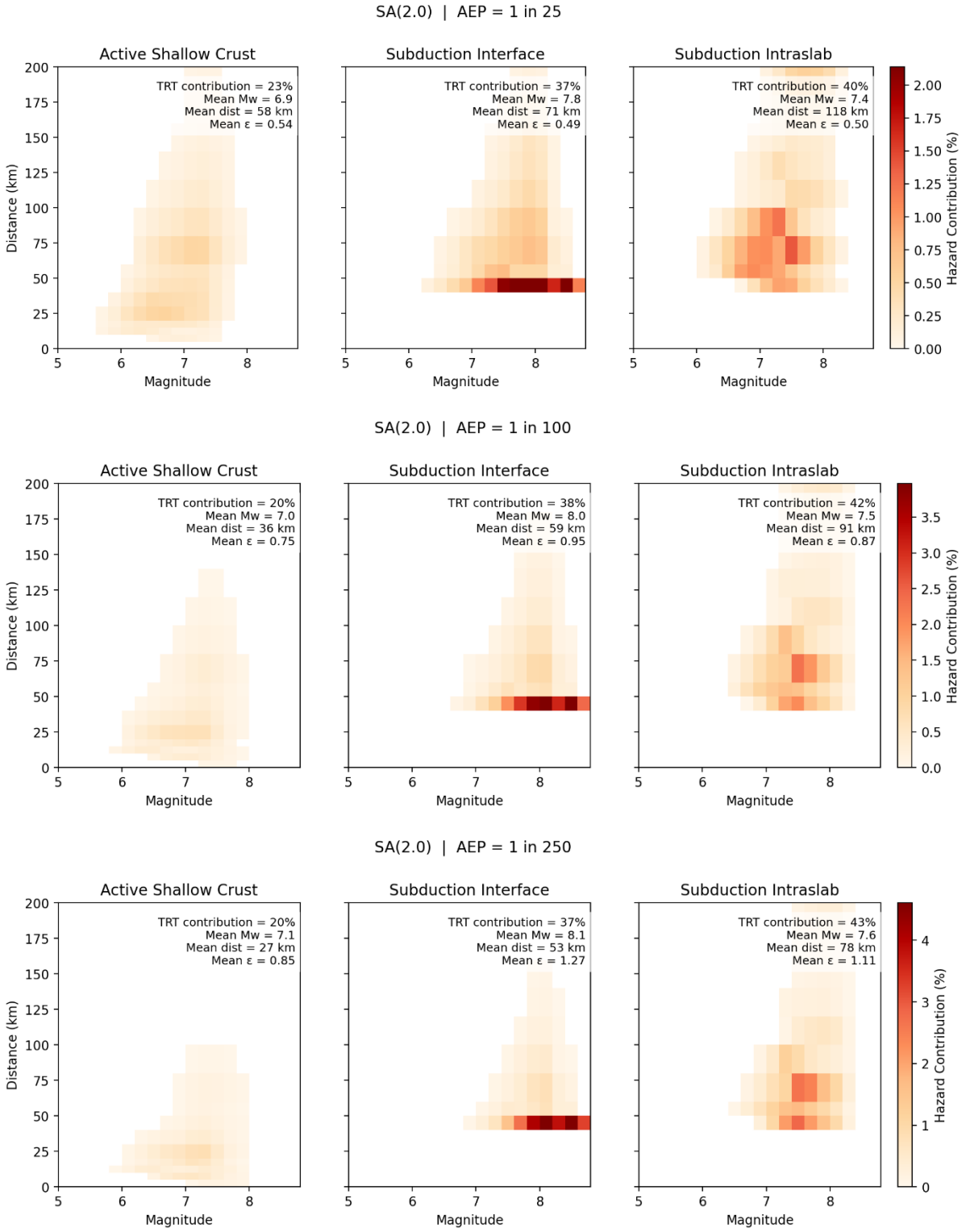

Figure Appendix C.5: SA(2s) hazard disaggregation by magnitude, distance and TRT for 1 in 25, 1 in 100 and 1 in 250 AEP and V_{s30} 375 m/s.

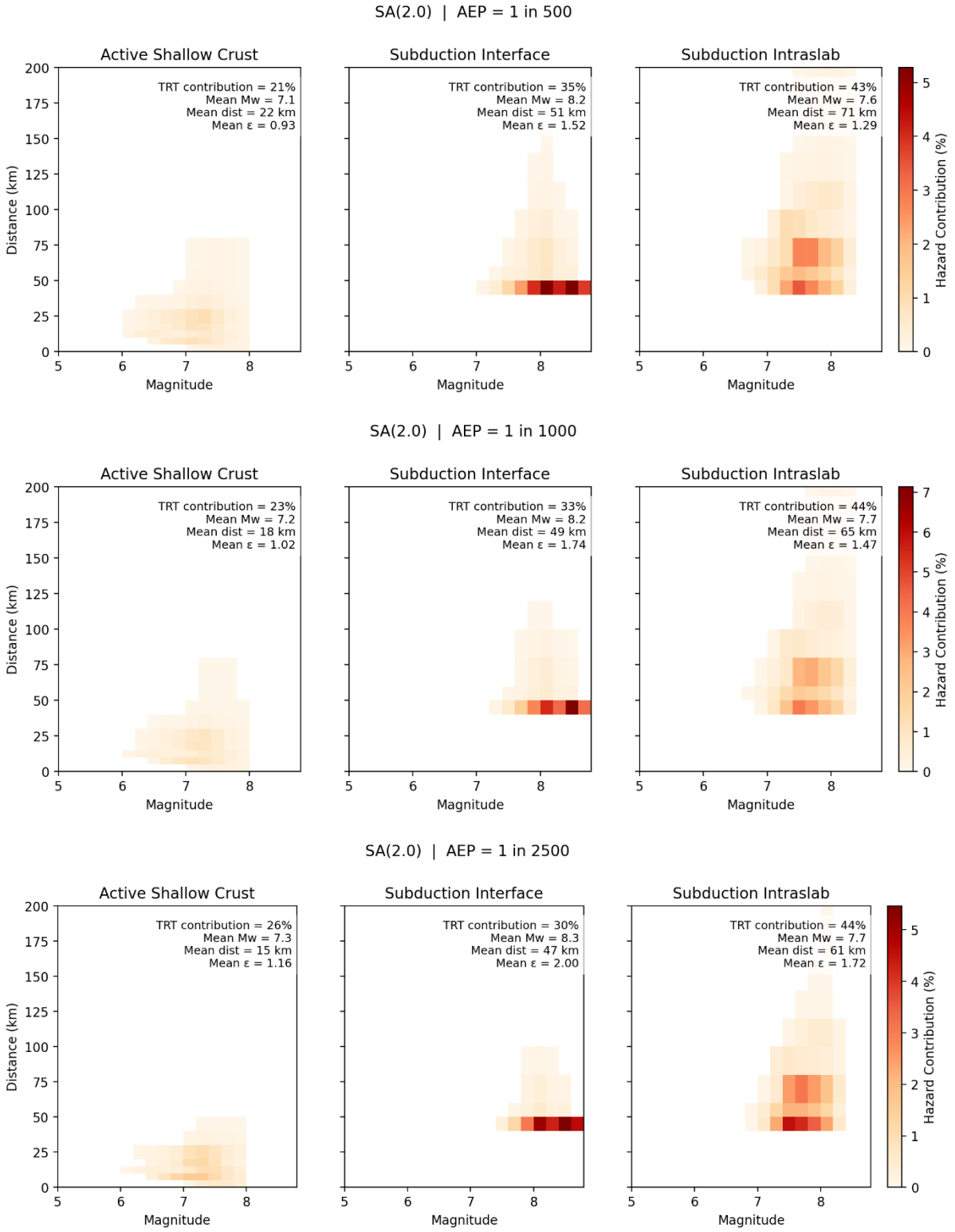

Figure Appendix C.6: SA(2s) hazard disaggregation by magnitude, distance and TRT for 1 in 500, 1 in 1000 and 1 in 2500 AEP and V_{s30} 375 m/s.

C2 Hazard disaggregation for V_{s30} 450 m/s

C2.1 PGA

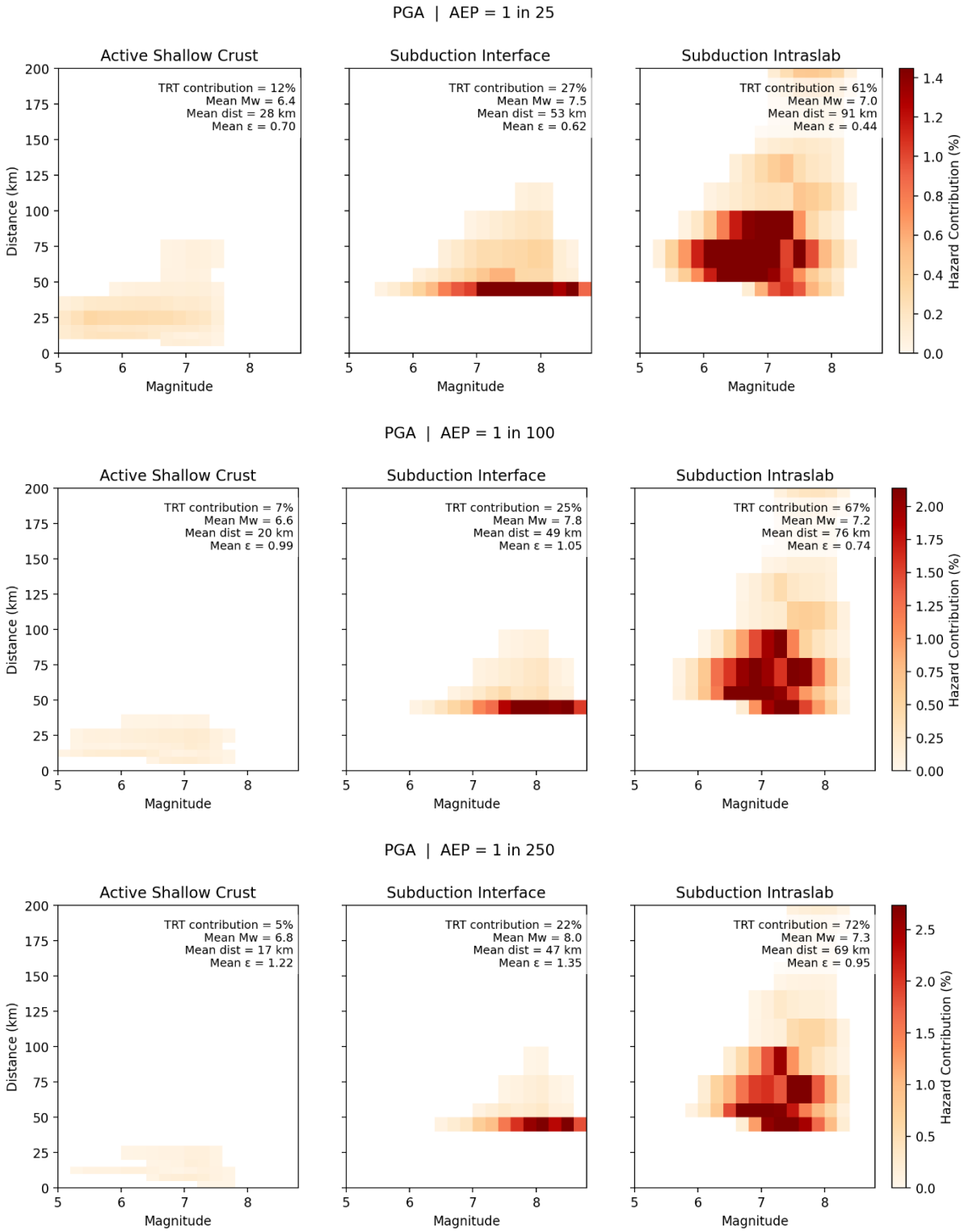

Figure Appendix C.7: PGA hazard disaggregation by magnitude, distance and TRT for 1 in 25, 1 in 100 and 1 in 250 AEP and V_{s30} 450 m/s.

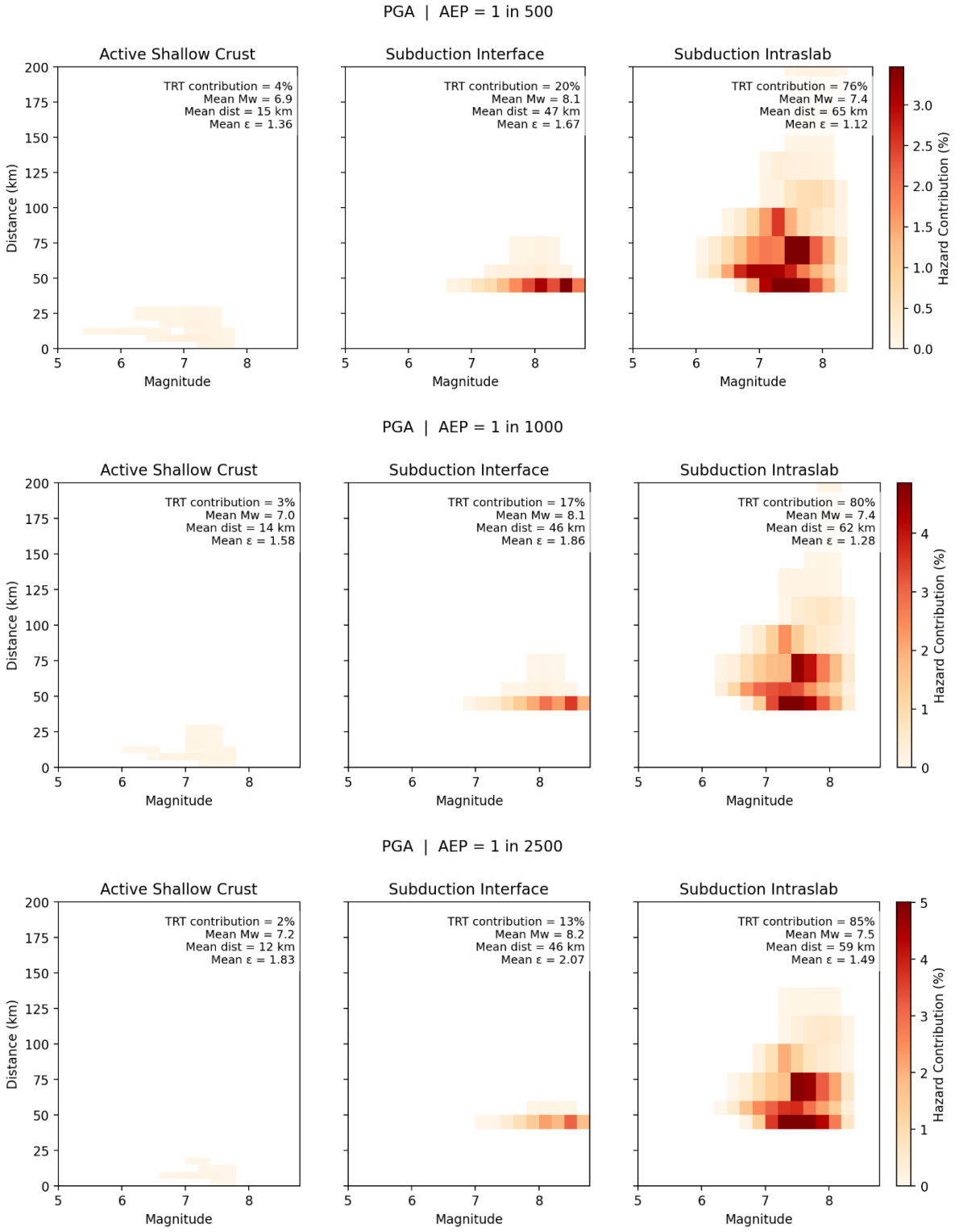

Figure Appendix C.8: PGA hazard disaggregation by magnitude, distance and TRT for 1 in 500, 1 in 1000 and 1 in 2500 AEP and V_{s30} 450 m/s.

C2.2 SA(0.5s)

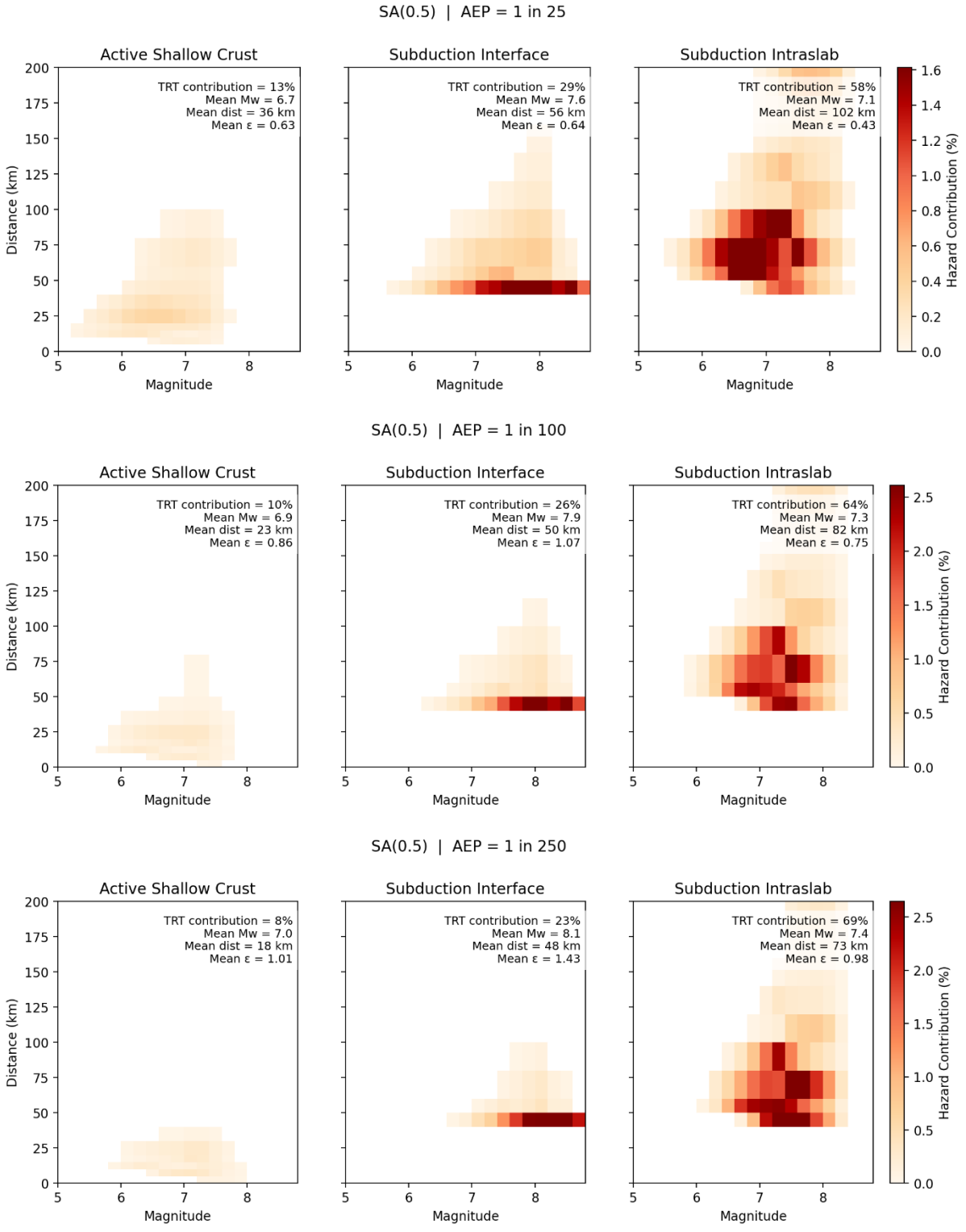

Figure Appendix C.9: SA(0.5s) hazard disaggregation by magnitude, distance and TRT for 1 in 25, 1 in 100 and 1 in 250 AEP and V_{s30} 450 m/s.

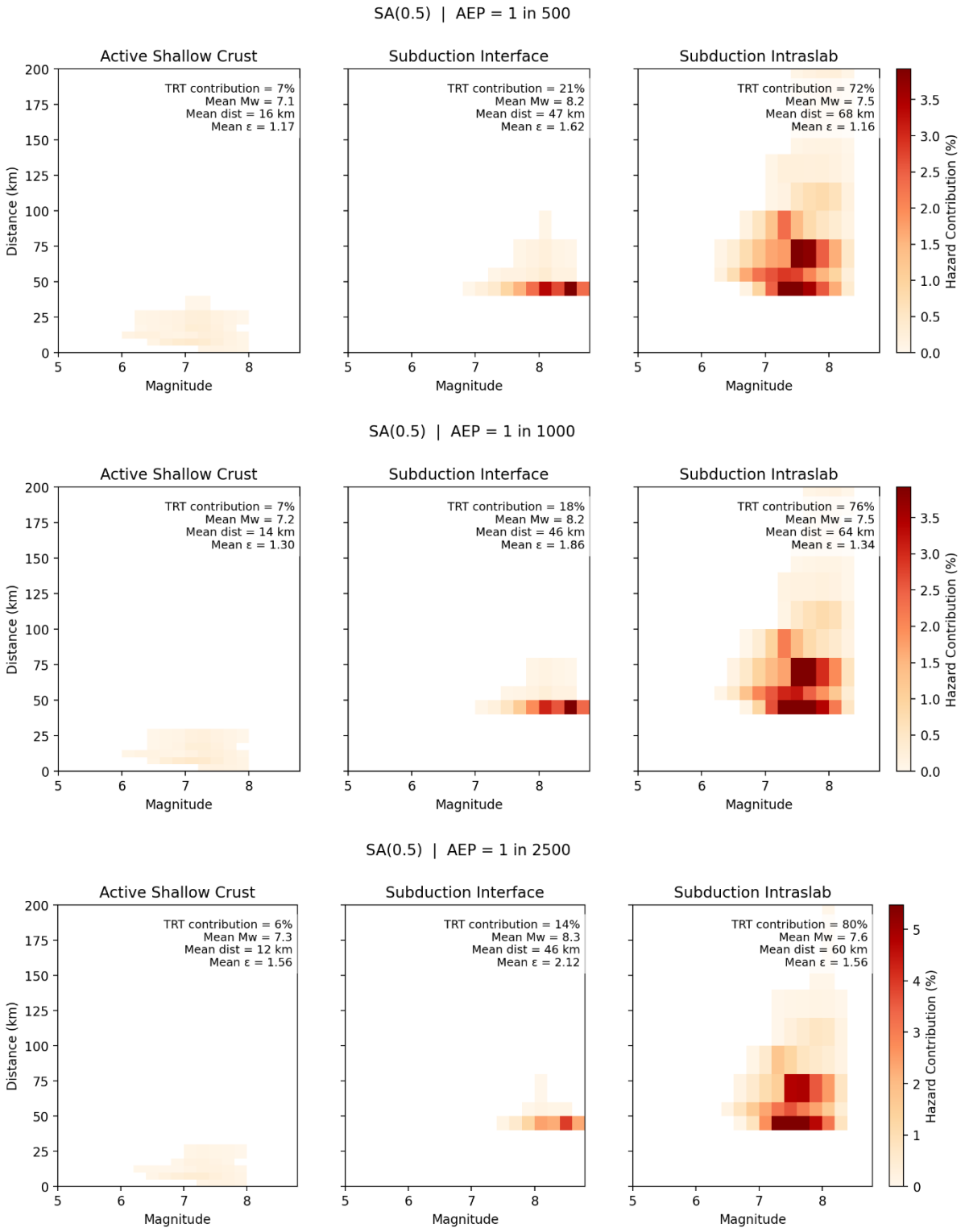

Figure Appendix C.10: SA(0.5s) hazard disaggregation by magnitude, distance and TRT for 1 in 500, 1 in 1000 and 1 in 2500 AEP and V_{s30} 450 m/s.

C2.3 SA(2.0s)

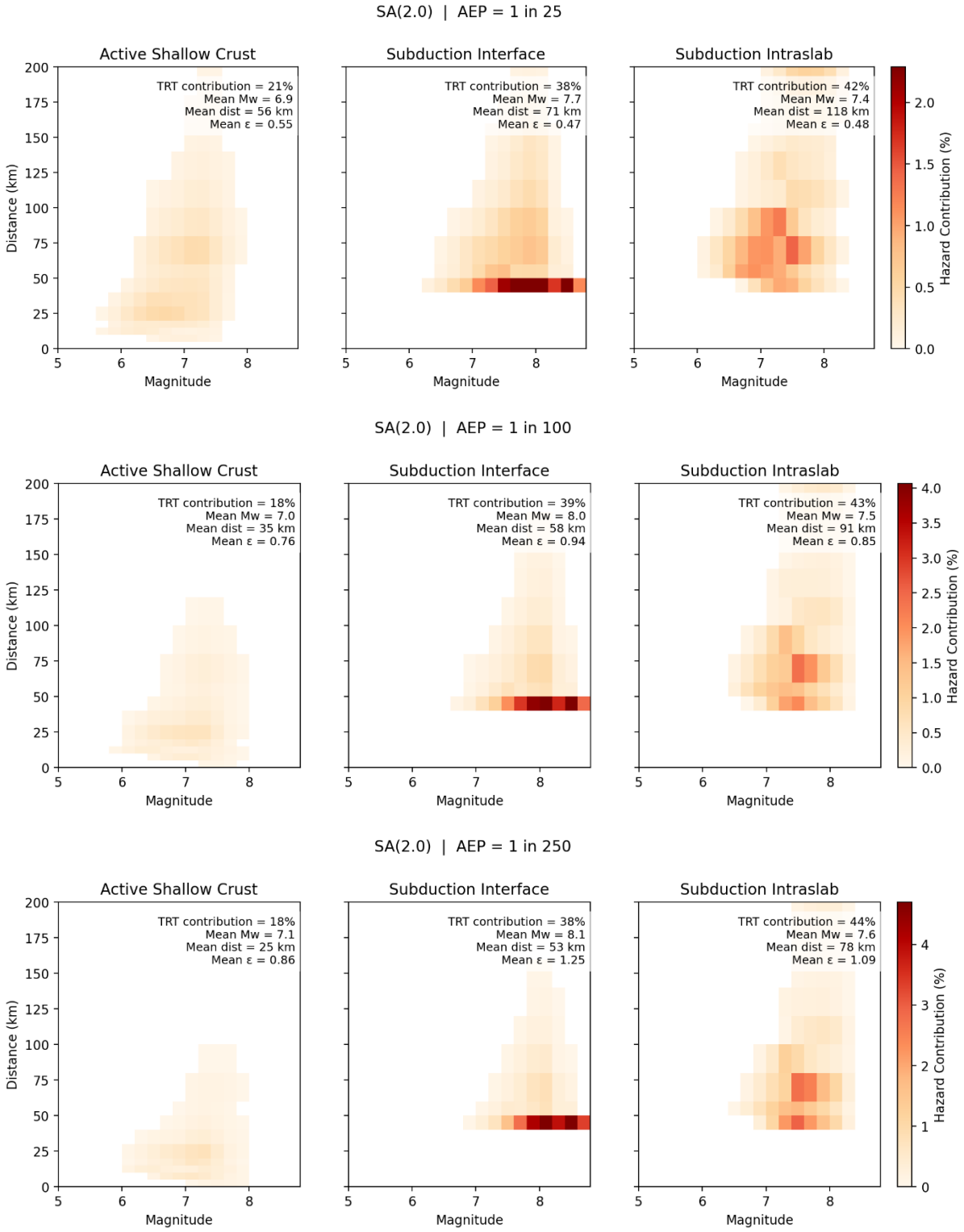

Figure Appendix C.11: SA(2s) hazard disaggregation by magnitude, distance and TRT for 1 in 25, 1 in 100 and 1 in 250 AEP and V_{s30} 450 m/s.

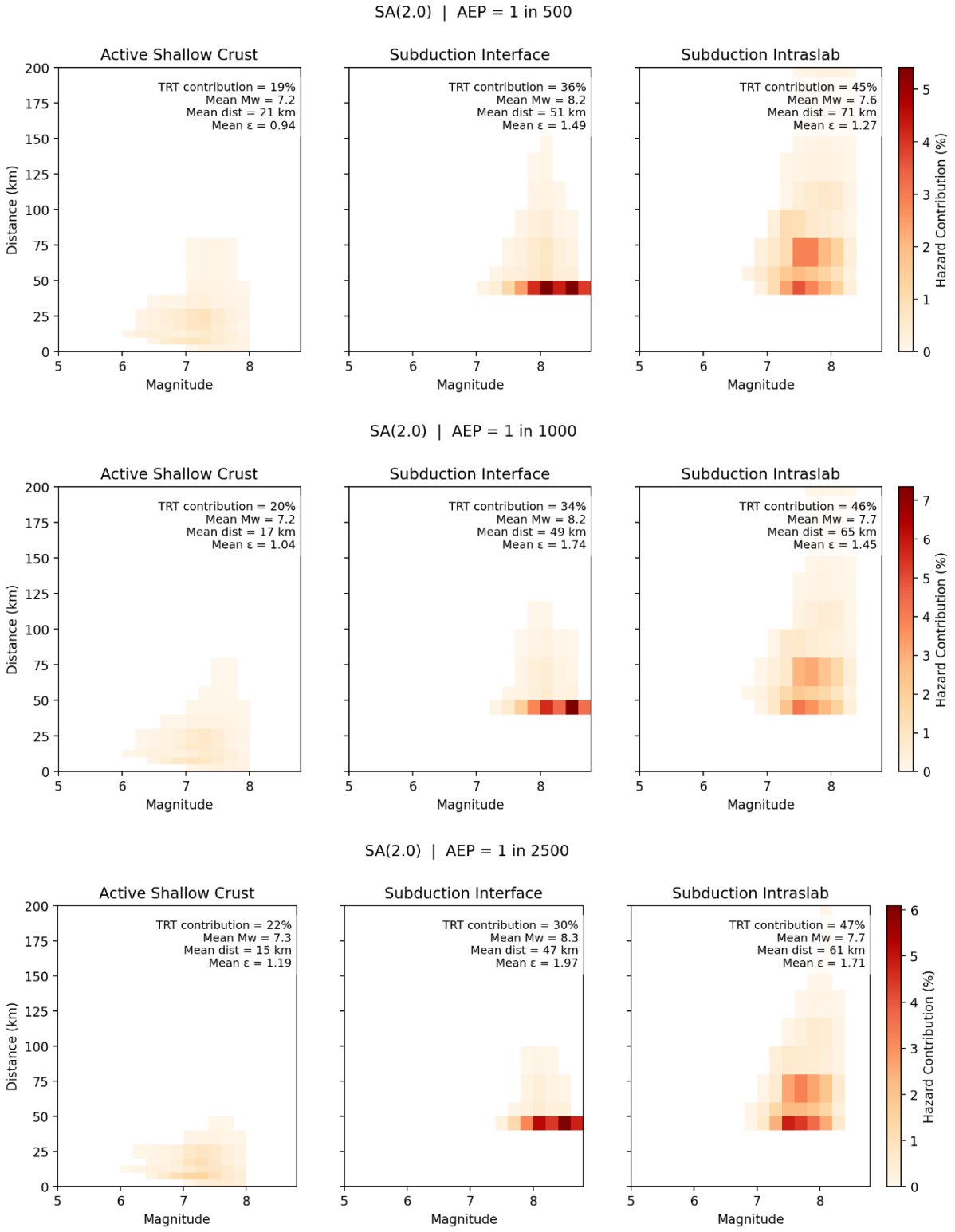

Figure Appendix C.12: SA(2s) hazard disaggregation by magnitude, distance and TRT for 1 in 500, 1 in 1000 and 1 in 2500 AEP and V_{s30} 450 m/s.

C3 Hazard disaggregation for V_{s30} 600 m/s

C3.1 PGA

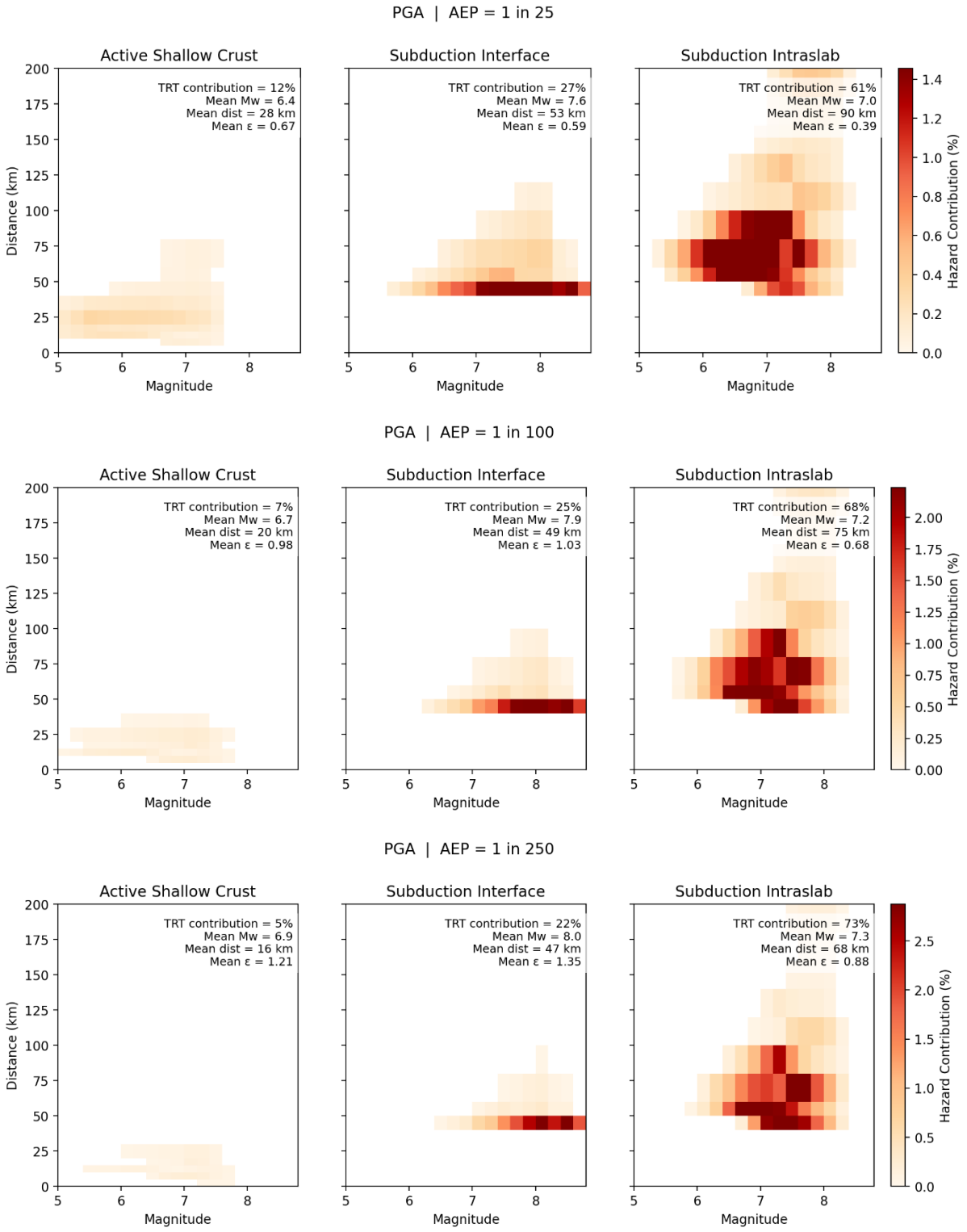

Figure Appendix C.13: PGA hazard disaggregation by magnitude, distance and TRT for 1 in 25, 1 in 100 and 1 in 250 AEP and V_{s30} 600 m/s.

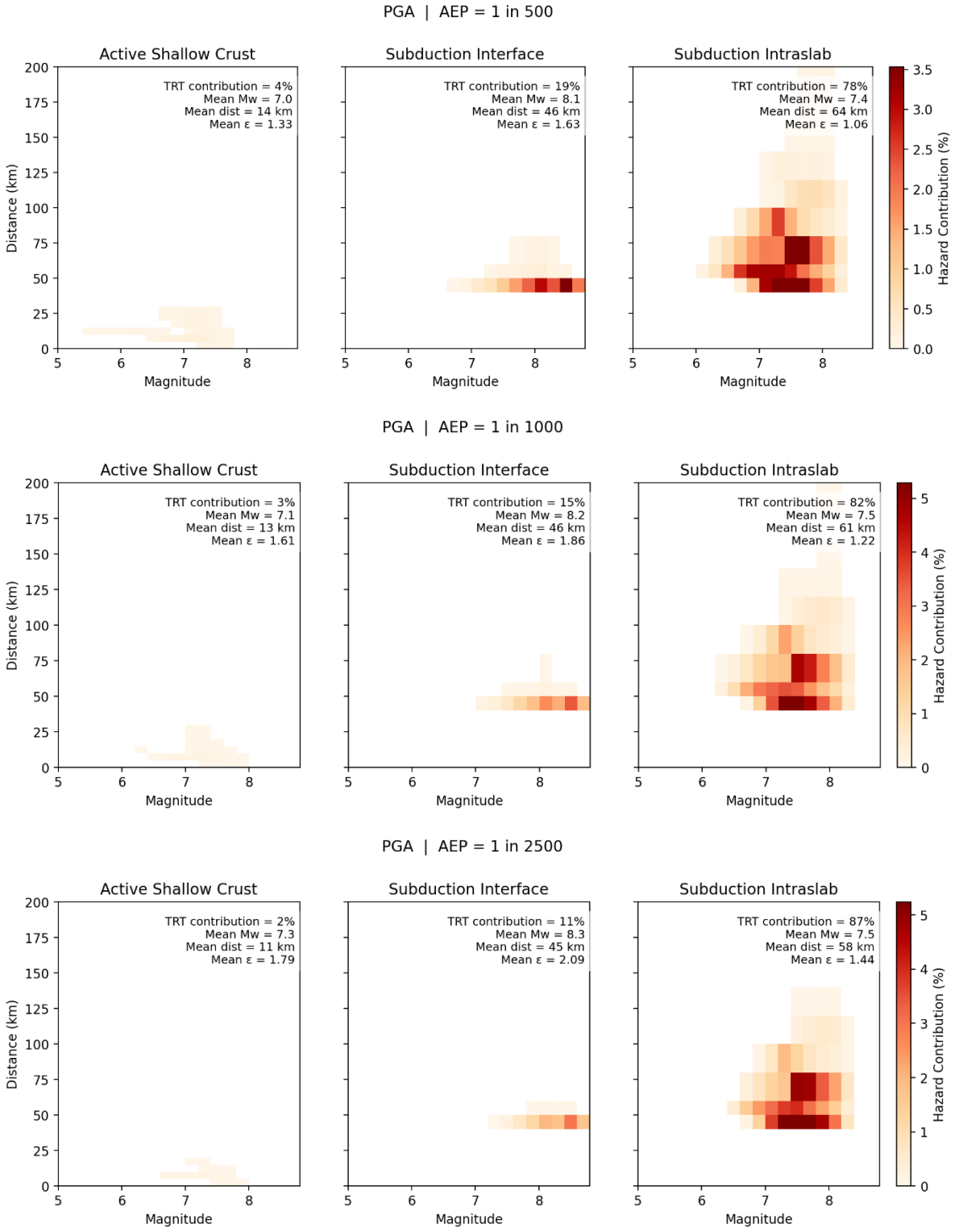

Figure Appendix C.14: PGA hazard disaggregation by magnitude, distance and TRT for 1 in 500, 1 in 1000 and 1 in 2500 AEP and V_{s30} 600 m/s.

C3.2 SA(0.5s)

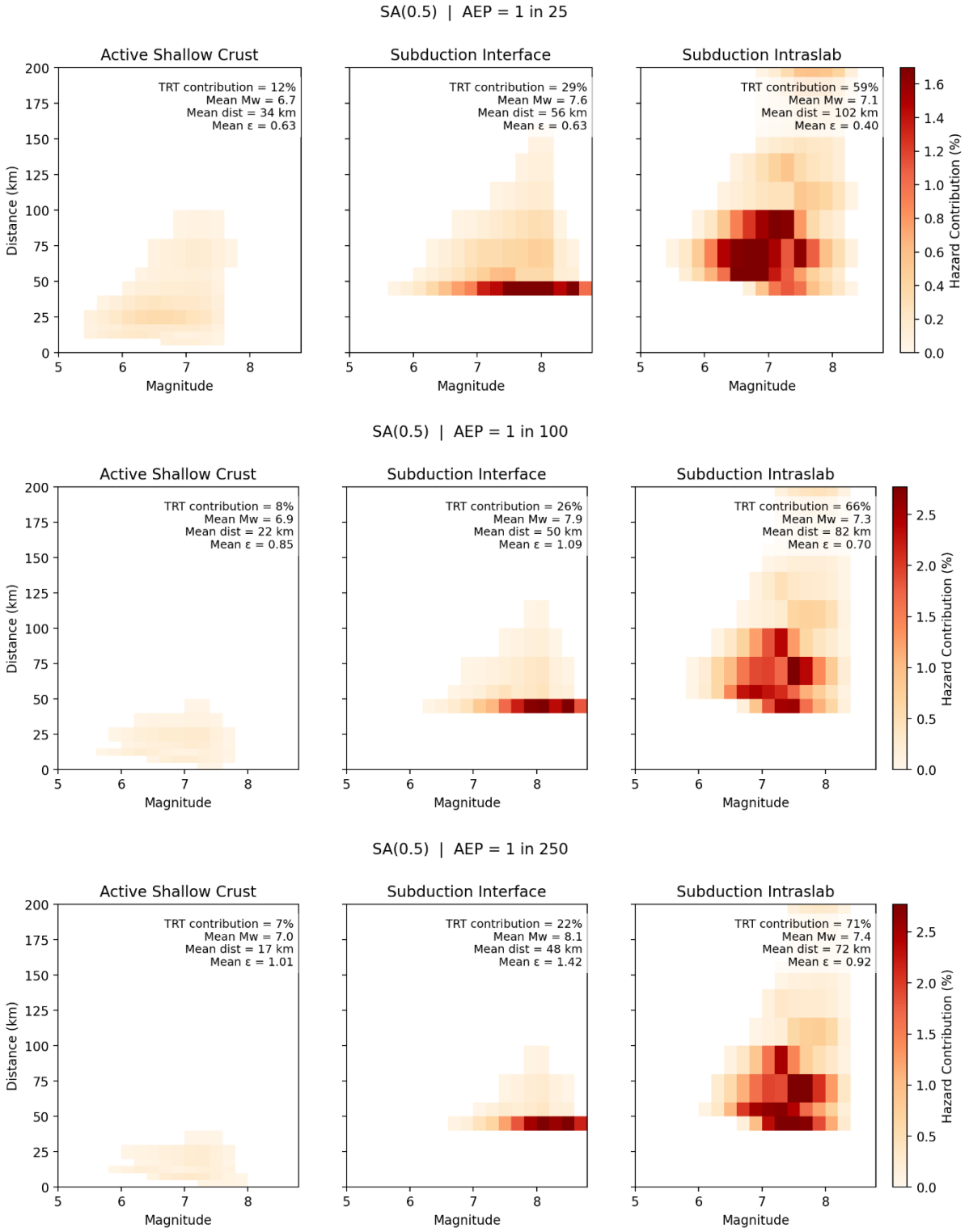

Figure Appendix C.15: SA(0.5s) hazard disaggregation by magnitude, distance and TRT for 1 in 25, 1 in 100 and 1 in 250 AEP and V_{s30} 600 m/s.

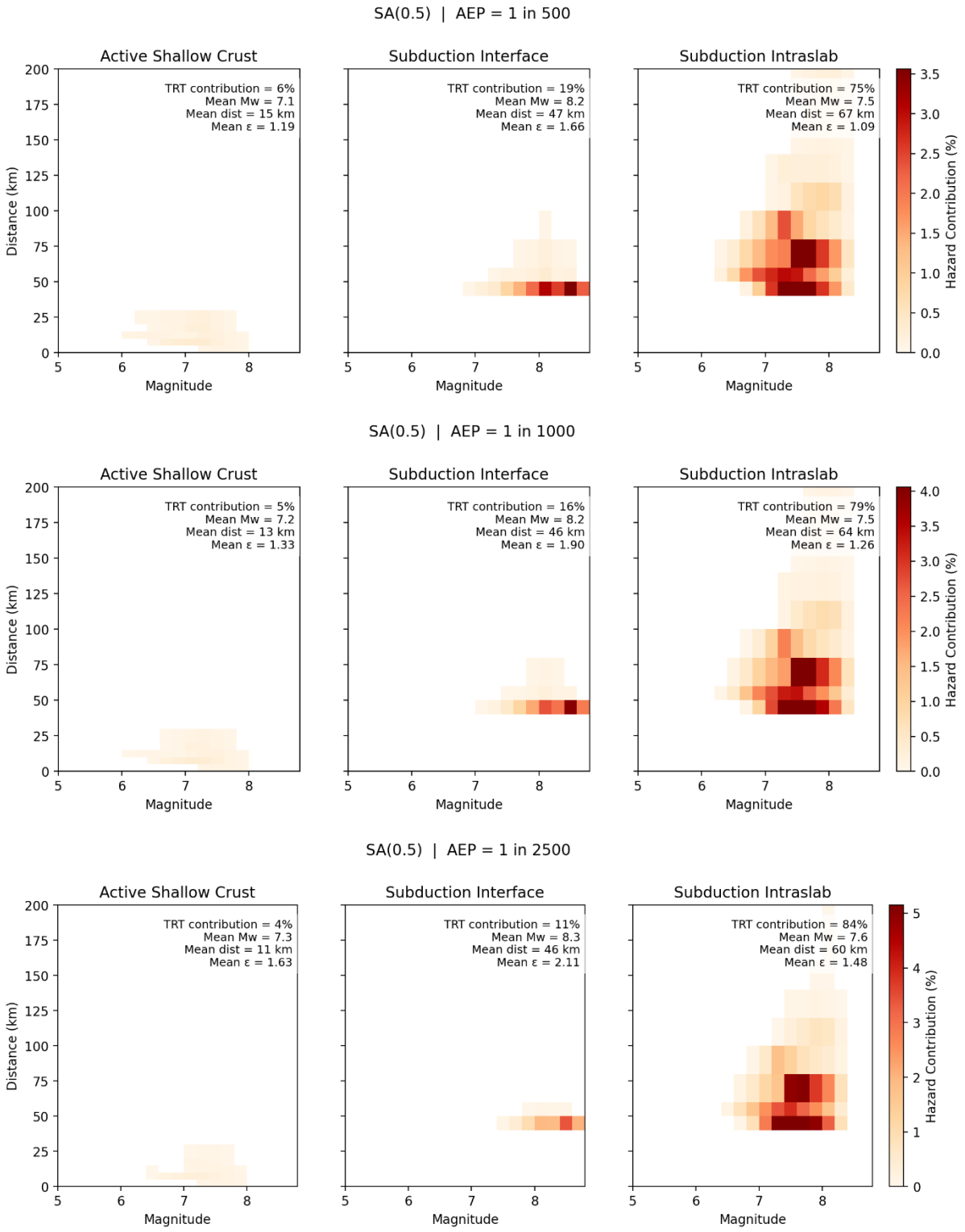

Figure Appendix C.16: SA(0.5s) hazard disaggregation by magnitude, distance and TRT for 1 in 500, 1 in 1000 and 1 in 2500 AEP and V_{s30} 600 m/s.

C3.3 SA(2.0s)

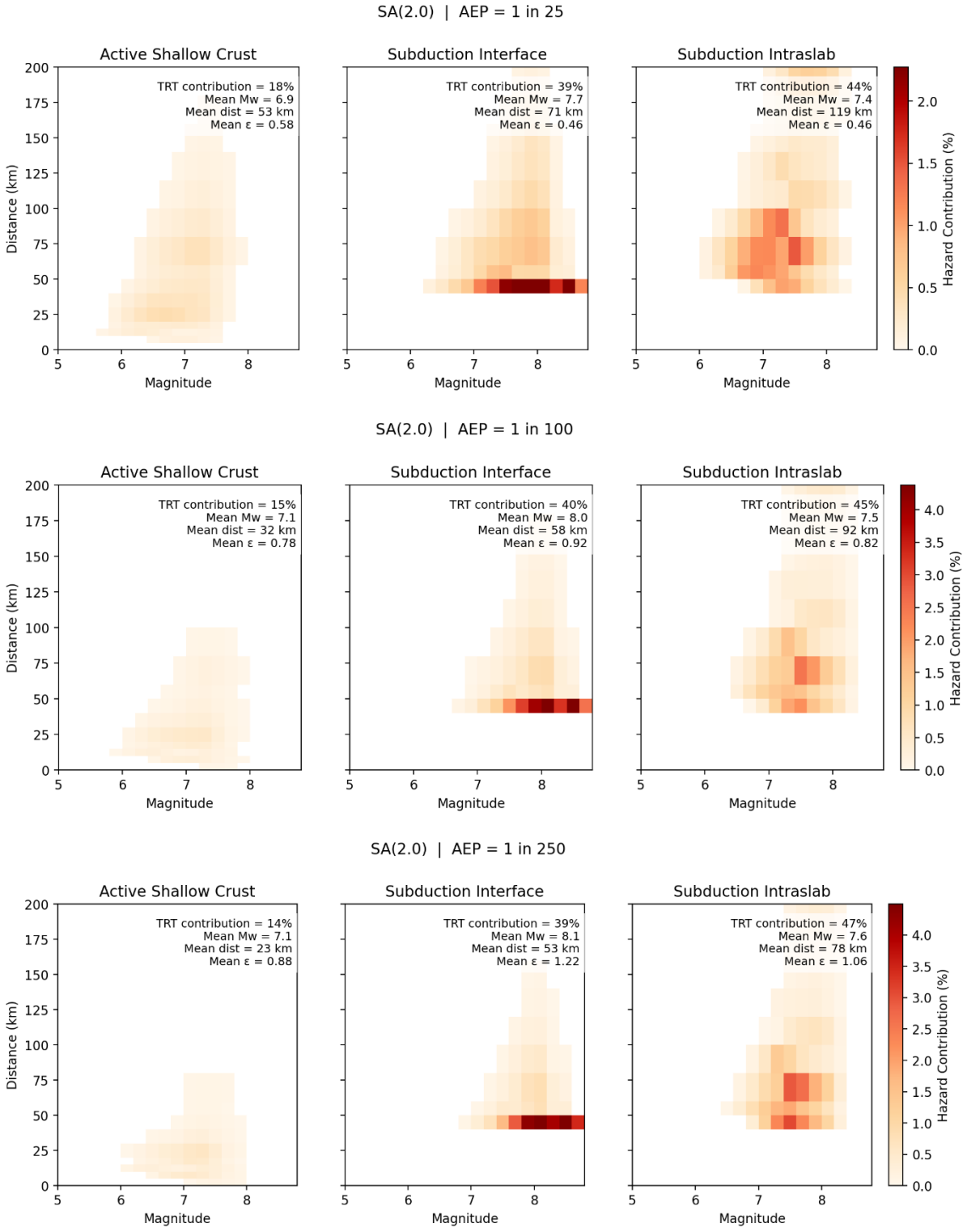

Figure Appendix C.17: SA(2s) hazard disaggregation by magnitude, distance and TRT for 1 in 25, 1 in 100 and 1 in 250 AEP and V_{s30} 600 m/s.

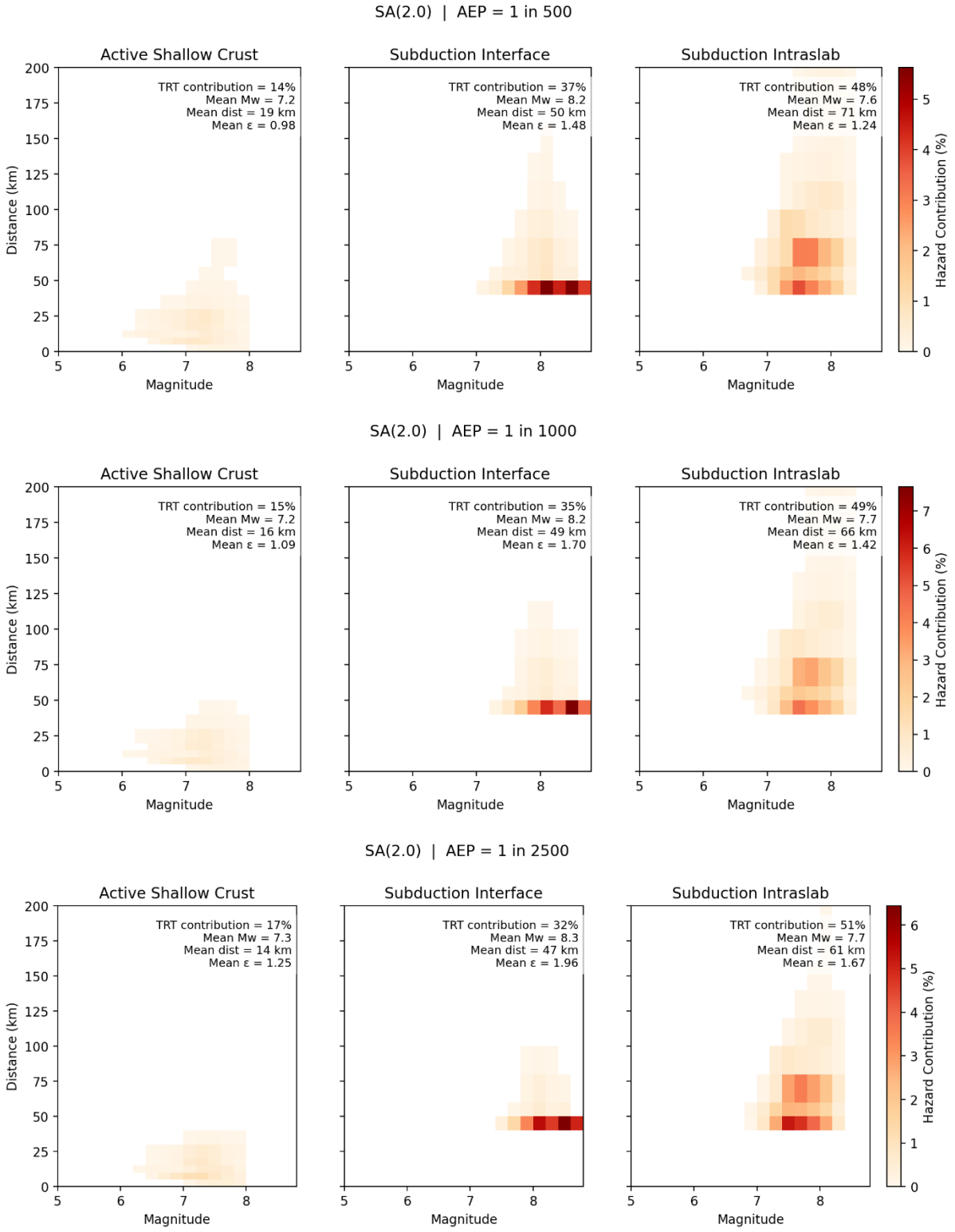

Figure Appendix C.18: SA(2s) hazard disaggregation by magnitude, distance and TRT for 1 in 500, 1 in 1000 and 1 in 2500 AEP and V_{s30} 600 m/s.

C4 Hazard disaggregation for V_{s30} 760 m/s

C4.1 PGA

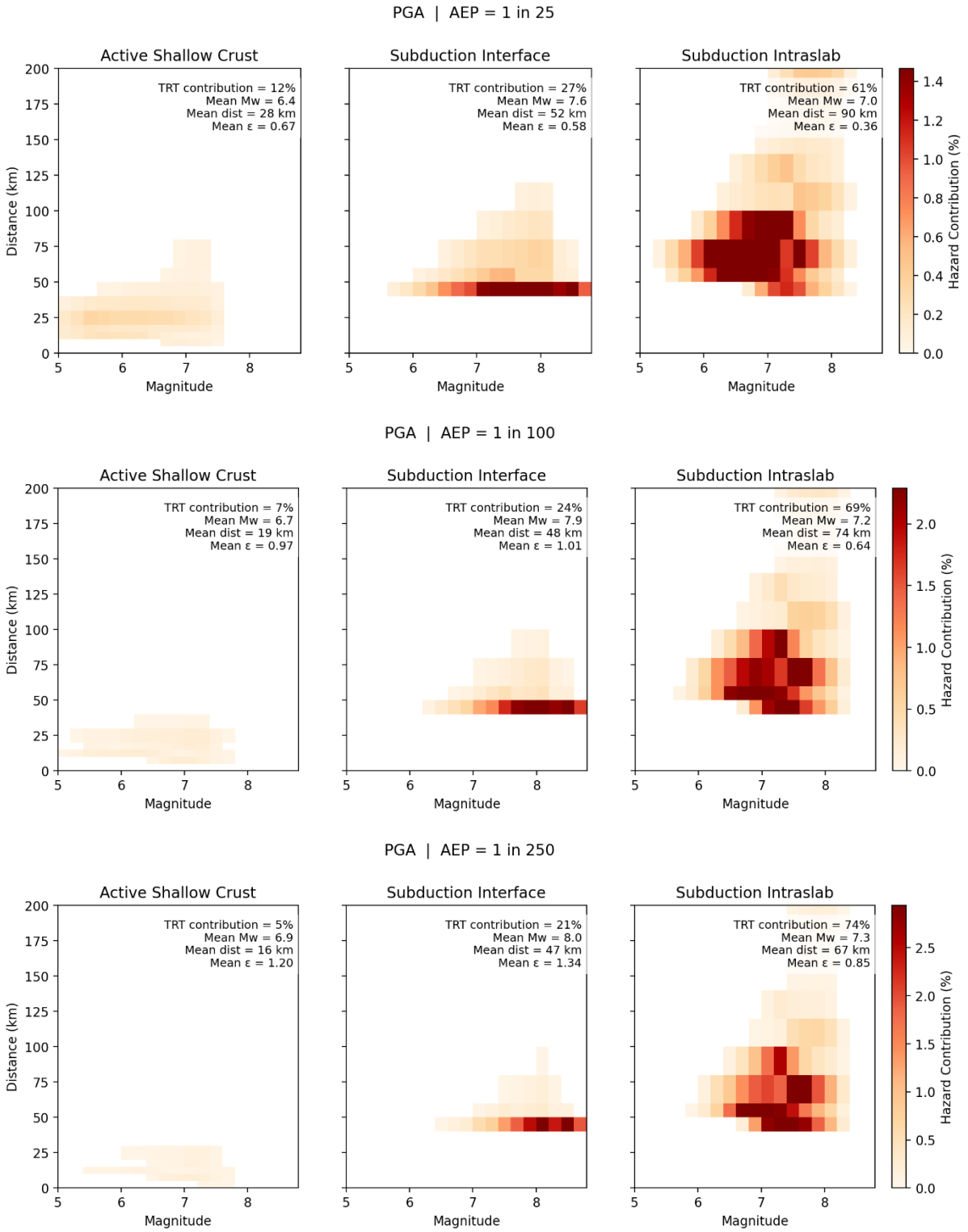

Figure Appendix C.19: PGA hazard disaggregation by magnitude, distance and TRT for 1 in 25, 1 in 100 and 1 in 250 AEP and V_{s30} 760 m/s.

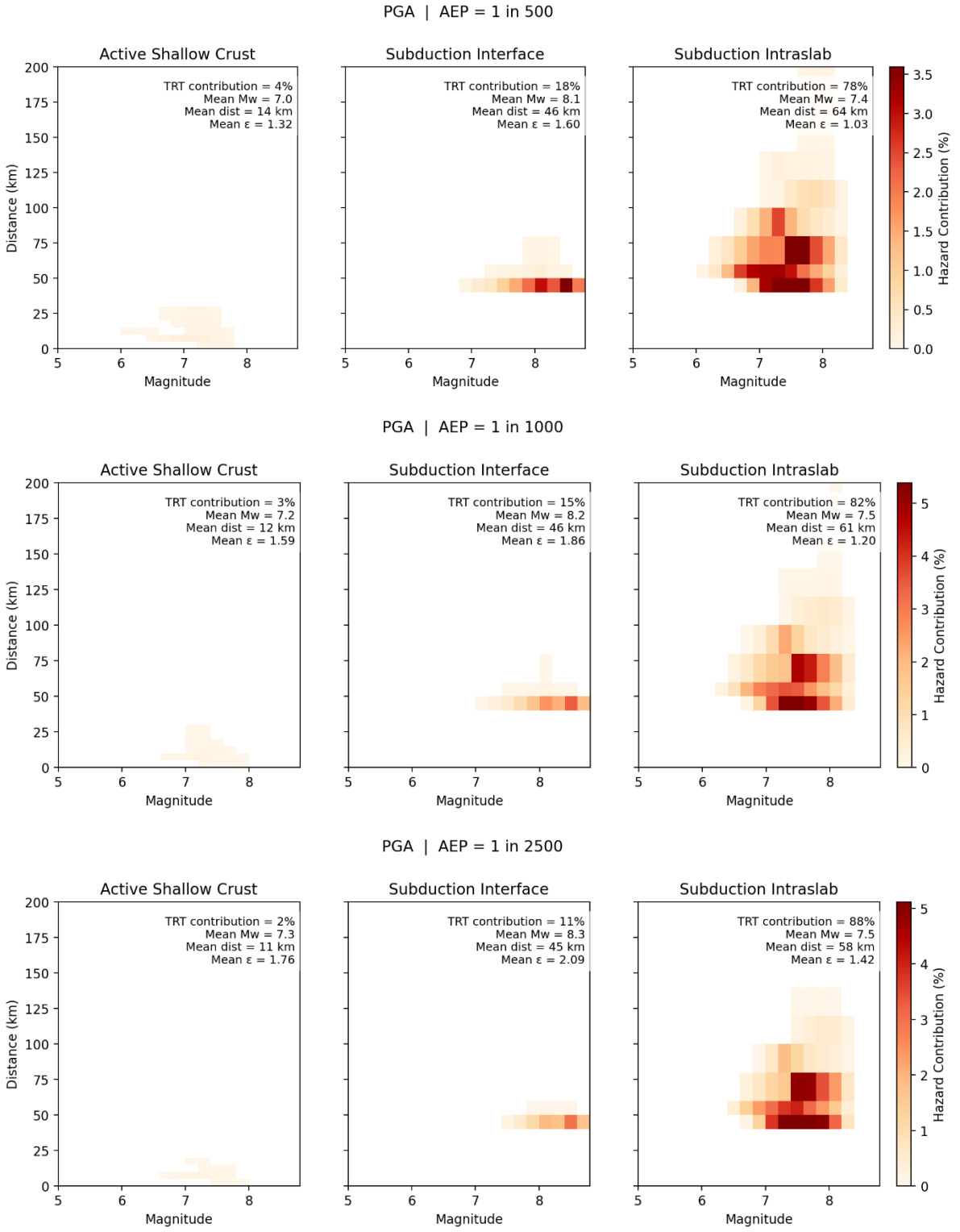

Figure Appendix C.20: PGA hazard disaggregation by magnitude, distance and TRT for 1 in 500, 1 in 1000 and 1 in 2500 AEP and V_{s30} 760 m/s.

C4.2 SA(0.5s)

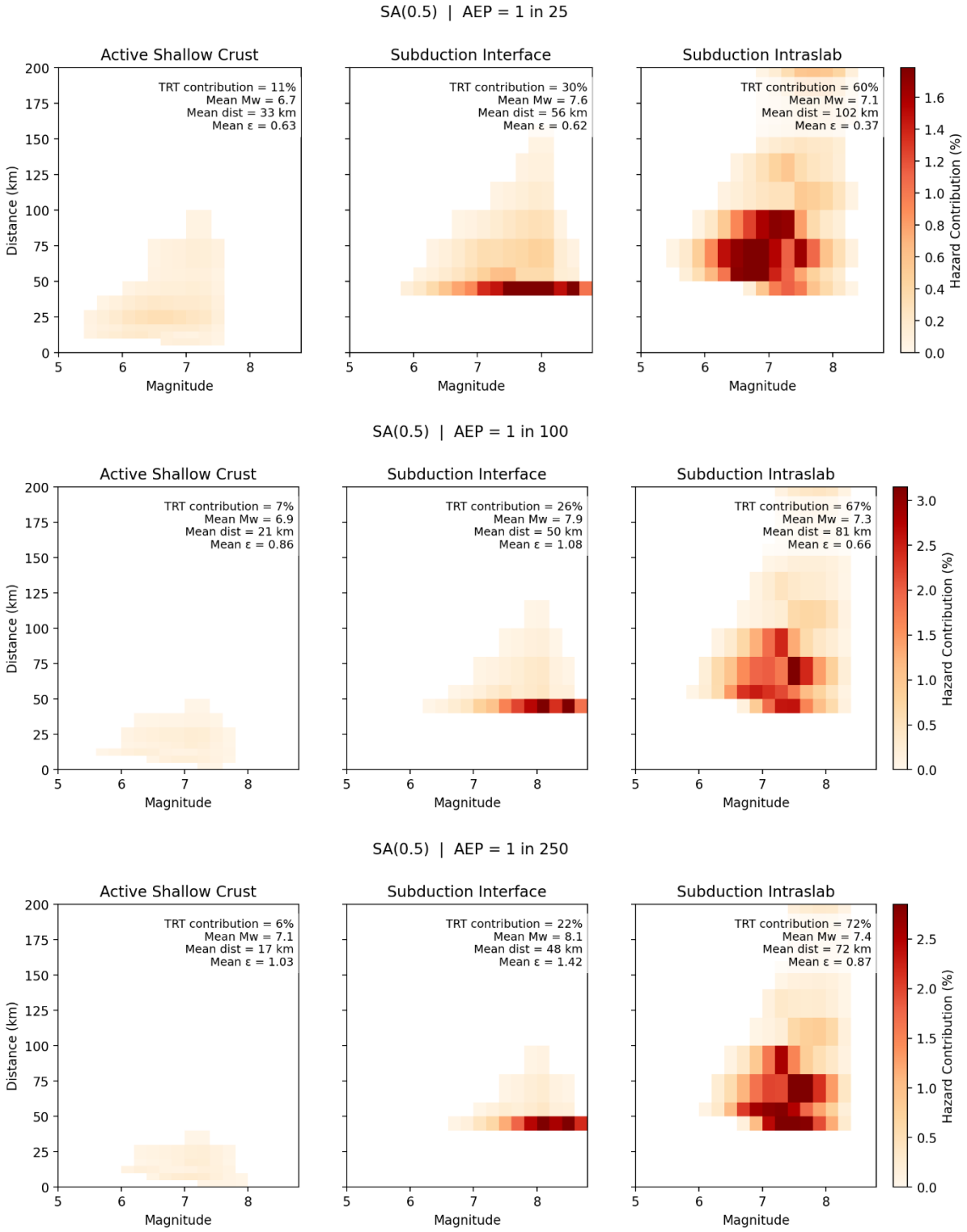

Figure Appendix C.21: SA(0.5s) hazard disaggregation by magnitude, distance and TRT for 1 in 25, 1 in 100 and 1 in 250 AEP and V_{s30} 760 m/s.

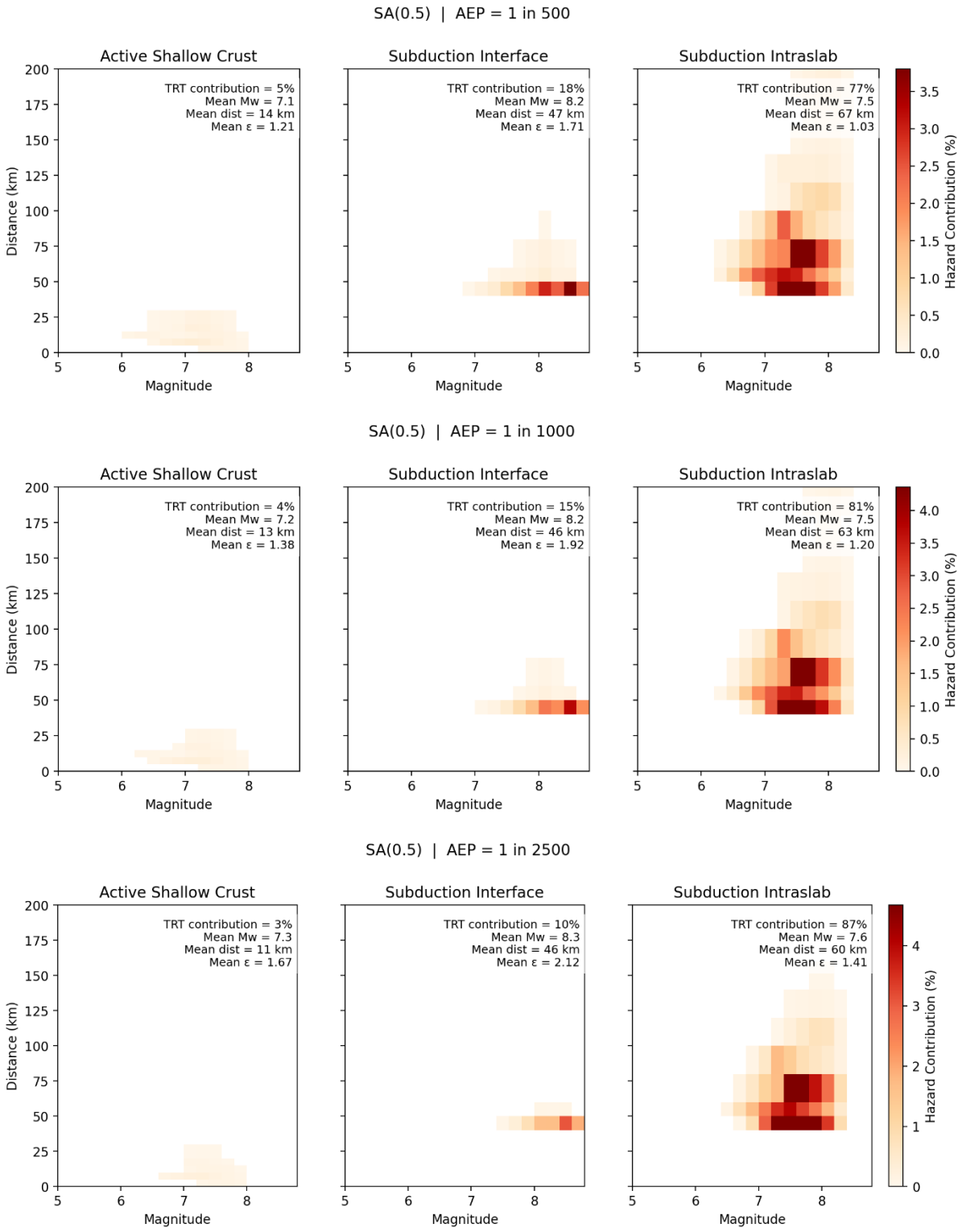

Figure Appendix C.22: SA(0.5s) hazard disaggregation by magnitude, distance and TRT for 1 in 500, 1 in 1000 and 1 in 2500 AEP and V_{s30} 760 m/s.

C4.3 SA(2.0s)

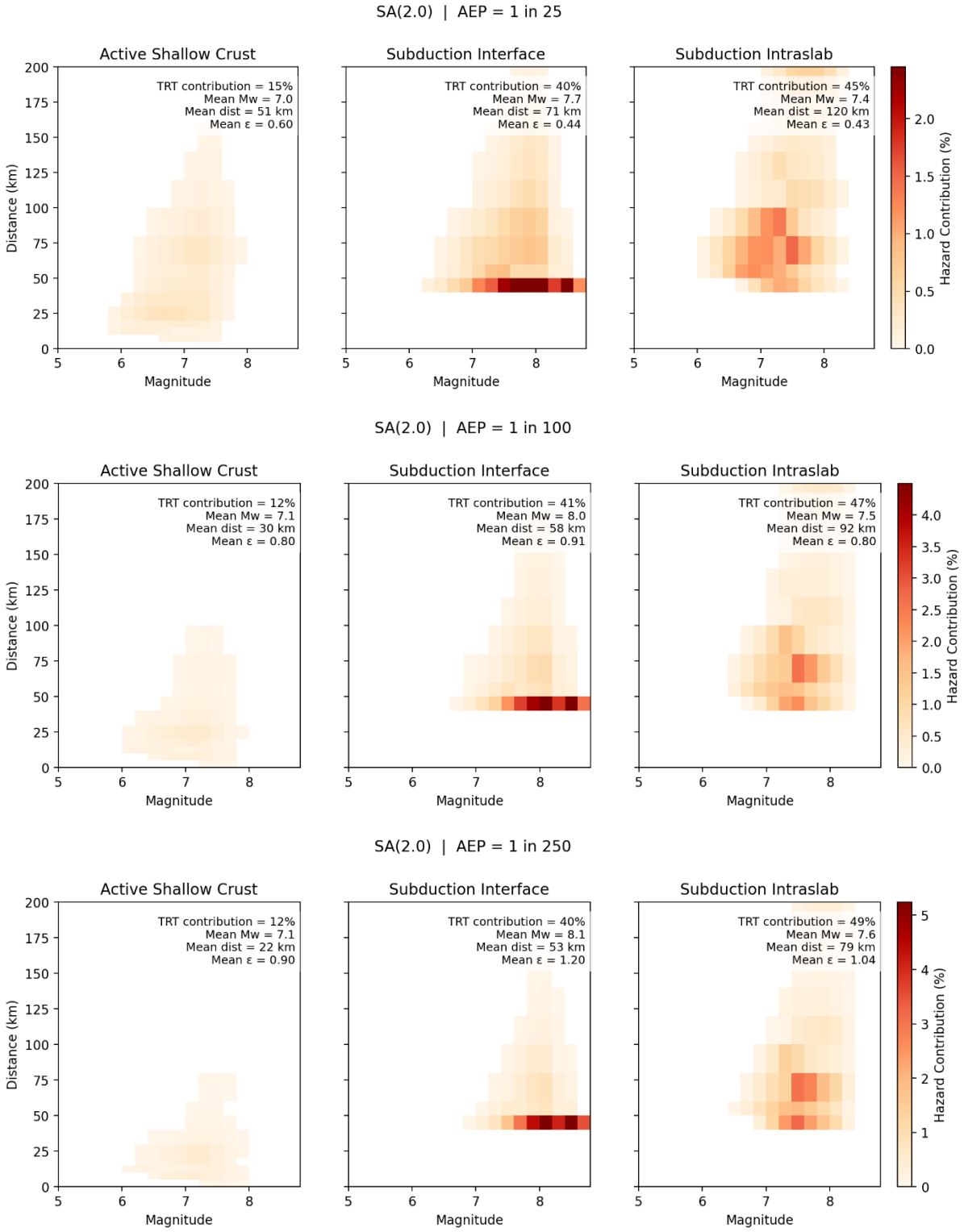

Figure Appendix C.23: SA(2s) hazard disaggregation by magnitude, distance and TRT for 1 in 25, 1 in 100 and 1 in 250 AEP and V_{s30} 760 m/s.

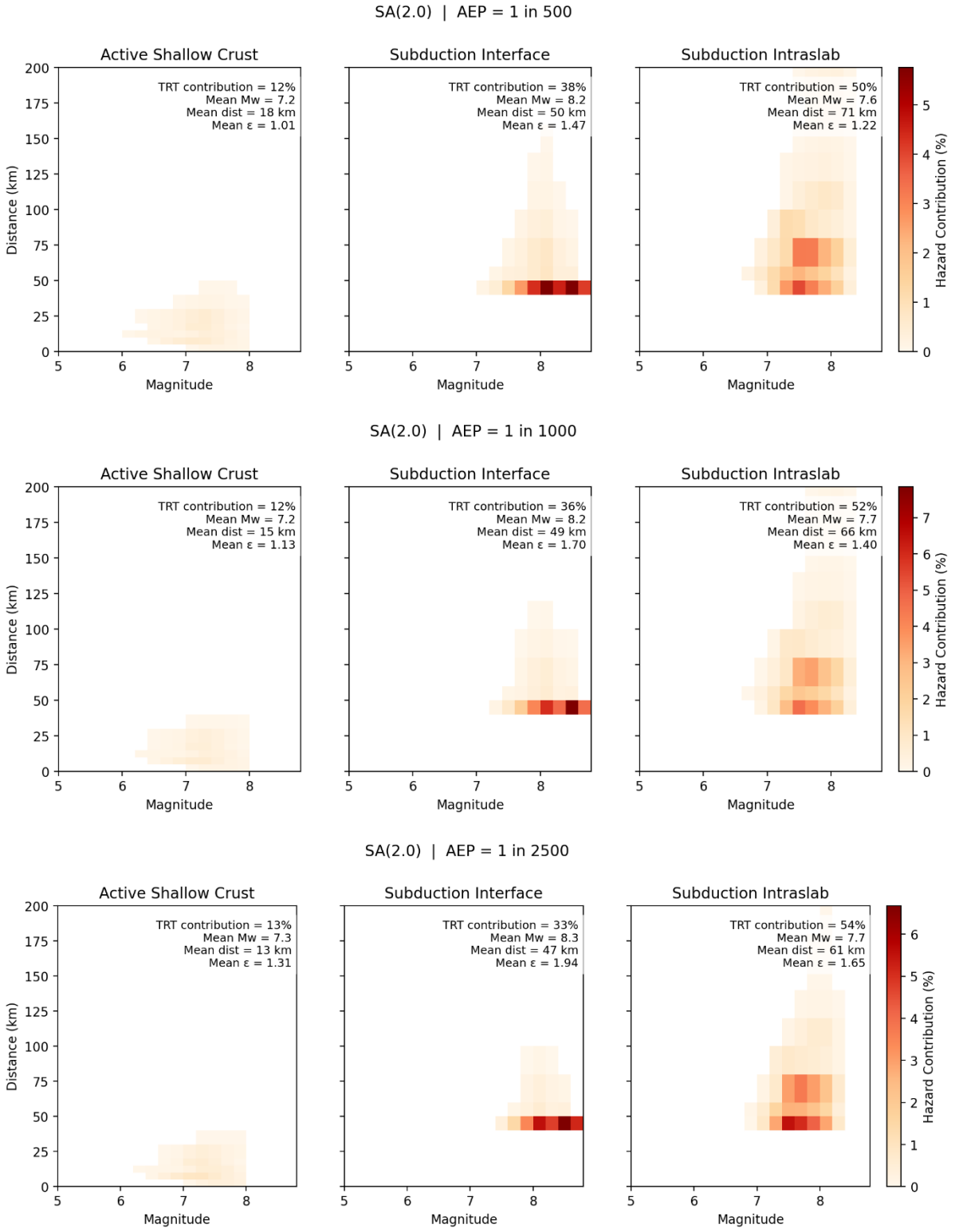

Figure Appendix C.24: SA(2s) hazard disaggregation by magnitude, distance and TRT for 1 in 500, 1 in 1000 and 1 in 2500 AEP and V_{s30} 760 m/s.



Together we create + sustain a better world